AN ELECTRICAL AND OPTICAL STUDY OF FLUIDS NEAR METAL SURFACES

by

Robert Stephen Day

A Thesis submitted for the degree of
DOCTOR OF PHILOSOPHY
of the University of London
and also for the
DIPLOMA OF MEMBERSHIP of the IMPERIAL COLLEGE

AUGUST 1972

Lubrication Laboratory,
Department of Mechanical Engineering,
Imperial College of Science and Technology,
London, S.W.7.

ABSTRACT

The existence and nature of relatively thick, highly viscous boundary layers at the interface between metal substrates and liquids is considered from the point of view of boundary lubrication.

All the apparatus used is based on the simple idea of displacing an oil film from a solid metal surface under the hydrostatic pressure of mercury. In this way the problems of contamination by dust particles and the effect of surface asperities are circumvented.

The thickness of the oil films was calculated from the measured capacitance of the metal-oil-mercury system. In many cases these calculations were checked interferometrically. The films were exposed to tangential shearing by forcing the mercury past them.

It has been found that, under favourable conditions, chemisorbed films of about 1,500 Å in thickness are capable of withstanding tangential shearing of 150 Newtons/metre^2, or more. The thickest and most shear resistant films are formed where the basic fluid and fatty acid additive have similar molecular dimensions. The interferometric topography of these films confirm that they consist of an interwoven fibrillar structure within which quantities of the non-polar solvent are trapped.

The mercury squeeze film apparatus has been developed for use as a thin film viscometer. With this technique the existence of physically adsorbed viscous polymolecular layers up to 10,000 Å thick has been established. Hydrogen bonding has been shown to play an essential role in the formation of these films, and a theory of their structure is proposed.

ACKNOWLEDGEMENTS

The author wishes to make grateful acknowledgement to the following, who contributed to or assisted this study:

Professor A. Cameron, for the opportunity to work in his Laboratory, for his encouragement and advice during the course of this investigation, and for the many hours of stimulating discussion;

Professor J.C. Anderson, who placed many of the facilities of his Laboratory at the author's disposal and for the helpful and encouraging discussions;

The National Aeronautics and Space Administration Lewis Research Centre for financing the author during the major part of the project, and the Monsanto Research Corporation for providing several fluids and the relevant data;

Mr. R. Dobson, for his timely encouragement, technical advice and constant generous help in the Laboratory;

My colleagues in the Lubrication Laboratory, especially Michael Stokes, Michael Sutcliffe, Richard Gentle, Andrew Smith, Warwick Grew, Hugh Spikes and Graham Paul, for their support and encouragement during this research, and many useful discussions.

Contents

Title page	1.
Abstract	2.
Acknowledgements	3.
Contents	4.
Chapter 1 Introduction and Rationale	8.
1.1 Boundary Lubrication	8.
1.1.1 Monomolecular Boundary Lubrication	10.
1.1.2 Polymolecular Boundary Lubrication	11.
1.2 Experimental Evidence of Thick Films	12.
1.2.1 Positive Results	12.
1.2.2 Negative Results	15.
1.3 Possible Mechanisms of Thick Film Formation	17.
1.3.1 Chemical Adsorption	17.
1.3.2 Physical Adsorption	20.
1.4 Summary	22.
1.5 Scope of the Research	23.
Chapter 2 Experimental Apparatus and Materials	24.
2.1 Introduction	24.
2.2 The Ball Apparatus	24.
2.3 The Shear Apparatus	26.
2.3.1 The Cell	26.
2.3.2 The Mercury Flow System	30.
2.3.3 Calculation of Shear	32.
2.4 Electrical Instrumentation	34.
2.4.1 Circuitry	34.
2.4.2 Calibration	38.
2.5 Optical Interferometric System	40.
2.5.1 Choice of 'White Light' System	41.

Contents continued.

2.5.2 Reflection Surfaces	42.
2.5.3 Collimation	44.
2.5.4 Optical Calibration	46.
2.6 Cleaning Techniques and Specification of Materials	48.
2.6.1 Cleaning	48.
(a) The Ultrasonic Agitation Bath	49.
(b) The Ionic Bombardment Apparatus	50.
2.6.2 Possible Contamination	52.
2.6.3 Specification of Materials	53.
Chapter 3 Early Experiments with the Shear Apparatus	56.
3.1 Introduction	56.
3.2 Experimental Technique and Early Results	56.
3.2.1 Original Experimental Technique	56.
3.2.2 Results and Discussion	57.
(i) Without Shear	57.
(ii) Shear	60.
3.3 Possible Mechanisms of Electrical Failure	63.
3.3.1 Bridge Formation	63.
3.3.2 Fritting	64.
3.3.3 Cavity Breakdown	64.
3.3.4 Ionic Conduction	65.
3.3.5 Proposed Mechanism	65.
3.3.6 Experimental Comparison	68.
3.4 Conclusions	70.
Chapter 4 Mechanical Properties of Thick Films	71.
4.1 Introduction	71.
4.1.1 Previous Studies of Thick Film Properties	71.
4.1.2 Proposed Experiments	77.
4.2 Revised Experimental Technique and Discussion	77.

Contents continued.

4.3 Results and Discussions	79.
4.3.1 Effects of Various Initial Conditions	79.
4.3.2 Residual Films of Various Fatty Acids	82.
4.3.3 Conductivity of the Various Residual Films	86.
4.3.4 Thick Rilm Recovery	91.
4.4 Interferometric Results and Discussion	94.
4.4.1 Topography of the Thick Films	94.
4.4.2 Variation of Thick Film Dielectric Constant	98.
4.5 General Discussion and Conclusions	101.
4.5.1 Summary of Results	101.
4.5.2 Discussion and Conclusions	102.
Chapter 5 Experiments with the Ball Apparatus	108.
5.1 Introduction	108.
5.2 Experimental Procedure	108.
5.3 Results (and Discussion)	109.
5.3.1 0.1% Stearic Acid in Hexadecane	109.
5.3.2 The Fluids Supplied by N.A.S.A.	114.
(a) The Esters	114.
(b) The Hydrocarbons	118.
(c) The Remaining N.A.S.A. Fluids	120.
5.3.3 Comparison of 'Wet' and 'Dry'-Cleaned Surfaces	123.
5.3.4 Synthetic Paraffin With and Without Antiwear Additives	125.
5.4 Summary	129.
5.5 Conclusions	132.
Chapter 6 Theory of Fluid Thinning Process	134.
6.1 Introduction	134.
6.2 Derivation of Theory	134.
6.2.1 Expression for $\int_0^h u\,dy$	138.
6.2.2 Expression for $(\frac{\partial u}{\partial x})_{y=h}$	139.

Contents continued.

6.2.3 Expression for $(\frac{\partial u}{\partial y})_{y=h}$ 140.

6.2.4 First Approximation 140.

6.2.5 Second Approximation 141.

6.2.6 Final Expressions for U, $(\frac{\partial u}{\partial y})_{y=h}$ and $(\frac{\partial u}{\partial y})_{y=o}$ 142.

6.3 The Electric Double Layer 146.

Chapter 7 Investigation of Physical Adsorption 150.

7.1 Introduction 150.

7.1.1 Physical Interactions 150.

7.1.2 Models for Physically Adsorbed Thick Films 152.

7.1.3 Types of Molecular Bonding 155.

7.1.4 Hydrogen Bonding 156.

(a) Viscosity Variations 158.
(b) Dielectric Constant Variations 161.
(c) Conductance Variation 162.
(d) Pyroelectric Behaviour 162.

7.2 Experimental Apparatus and Procedure 163.

7.3 Results and Discussion 167.

7.3.1 The Pure Hydrocarbons 167.

7.3.2 The Esters 169.

7.3.3 The Alcohols 171.

7.3.4 The Fatty Acids 173.

7.4 Summary and Conclusions 176.

7.4.1 Proposed Structure of Physically Adsorbed Films 177.

Chapter 8 Conclusion and Future Work 182.

8.1 Shear Strength of Chemisorbed Thick Films 182.

8.2 Investigation of Physical Adsorption 182.

8.3 Possible Future Research 183.

Appendix A The Effect of Turbulence in the Cell Apparatus 186.

Appendix B Tables of Results obtained by Fuks 189.

Appendix C Computed Solution of Differential Thinning Equation 190.

References 198.

CHAPTER 1

INTRODUCTION AND RATIONALE

This thesis deals with some properties of the various polymolecular boundary layers whose importance to lubrication remains the subject of much conjecture. Extensive research has been carried out in the realm of boundary lubrication during the past century and this chapter contains a brief survey of the most relevant of this work. Detailed discussions of more specialised branches of this field are deferred until the appropriate sections of the later chapters.

1.1 Boundary Lubrication

When two clean solid surfaces are rubbed together power is dissipated in the contact regions which can be attributed to a frictional force acting between the two materials. In these contact regions seizing and tearing may occur and high temperatures are generated at the interface. The resulting erratic and rough sliding motion between the damaged surfaces obviously decreases the efficiency and lifetime of any moving machinery. This problem is reduced by introducing a lubricating fluid between the surfaces which reduces the amount of contact and the frictional force.

If this fluid film is thicker than the combined surface roughness preventing any metal-metal contact, then all the shearing will take place within the lubricant. The resulting coefficient of friction is suitably low, depending mainly on the fluid viscosity rather than on the properties of the opposing surfaces. The classical hydrodynamic behaviour of the lubricant under these conditions was formulated by Reynolds in 1886 (1), and is termed 'hydrodynamic

lubrication'.

When high loads are applied across surfaces with high moduli of elasticity the fluid viscosity increases with pressure. Deformation of the metal surfaces takes place producing extreme local pressures in the lubricant, accompanied by large viscosity increases. These conditions were first documented by Ertel-Grubin (2) as recently as 1947, and are known as 'elastohydrodynamic lubrication'. Typical film thicknesses in this regime are of the order of several hundred nanometers so that solid-solid contact, if it should occur, makes a negligible contribution to the friction coefficient.

At extreme loads and low speeds these coherent lubricating films cannot be maintained and the system enters the realm of 'boundary lubrication'. This form of lubrication prevents the surfaces reverting to dry, unlubricated conditions. It also occurs in most machines on stopping and starting prior to the establishment of hydrodynamic or elastohydrodynamic conditions. The boundary lubricants somehow modify the solid surfaces, by physical adsorption and/or chemical reaction, producing a surface film which is more easily sheared than the actual metal. For this reason the physical and chemical properties of the solid surfaces are of prime importance in boundary lubrication. Their crystalline form, degree of oxidation and other chemical modifications critically effect their ability to physically adsorb and chemically react with constituent molecules of the lubricant. The viscosity of the fluid, so important in the two forms of full-film lubrication is negligible in this context. What is important is the property of a fluid which enables it to be

a good boundary lubricant termed its 'oiliness', and sometimes its 'body'. Just what this property is and how it functions is an unsolved problem about which there is a large amount of confusion and disagreement. In fact, boundary friction is the result of many interactions, known and unknown, under many constraints and should not, therefore, be thought of as a rigorously defined process. Boundary lubrication may be split into two main categories, involving monomolecular and multimolecular layers of the lubricant on the surfaces.

1.1.1 Monomolecular Boundary Lubrication

Early research by Rayleigh (3) was expanded by Langmuir (4) who showed that a film of fatty acid floating on water could be reduced to a close-packed monomolecular layer. He demonstrated how the thickness of this monolayer, its structure, orientation and packing density could be deduced. By passing a specimen through the air/water interface he transferred these monolayers onto the surfaces of various solids where their lubricating properties could be studied. By this method he found that the presence of a single layer of lubricant reduced the coefficient of friction on many surfaces to the order of 0.1.

Extensive research into the properties of monolayers on a large range of surfaces has been carried out since, most notably by W.A. Zisman, and his co-workers (5-10). Using a similar technique to obtain retracted monolayers on glass plates, they measured the coefficients of friction under varying conditions for a stainless steel slider. Some of these results are discussed later.

As a result of this research a school of lubrication has formed, which believes that boundary lubrication is effected solely by the presence of a chemisorbed and/or physically adsorbed monolayer on the rubbing surfaces. The possibility of an organised polymolecular layer existing under boundary lubrication conditions was suggested by Sir William Hardy (11, 12) in the early part of this century. He thought that even if these layers were not necessary for successful lubrication they were very probably present.

1.1.2 Polymolecular Boundary Lubrication

Hardy's model of boundary lubrication, under the most extreme conditions comprised of plane parallel surfaces separated by two adsorbed monolayers. More important to this research, he defined the adsorbed state of matter as being distinct from any other state, and suggested that the range of metallic surface forces may extend several hundred nanometers into the lubricant. Within this range he postulated that the constituent lubricant molecules were orientated, producing a thick ordered polymolecular film. His theory was based on the results of experiments on adhesion and observations of the fldatation of metal surfaces on stable gas films approximately four microns thick. At this time Trillat (13) had detected ordered films of fatty acids 10,000Å (1,000 nanometers) thick using x-ray and electron diffractometry, results which experimentally supported Hardy's theories.

As a result of Hardy's ideas the theory of polymolecular boundary lubrication has grown. Its adherents assert that not only are these multilayers present, but that they are very necessary to provide the degree of lubrication observed practically. Experimental evidence

of the existence of these thick films, or multilayers, was plentiful. A comprehensive review of this research is found in Smith's Ph.D. Thesis (14), but a brief account of the most important of this work is given here.

1.2 Experimental Evidence of Thick Films

Although a large amount of research has been carried out on thick films not all the results confirm their existance. This section is therefore subdivided into the evidence for thick films, and that against.

1.2.1 Positive Results

Early work by Duff (15), revealed apparent evidence of long range ordering in solutions of fatty acids by their anomolous flow through capillaries. Barnard and Wilson (16) and Dover (17), obtained similar results in capillaries of 0.3mm. bore, showing that complete clogging occurred after several hours of flow. On removal of the acid with pyrophoric iron however, no clogging occurred.

In 1940, Needs (18), using a parallel plate squeeze film viscometer, investigated the behaviour of films of vegetable and mineral oils compressed between steel surfaces. He reported thick residual films between 7,500 Å and 10,000 Å, and went on to measure some of their mechanical properties. Some of these results are reported in chapter 4.1.

Tausz and Szekely (19) obtained films of mineral oils between a steel ball and mercury. They calculated the thicknesses from the capacitance measured across the oil film by a bridge. Polar and non-

polar oils were tested, the former producing stable residual films 1,000 Å thick as opposed to less stable, but thicker films (5,000 Å) for the non-polar oils.

Deryagin's early work on the anomolous flow of thin films of water in various apparatus met with mixed success. The flow of bubbles through capillaries indicated films 1,000 Å thick (20). He then reported rigid films of water 1,500 Å thick on flat metal surfaces (21-23) and 300 Å thick formed by water between hydrogen and mica (24, 25). He later retracted some of these results as the possibility of them being caused by dust could not be ruled out (26).

In 1949 Henniker (27) produced a review of the research done on thick film phenomena up to that time. The volume of this work is indicated by the fact that he discussed 174 references. Although the results reviewed were generally affirmative, Henniker considered that the evidence was inconclusive in the light of the ambiguity of much of the work. Again, the possibility of contamination, whether by dirt, impurities or surface ions, was the recurring criticism.

The later work by Deryagin is more impressive (28-30). He and his co-workers deduced viscosity variations in polymer solutions from observations of the profiles of fluid drops placed on polished metal surfaces and subjected to tangential air blasts. This technique is known as the 'blow-off' method which circumvents most of the contamination criticisms. Interferometric measurements of the profile of the fluid drops revealed continuous variations in viscosity in films up to 2 microns thick. By using ellipsometry, Deryagin showed that solutions of stearic acid in hexadecane produced structured, but heterogeneous boundary films between 100 Å and 1,000 Å thick.

Other important recent work was done by Fuks (31-33) and Cameron (34) and their collaborators. Each group used a type of falling plate viscometer to detect the presence of rheological anomolies and/or thick films. The more elaborate apparatus was used in the extensive work done by Fuks. Not only did he find strong evidence of thick films for many varied solutions of fatty acids in several solvents, he also measured some of the mechanical properties of these rigid layers. His work is discussed in more detail in chapter 4.1..

Cameron's simpler form of falling plate viscometer produced residual films for several fatty acid solutions in hexadecane. By using fatty acids of systematically increasing hydrocarbon chain lengths he also showed a 'chain matching' effect. This indicates enhancement of the final residual film thickness and of the anomolous viscosity increments during thinning when the solvent and fatty acid are of similar molecular weight. This is discussed later in chapter 4..

The most recent work reported by Smith (14) and Cameron and Smith (35), is the most conclusive to date. Many fluids were tested by displacing films from metal surfaces (both flat and spherical) by the hydrostatic pressure of mercury. The film thicknesses were calculated from the capacitance across the mercury-test fluid-metal substrate system, measured by an autobalance bridge. Although the technique resembles that used by Tausz and Szekely, mentioned earlier, the circuitry was very much more refined to overcome the problem of dielectric breakdown. Residual films of various thicknesses (500 Å to 5,000 Å) were produced for many solutions of fatty acids in sat-

urated hydrocarbons, producing further evidence of chain matching. These films were shown to be chemical in nature as they only formed on metal substrates in the presence of water and/or the metalic oxides and hydroxides. Further proof of these films' existence, and of their chemical nature, was given by electronmicroscopy. Electronmicrophotographs were produced showing reaction product in the form of fibres up to 5,000 Å in length, enmeshed on the oxidised metal substrate. No fibrils were observed on oxide-free substrates, produced by ionic bombardment in vacuo.

1.2.2 Negative Results

Bulkley (36) repeated the work of Barnard and Wilson (16) and of Dover (17) on the flow of polymolecular solutions in capillaries. Prior to the testing, however, he filtered these solutions, and found no evidence of anomolous flow above 4,000 Å. His results do not, therefore, exclude the possibility of residual layers in the order of 1,000 Å thick, although they differ markedly from those of the other workers.

Several workers had produced rather unsystematic results for the adsorption of vapours near saturation onto quartz, glass and platinum surfaces. Thicknesses were reported varying from 3,000 Å to a mere 25 Å. Bowden and Throssel (58) demonstrated that extreme cleanliness was essential for reliable results using electron bombardment and outgassing in vacuo. Their much more thorough technique revealed that not more than two molecular layers of water were adsorbed from the vapour onto gold and platinum substrates. Any thicker films produced, they concluded, were caused by contamination of these surfaces.

Bastow and Bowden (37) repeated the experiments of Hardy (11, 12) with various organic vapours and air, finding no evidence of flotation above 0.4 microns for any medium. In 1935 the same workers studied the flow of water, various organic liquids and ionic solutions radially through a narrow gap between circular glass and stainless steel plates (38). They detected no anomolous viscosity increases for gaps down to 1,000 Å with the exception of ammonium oleate, which is known to have liquid crystal properties. They concluded that those results where thick films were observed must be attributed to the presence of dust and contamination.

In a critical review of the most important research in this field, produced in 1969 by Hayward and Isdale (39), the authors came to the same conclusion as Bastow and Bowden, i.e. 'in those experiments where great care was taken to exclude dust, no anomolous effects were found'. They carried out experiments to prove their point using the experimental technique, devised by Griffiths in 1920 (40), where a ball was lowered through a ring submerged in the test fluid. The precision of their specimens was determined to be such that the diametral clearance was 13,000 $\pm$ 10,000 Å. Not surprisingly, when unfiltered kerosene was used the ball would not pass through the ring. When kerosene plus long chain polymer thickening additives were filtered and used the ball passed through the ring 80% of the time. They did not report any results where solutions of fatty acids in hydrocarbons were tested, which is rather surprising in the light of the positive results of many workers.

1.3 Possible Mechanisms of Thick Film Formation

If the research in the previous section is systematically reviewed the following important points emerge:

(i) Of all the experimental techniques employed few were well suited for measuring residual layers between 500 Å and 5,000 Å to a reasonable degree of accuracy. Those that satisfied this criterion were Deryagin's 'blow off' technique, Smith and Cameron's mercury squeeze-film apparatus and Fuks' falling plate viscometer.

(ii) The techniques employed by Deryagin and Smith and Cameron, unlike that of Fuks, overcome the problems of dust and impurity contamination. The mercury squeeze-film technique also overrides the problem of surface roughness to a large extent.

(iii) None of the workers who produced negative results used either Deryagin's or Smith and Cameron's experimental techniques. In some cases the most prolific thick film forming solutions were not even tested.

It seems reasonable, therefore, to accept the existence of polymolecular boundary layers on the strength of the results of Deryagin, Fuks and Smith and Cameron. It is interesting, however, to note that these workers do not agree on the mechanisms of formation of these thick films.

1.3.1 Chemical Adsorption

The significance of chemical reactions between the various materials present in a boundary lubrication system has been the subject

of much less research than has that of physical interactions. This is almost certainly due to the existence of well tried formulae concerning the thermodynamics of adhesion of molecules at various interfaces. The extensive research carried out on monolayers bears this out. The mechanism of chemisorption, however, remains uncertain on several points. It is in the body of the film, where the mobility, cohesion and adhesion of the reaction product coupled with the mobility and degree of attraction to the interface of the unreacted molecules (fatty acids) that the difference between chemi- and physisorption manifests itself.

The possibility of chemisorption occurring in boundary lubrication has been known for some time. Frewing (41) showed that transition temperatures of friction of mild steel measured on a Bowden-Leben machine occurred at the melting points of hexadecane, diphenylmethane, paraffin wax and several aliphatic alcohols, amides and ketones. In the case of the much more chemically reactive fatty acids, however, the transition temperature was always above the melting point of the acid, approaching that of the metal salt. As the melting point of the pure soap is not exactly known the results are not entirely conclusive. On purely physical considerations, however, the energy of the adsorption of the corresponding acids, amines and alcohols should be very similar. It appeared, therefore, that in the case of the acid some further adsorption process was taking place. Bowden, Gregory and Tabor (42) found similar results to Frewing on different metals (e.g. Cadmium) and interpreted them as indicating chemical reactions were taking place between the fatty acids and metals. Gregory and Spink (43) using a mixed monolayer of stearic acid and calcium

stearate on several substrates found evidence of chemical reaction on copper, but not on platinum. The work of Greenhill (44) supported these results.

The effect of the presence of water and oxygen on the reaction between metals and fatty acids was studied by several workers. These include Prutton, Frey and Turnbull (45), Dennison (46), Tingle (47, 48), Shooter (49), Rowe (50), and Russell et al (51). Their results, obtained by various techniques, showed that the metallic oxide was essential for any chemical reaction between the surface and the fatty acid. Lancaster (52), (53) found that water was necessary for the reaction between these metallic oxides and the fatty acids. The divergence between Lancaster's results and those of Prutton et al is probably due to incomplete drying of the chemicals in the latter's work.

Further evidence from previous research of the necessity of both water and oxygen being present, in some relatively free state, for chemical reaction to occur between metals and fatty acids was reviewed by Smith (14). He went on to establish that stearic acid solutions in hexadecane behaved very differently from equivalent solutions of hexadecylamine on several substrates. He showed that on unreactive substrates, i.e. platinum and gold in atmospheric conditions and steel and chromium in the absence of the oxide layer and water, neither the amine nor the acid produced a residual film. In the presence of the oxide, however, in normal atmospheric conditions the acid produced thick residual films on both chrome and steel, whereas no films were produced by the amines. He then showed that these thick films increased in thickness on both substrates with increasing temperature

until the region where the reaction product could be expected to melt and/or dissolve. Finally he produced electronmicrophotographs of the actual reaction product on a steel substrate. These showed that the films were of a fibrillar nature, similar to grease structures, the fibrils varying from 1,000 Å to 5,000 Å depending on the likelihood of chemical reaction.

These results seem conclusive. It appears reasonable to suppose, therefore, that the thick films reported by Fuks are also chemisorbed, at least where fatty acids and metal surfaces are concerned. In Fuks' apparatus apparently no attempt was made to isolate the test fluids from possible contaminants apart from the actual test surfaces. It is quite possible therefore, that the results produced with the quartz discs are affected by the reaction product (or soap) produced by chemical attack by the fatty acids under test on some metal constituents of the fluid container. No attempt is mentioned to remove either water or oxygen from the test area.

1.3.2 Physical Adsorption

In the majority of cases, those workers who have accepted the existence of polymolecular boundary layers have automatically assumed that they were the result of some form of long range physical force or forces. As this concept is dealt with in more detail in chapter 7.1 and 7.2 only a brief description will be given here.

Since Hardy first postulated that thick films were produced by purely physical interactions (11, 12) several more intricate physical theories have evolved. Many of these, most notably that of Deryagin are reviewed by Akhmatov (54). More recently, Allen and

Drauglis (55) have produced a rather elegant theory concerning the adsorption of stearic acid on an iron oxide substrate where all interactions, apart from the initial monolayer adsorption, are of a purely physical nature.

There is a great deal of experimental evidence for thick films which were either purely or predominantly physical in nature. Much of this work has already been mentioned in section 1.2.1, and consists mainly of the research where chemisorption may be ruled out.

Those results produced where the substrate was of glass or quartz and/or where non-reactive polar molecules were used as lubricant may either be interpreted as evidence of physically formed thick films, or disregarded as being caused by dirt particles. The later work of Deryagin, however, is not so easily discredited (26, 28 to 30). The work of Fuks (31-33) may also, in part, be interpreted as giving evidence of the existence of physically adsorbed thick films, although doubts invoked by his experimental technique have already been mentioned.

The Langmuir-Blodgett technique for the deposition of known numbers of accumulated monolayers has been used by many workers (56, 57, 43, 44) to investigate the lubrication properties of such 'artificial' multilayers deposited on metals. For technical reasons calcium stearate was used to some extent in most of these experiments. The coefficient of friction was reduced to 0.1 by a single layer, but this exhibited little durability. A greater number of layers survived the tests better, and 53 layers apparently survived indefinitely, this being attributed to film repair by superfluous material. Transition temperatures were observed in a number of cases in the

region of the melting point of lubricant film under test, but Frewing (57) found a dependence of this effect upon the number of layers used, presumably due to modified energetics at the surface. The lack of durability of the built-up film was attributed to its lack of adhesion at the surface, a result of its artificial deposition. Bickerman (59) reported that such films do not always follow the surface topology, and may be likened to a net draped over an irregular surface. The durability of the thicker film may then be attributed to the presence of a static reservoir of material from which local breakages may be repaired. On the other hand, the monolayers produced by retraction reported by Zisman et al. (6 - 9) exhibited extremely high resistance to repeated sliding, withstanding pressures as high as 100,000 p.s.i. At the time it was asserted (6) that these results were conclusive evidence that condensed monolayers could account for all boundary lubrication phenomena.

The purely physically attached multilayers obtained with the Langmuir-Blodgett technique must be accepted as evidence of the possibility of such films building up naturally. The degree of adsorption of the initial monolayer was artificially slight and yet the multilayers remained stable. This suggests that on the very strongly adsorbed initial layers revealed by Zisman such physical multilayers would be both more probable and more strongly adhered overall.

1.4 Summary

The ability of solutions of fatty acids in hydrocarbons

to produce thick residual films has been shown to be very probable. The evidence that these films are of a predominantly chemical nature is more impressive than that for purely physically adsorbed multilayers. This is not, however, conclusive proof that physical multilayers do not exist in lubricating systems. The most satisfactory conclusion to be drawn is that both mechanisms coexist to varying degrees in many of the systems. The chemisorbed films produced under the optimum conditions appear to mask the presence of any physical interactions. From this it seems that of the two mechanisms the chemical process produces the more durable thick films.

1.5 Scope of the Research

The initial aim of the work described in this thesis was to investigate some of the mechanical properties of the predominantly chemisorbed thick films produced by solutions of fatty acids in hydrocarbons. The effects of varying the concentration and hydrocarbon chain length of the acids was to be explored.

During this work it became apparent that the technique used was indicating variations in some physical properties of several of the fluids being tested. Not all these fluids produce chemisorbed thick films. The technique was therefore adapted to the purpose of investigating the extent and nature of these variations. Comparatively simple fluids of known molecular structure were used to clarify the processes.

CHAPTER 2

EXPERIMENTAL APPARATUS AND MATERIALS

2.1 Introduction

The advantages of the mercury squeeze film technique, used by Smith and Cameron (1), have been appraised in the previous chapter. The mercury flows around any dust particles in the oil or protruberences of the metal surface so that the residual film detected must be caused solely by the lubricant itself. The equipment used in this research was developed from their ball apparatus, described in this chapter. A system in which the behaviour of thick films undergoing shear could be investigated both electrically and optically is also discussed. The evaluation of a further improvement of the ball apparatus is deferred until chapter 7 where its development becomes clear from the text.

2.2 The Ball Apparatus

Mercury was used to displace an oil film by hydrostatic pressure from the surface of a polished steel ball of 0.25 inch (6.4 mm.) diameter. A copper wire was attached to the ball by a conducting epoxy resin and insulated with a teflon sleeve. This wire passed through a stopper which supported the guard coil surrounding the ball and prevented damage to the oil film caused by contact with the test tube wall. The stopper fitted a test tube containing the reservoir of mercury and, later, the test fluid.

The thickness of the oil film was calculated from the capacitance measured across the mercury-oil film-metal system, as described in section 2.4.1. For this purpose the autobalance bridge was connected

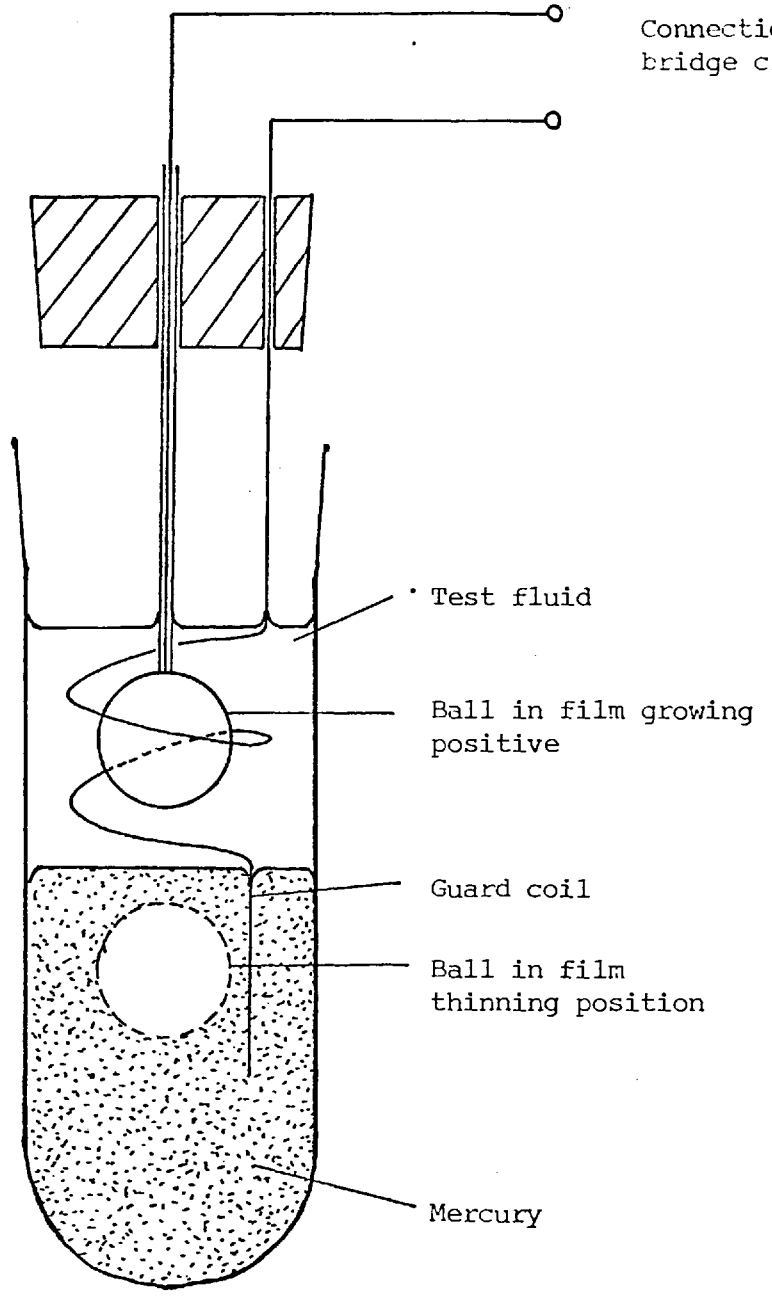


Fig. 2.1 Schematic representation of Ball Apparatus

across the copper wire and the guard coil, which was long enough to be always in contact with the mercury. A schematic representation of this apparatus is shown in fig. 2.1.

2.3 The Shear Apparatus

In this apparatus , which is shown in the photograph, fig. 2.2, the oil film was not only displaced by hydrostatic pressure, but also by the tangential shear created by forcing the mercury past it. A cell was used instead of a ball so that flat chrome surfaces replaced the ball as substrates and capacitor plates. These plates were later made semi-reflecting so that the films could also be observed by optical interferometry whilst undergoing shear. This cell and the mercury flow system are described in detail below.

2.3.1 The Cell

A diagrammatic representation of a typical cell is shown in fig. 2.3a. The capacitor plates where the oil film thicknesses were measured form the heart of a cell. These conducting chromium layers were vacuum deposited onto the surface of a microscope slide. Several variations in shape and number of the plates were experimented with in the early work. The most satisfactory arrangement was that shown in fig. 2.3b with three square plates each of one cm^2. (10^{-4} m^2.) area, which was used in all the later research. The optimum thickness of these layers giving both good conductivity and reasonable interference fringes is discussed later in section 2.5.2. Insulated copper wires were attached to the ends of the narrow chromium connection strips using the conducting epoxy resin.

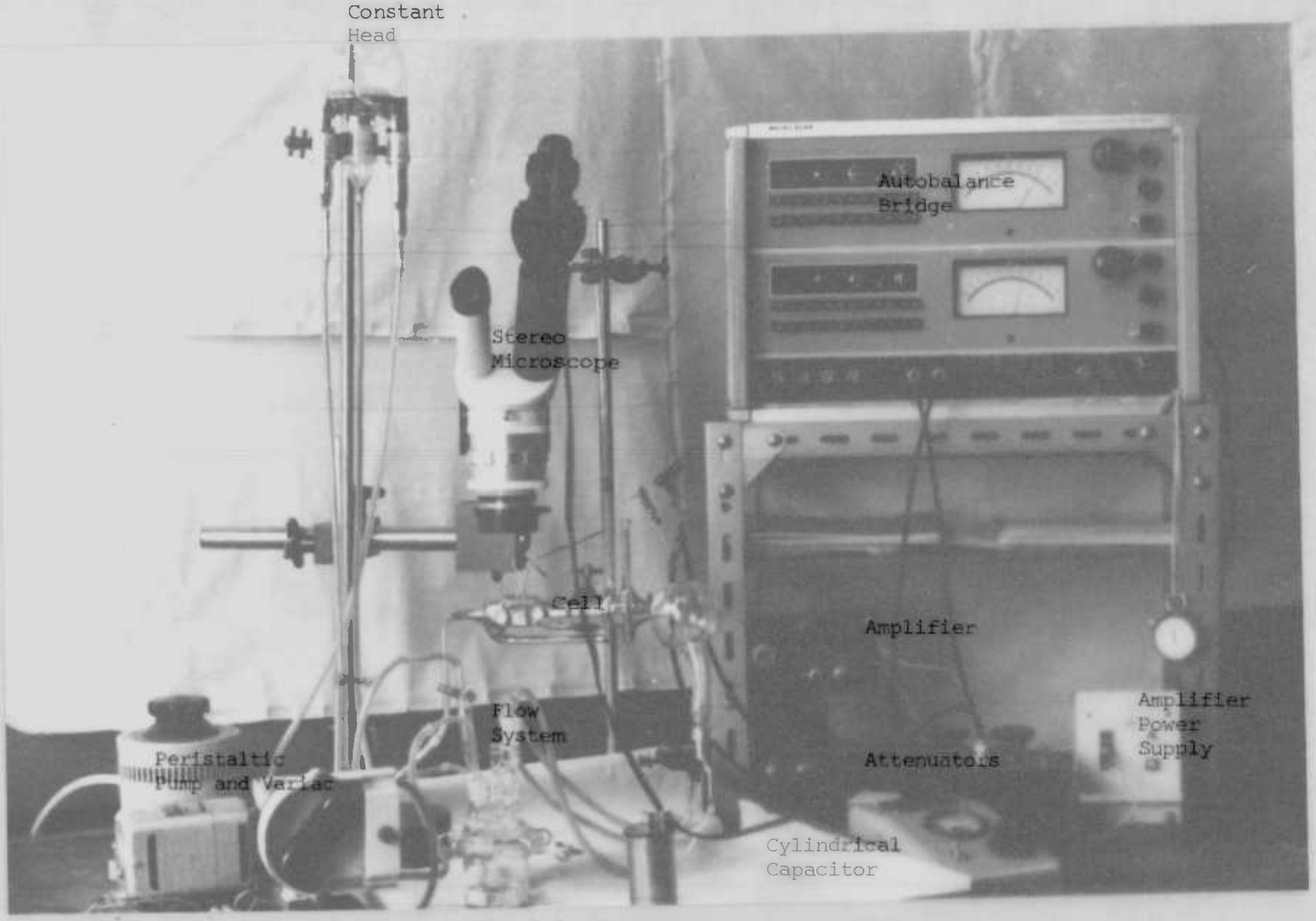


Fig. 2.2 General view of apparatus

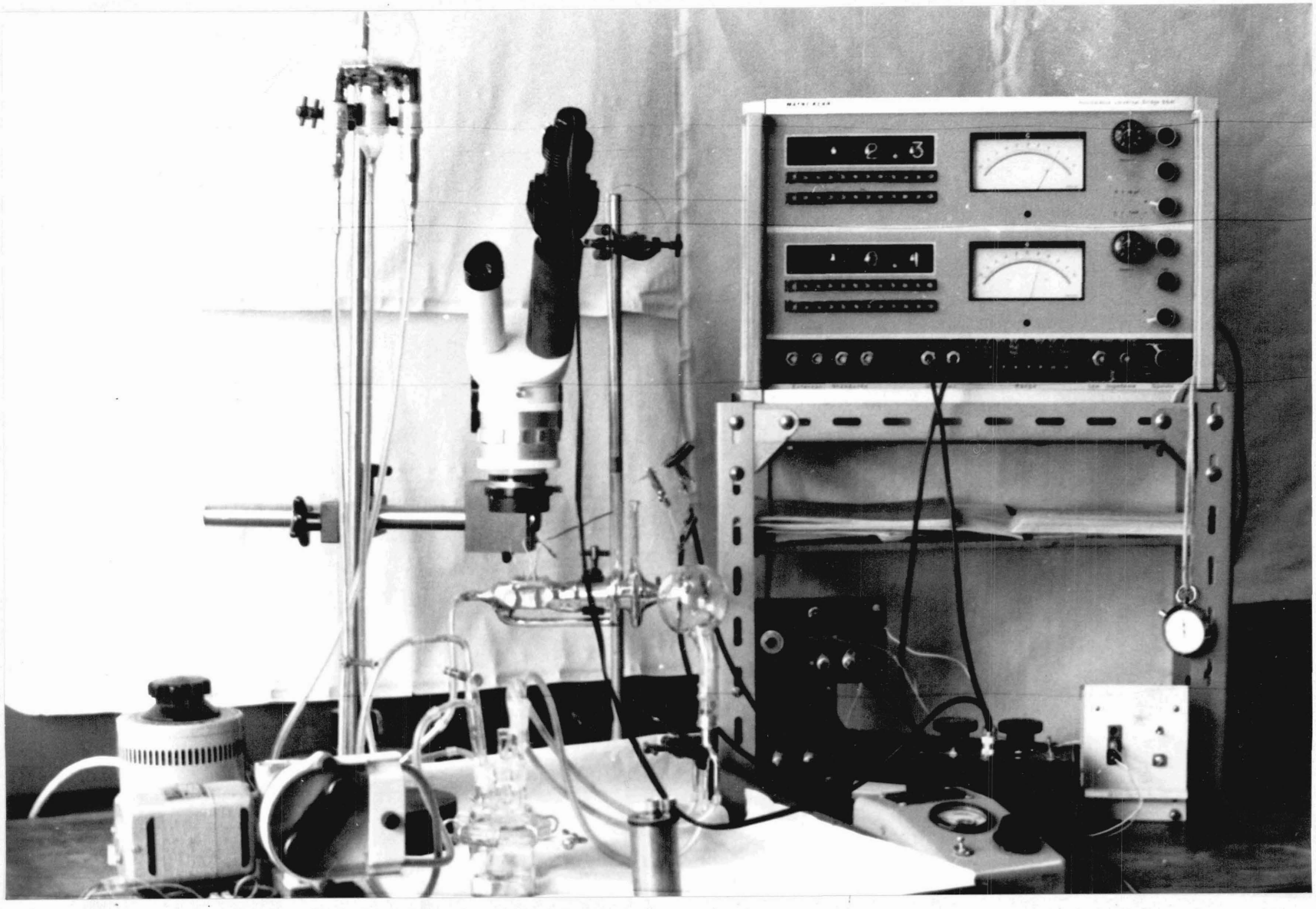


Fig. 2.2 General view of apparatus

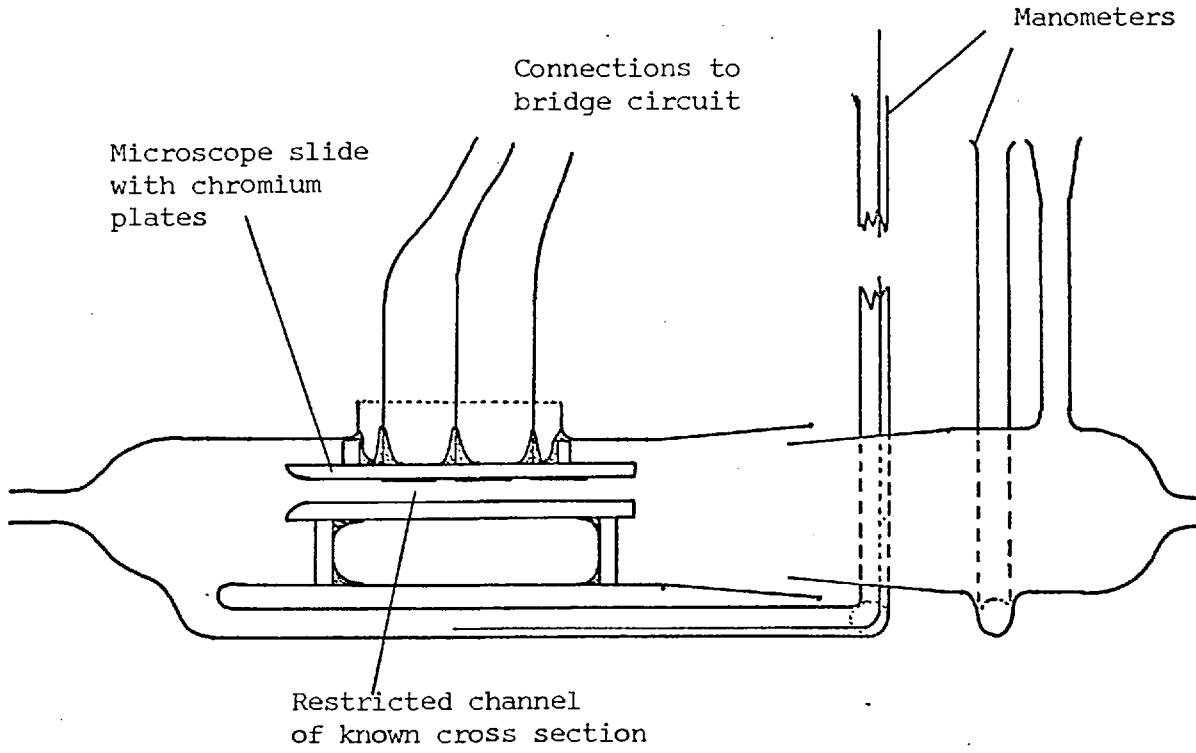


Fig. 2.3a Cell Apparatus

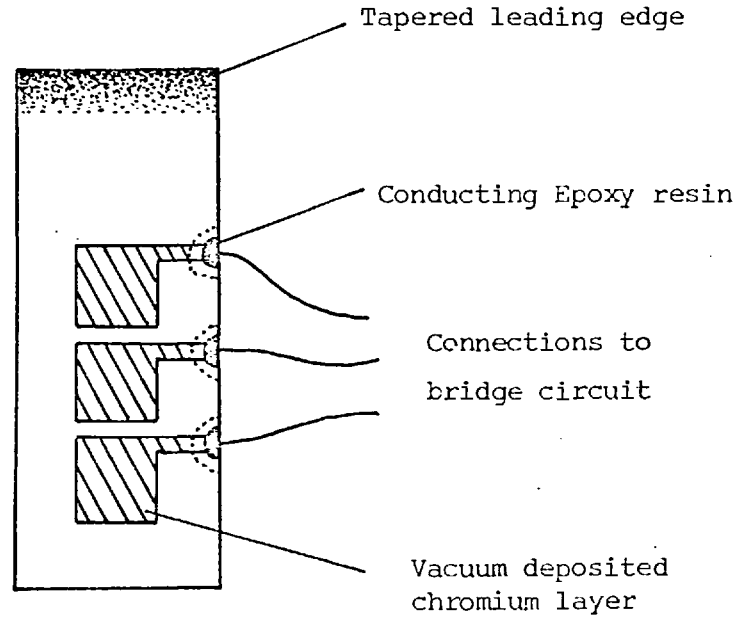


Fig. 2.3b. Capacitor Plates

The microscope slide needed to be incorporated into a channel through which the mercury should flow. Its cross section was an important factor in the magnitude of the shear imparted on the oil film by the motion of the mercury. In the earlier cells this channel was formed by placing the slide over an indentation cut in a block of P.T.F.E. having the same length as the slide. The indentation was 1.2 cm. (1.2×10^{-2} m.) wide and of varying depth for each cell. The sides and bottom were polished and the inlet region tapered to reduce the possibility of turbulence. The microscope slide was fixed with the chromium capacitor plates facing inwards such that one of the indentation walls came between these plates and the connecting wire junctions. An epoxy resin was applied to the outer edge of the P.T.F.E. wall-microscope slide junctions to seal the unit. In later cells, when the channel depth required was much smaller, a second microscope slide was used in place of the P.T.F.E. The separation of the slides was determined by two narrow strips of glass which were positioned similarly to the P.T.F.E. walls. Again, the inlet region was tapered and the unit was sealed on the outer edges using an epoxy resin. In both cases the danger of contamination of the oil under test was reduced to a minimum as the inner walls of the channel consisted only of glass, the chromium capacitor plates, and sometimes P.T.F.E..

This completed section was placed in the glass cell casing under the 'window' through which the connecting wires were drawn. It was secured and made flush with the casing using epoxy resin which also served to insulate the join of the connecting wires to the narrow chromium strips.

The cell casing was made of glass to facilitate cleaning.

The glass proved very useful during experiments in the detection and rectification of minor problems, e.g. trapped air bubbles; the presence of dirt particles, etc. Once a satisfactory design for this casing had been proved and tested experimentally a carbon mould was built so that similar casings could be quickly produced by a glass-blower.

The 'window' in the casing was necessary to facilitate the interferometric study of the oil films which could be observed directly through the semi-transparent chromium capacitor plates. There were three vertical glass tubes, one in the actual cell and two in the fitting cone. Two were used as manometers at either end of the channel so that the pressure drop across it could be measured. This was used in the calculation of the shear applied to the oil film. The third tube was used to introduce the test oil. The manometer tube in the cell contained a wire which acted as a connection for the mercury to the bridge circuit.

2.3.2 The Mercury Flow System

This consisted of five basic parts, see fig. 2.4, of which the cell section has already been described.

A peristaltic pump drove the mercury through the circuit. The mercury was simply forced around by the compression of the silicone tubing by the rotor, so there was no risk of contamination. The pump motor speed was controlled by a variable transformer. The mercury was pumped up to a constant head device where the intermittant flow of the pump was smoothered. The flow of mercury from this constant head into the cell was regulated by a screw clip on the tubing. After

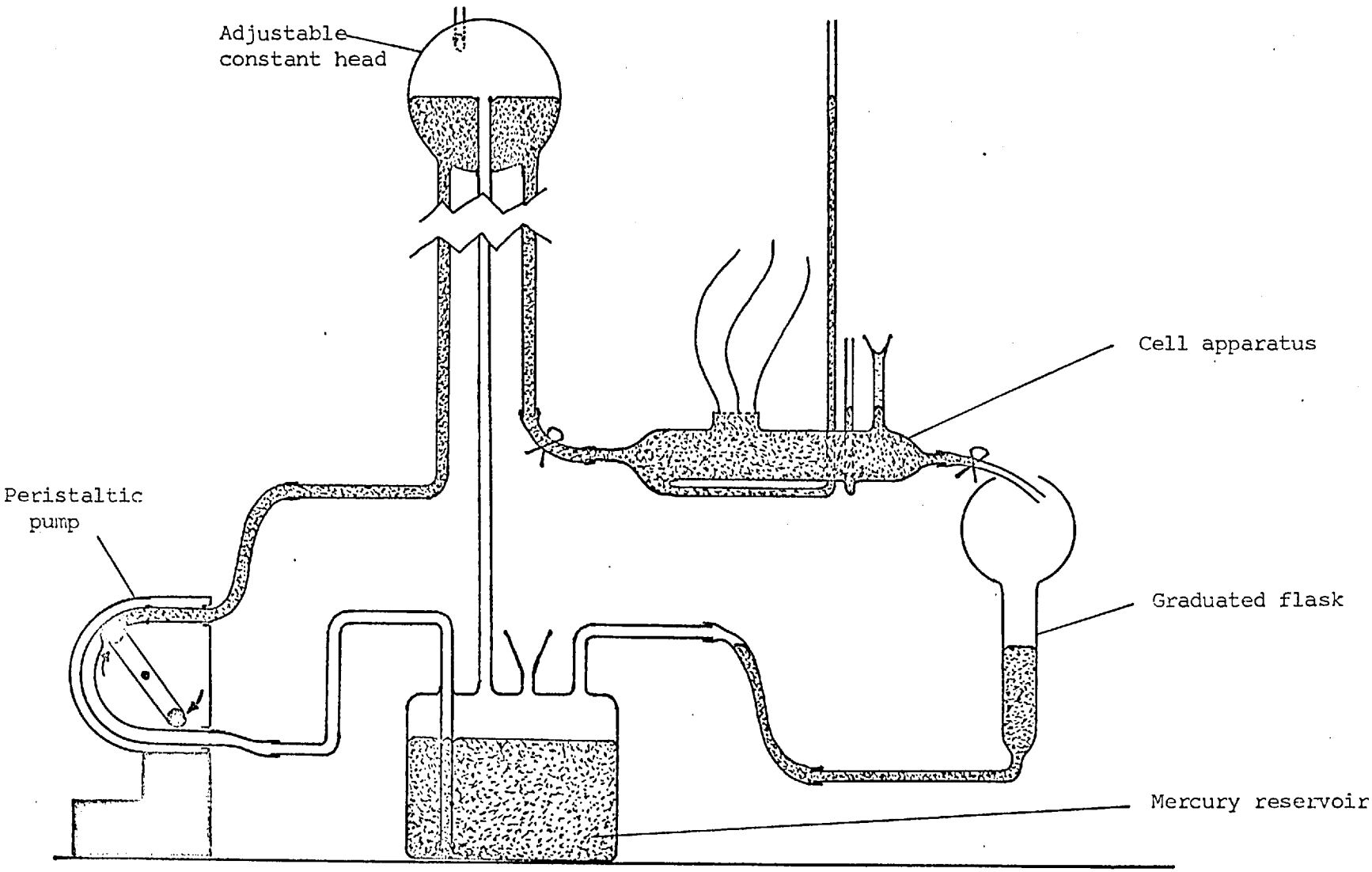


Fig. 2.4 Schematic Representation of Mercury Flow System

passing through the cell the mercury poured into a spherical container with an outlet stem which was graduated in cubic centimeters. This flow was used initially to calculate the shear applied in the cell. The mercury then emptied into the reservoir which also took the overflow from the constant head. The pump sucked the mercury from the very bottom of this reservoir so that any substantial amount of the test fluid carried this far from the cell was trapped, due to the greater density of mercury. The spherical container and constant head device acted as test fluid traps in a similar way, so there was little likelihood of oil being recirculated back to the cell.

These sections were all of glass and came apart into smaller units for easy and thorough cleaning and replacement when necessary. The sections were linked by the same silicone tubing used in the pump. This simplified the movement of the constant head device for variation of the shear and enabled, with the use of screw clips, the flow to be varied or stopped wherever necessary. The tubing was semi-transparent and easy to clean. It was tested for adsoprtion and possible contamination as described later (section 2.6.2). No contamination was found.

2.3.3 Calculation of Shear

In the early experiments when comparatively low shear was applied it was calculated from the flow rate through the cell. This rate was measured in the graduated flask described earlier. The equation used was simply that for fully developed non turbulent or laminar flow in a channel with parallel walls, i.e.

$$\tau = 6\eta q/h_c^2 \qquad (2.1)$$

where q = rate of flow of mercury

η = absolute viscosity of mercury

h_c = separation of channel walls

and τ = shear applied at the walls.

The assumption of non-turbulent flow was justified by calculation of the Reynolds Number for the variety of channel separations and maximum fluid velocities used. In this early work the value never exceeded 800.

Once it was realised that the resistance to shear of the residual films was much greater than initial results had indicated, the rate of flow was increased and the cell minimum cross-section reduced to achieve larger tangential shear. Measurement of the rate of flow became much less accurate, so the pressure drop exhibited by the two manometers was used to calculate the shear. Again, laminar flow was assumed and the same equation translated in terms of pressure used to calculate the shear, i.e.

$$\tau = \tfrac{1}{2} h_c \frac{dp}{dx} \qquad (2.2)$$

$\frac{dp}{dx}$ was initially taken as $\frac{\Delta p}{L}$

where Δp was the pressure drop across the cell

and L was the length of the restricted channel.

The Reynolds Number calculated for the maximum flow in the cells with channel depth of 0.25 mm. (2.5×10^{-4} metres) now approached 2,000. The possibility of turbulent flow was considered therefore, and is discussed in Appendix A.

Also, the magnitude of the entry length, i.e. the distance from the beginning of the channel to the point where a fully developed parabolic velocity profile is achieved, was calculated. This entry

length, L', was given by the equation:

$$L' = 0.029\ R_e \times h_c \qquad (2.3)$$

where R_e is the Reynolds Number.

This equation has repeatedly been shown to be in good agreement with experimental results. Substituting the value for h_c and a value of 2,000 for R_e gives:

$$L' = 1.0 \text{ cm. to } 1.3 \text{ cm.}$$

The cells were therefore built such that the first capacitor plate was positioned at least 4 cm. from the beginning of the restricted channel. The comparative shortness of the entry length made the assumption that $\frac{dp}{dx} = \frac{\Delta p}{L}$ a good approximation as long as laminar flow persisted.

2.4 Electrical Instrumentation

2.4.1 Circuitry

The basic method of measuring the thickness of the oil films in all these experiments was to measure the capacitance of the system. From this capacitance, the film thickness was calculated, using the formula

$$h = \frac{\varepsilon' \varepsilon_o A}{C} \qquad (2.4)$$

where A is the area of the metal capacitor plate

ε' is the relative permittivity of the dielectric material, i.e. the test fluid

ε_o is the rationalised permittivity of free space

h is the oil film thickness.

The values of ε' of all the test fluids used were measured

in a simple apparatus of known separation at the operating frequency of 1 kHz. Using this expression the variation of the thickness of the test fluid with time could be tabulated, both for the thinning of the fluid under the hydrostatic pressure of the mercury and for the thinning of the fluid as shear was applied by pumping the mercury past it.

The basis of the electrical system used for these capacitance measurements was a Wayne-Kerr Autobalance Universal Bridge, type B641. This bridge operates on the transformer ratio arm principle (2) and, presents to the test capacitor, over the capacitance range met in these experiments, a peak voltage of 40 mVolts. Such a voltage is sufficient to cause dielectric breakdown of all the fluids used in this work at the very low film thicknesses encountered. Smith devised a system to overcome this same problem and a detailed account of the circuitry and specification of his apparatus is given in his Ph.D. thesis (3).

A replica of this electrical system, with the exception of the Autobalance bridge, was used in this research. The voltage applied to the oil film was reduced by inserting an attenuator between the E terminals of the bridge and the capacitor, and an amplifier between the capacitor and the bridge's I terminals. Figures 2.5a and 2.5b are much simplified circuit diagrams of the unmodified and modified bridge circuits respectively. The original bridge applies a voltage V_x to the unknown admittance, through which current i_x is passed. Adjusting the standards G_s and B_s brings i_s into balance with i_x, where G_s and B_s respectively represent a set of shunt connected conductance and capacitance standards.

By inserting the attenuator R_1 and R_2 the voltage across

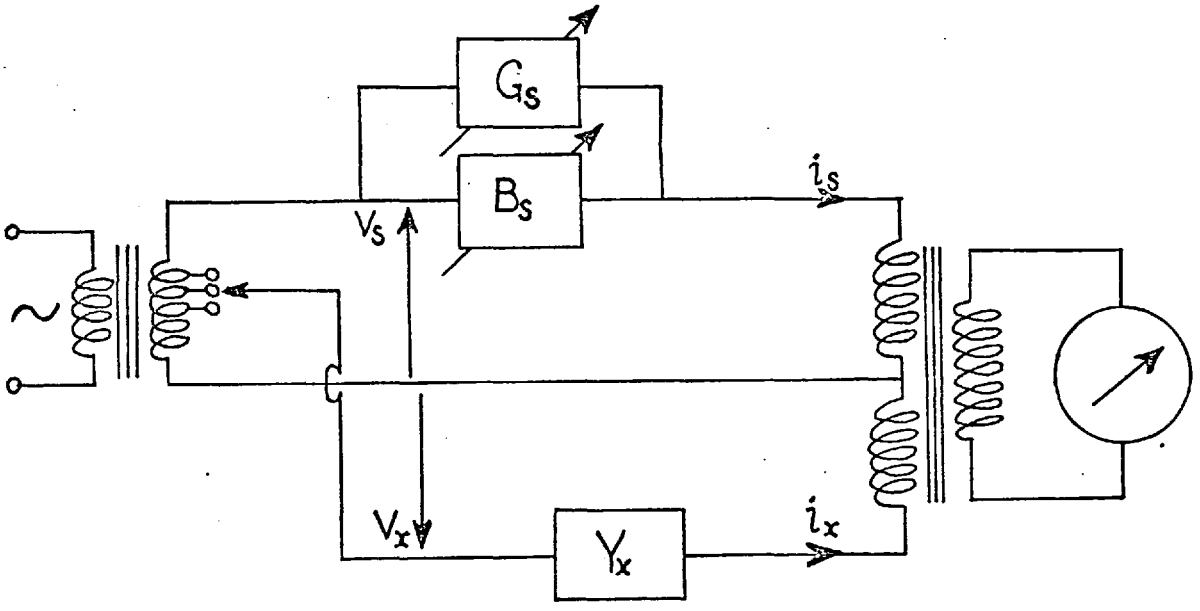


Fig. 2.5a Unmodified Circuit Diagram

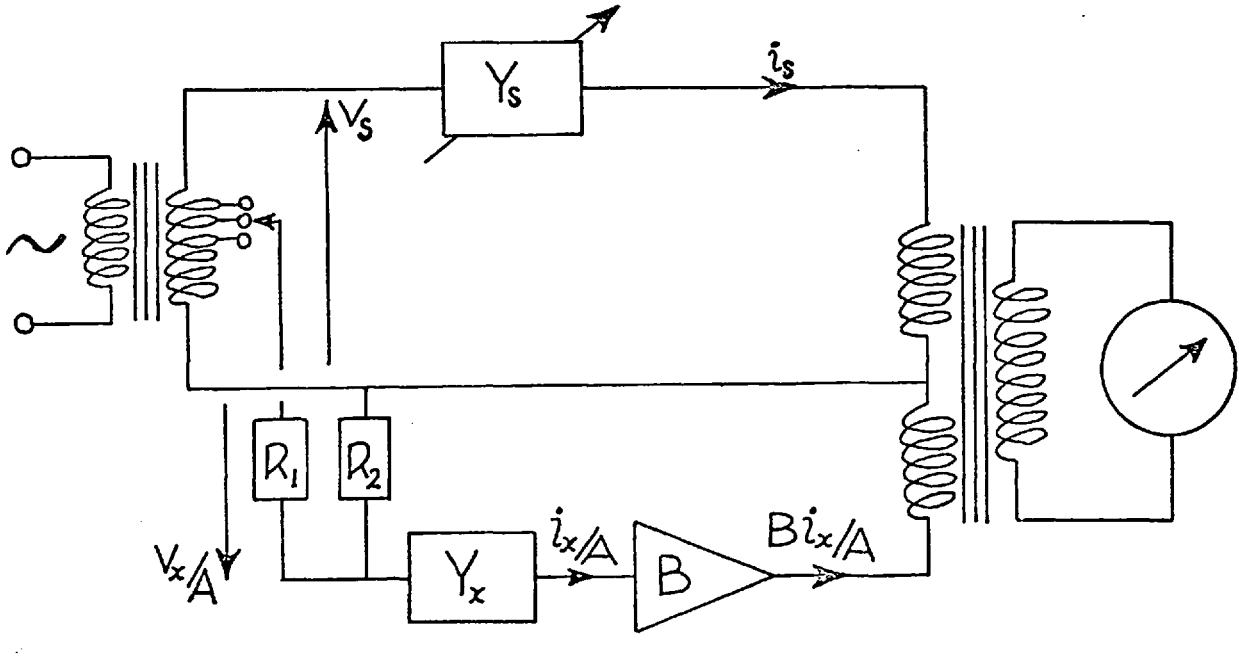


Fig. 2.5b Modified Circuit Diagram

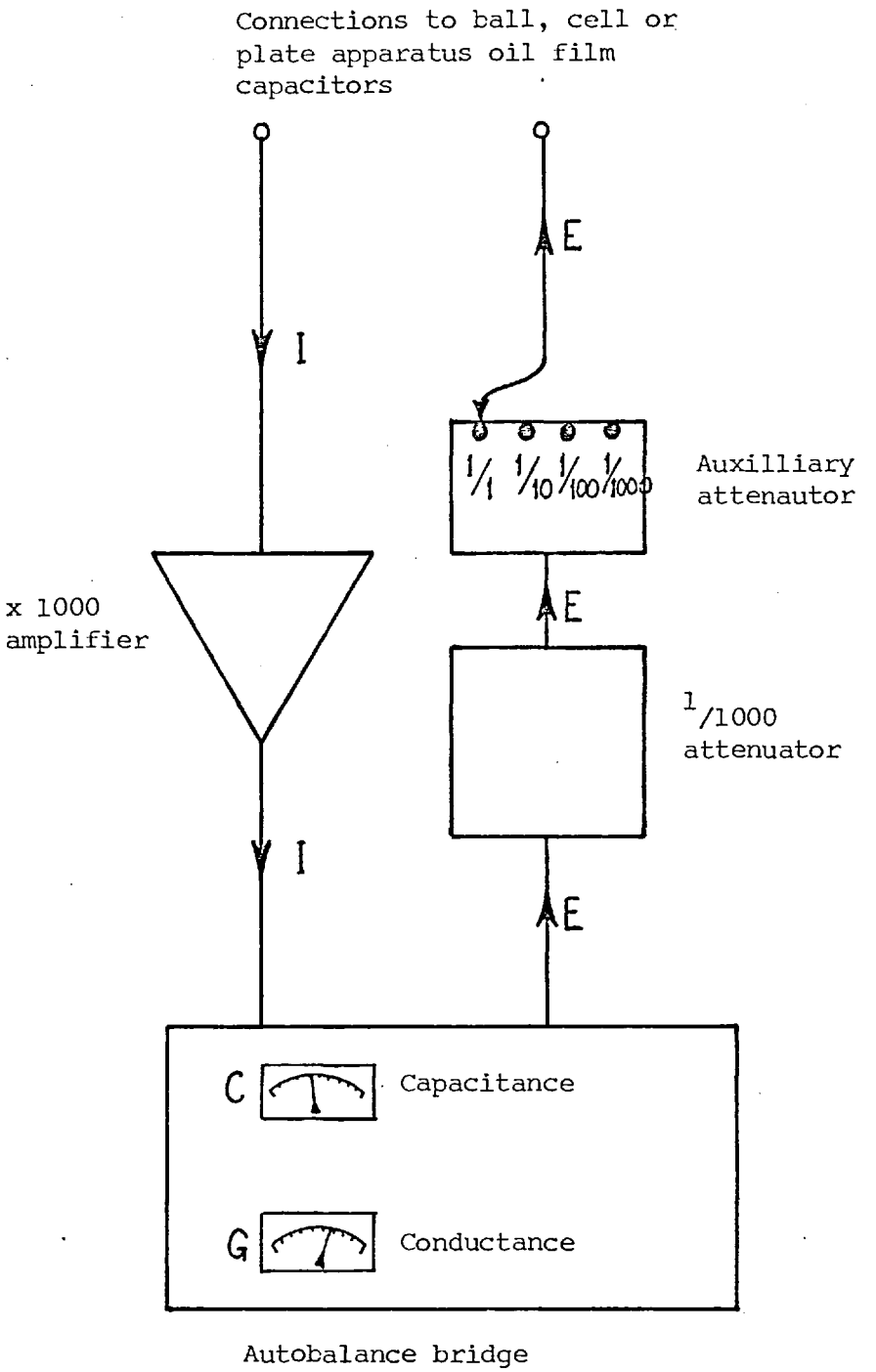


Fig. 2.6 Schematic representation of electrical circuitry used with shear, ball and plate apparatus

Y_x is reduced to V_x/A. The resulting current i_x/A is boosted by the amplifier to give the output current $i_x B/A$. By setting B equal to A, the bridge can be used in the same way as before modification.

In practice A and B were each set at 1,000, thereby reducing the peak voltage applied to the oil film to 40μV. This voltage was sufficiently small to avoid dielectric breakdown of most oil films even below 50 nm. (500 Å) as long as bulk electrical properties were retained. During the experimental work, an extra variable attenuator, able to reduce the voltage by factors of 10, 100 and 1,000 was built, so that films below 500 Å could be measured. This attenuator was inserted in the circuit in series with the other. It was switched into the circuit whenever a large value of capacitance or conductance caused saturation in the amplifier. Its use was limited by electrical noise interfering with the bridge readings, especially for lower values of capacitance. The complete system, as shown in fig. 2.6 was calibrated to give capacitance measurements of an accuracy of ± 2% for low conductance.

2.4.2 Calibration

The importance of evaluating the capacitance readings in the light of the corresponding conductance values in this research is discussed later in this thesis. The validity and accuracy of any capacitance readings could be checked by referring to the calibration curves shown in fig. 2.7. These were obtained by measuring the capacitance and conductance of a series of combinations of capacitors and resistors using the unmodified bridge which has an accuracy of 0.1%. These

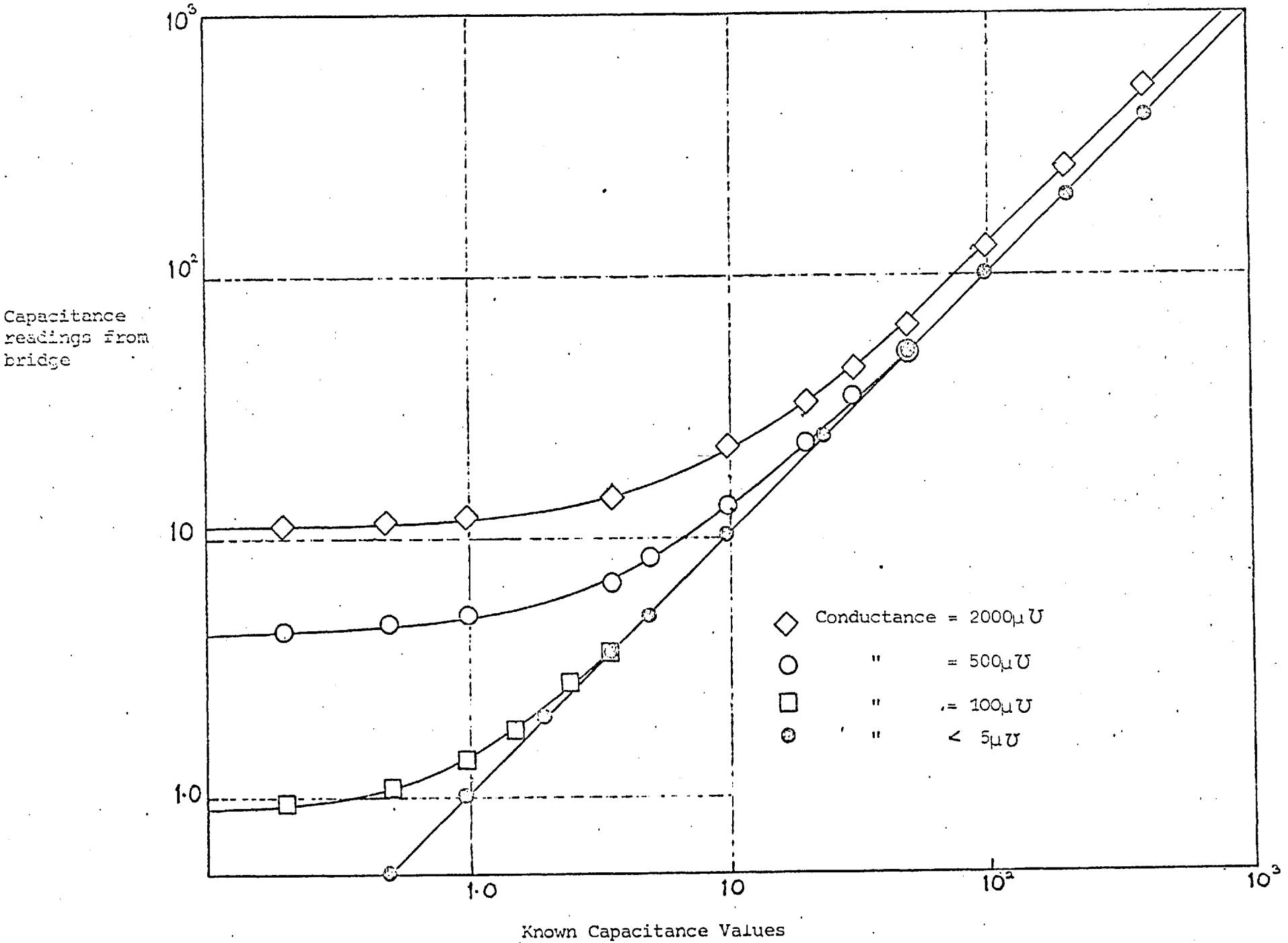


Fig. 2.7 Calibration of Capacitance Readings for 1000 x Amplifier

accurate values were plotted against the corresponding values measured in the modified bridge circuit for the 1/1000 attenuator, the extra attenuator being used whenever necessary. The attenuation and phase controls were adjusted initially to give agreement between the two readings of a middle range value capacitor with the bridge set for calibration.

The curves show that, for low conductance, accurate calibration, within the linear region, was possible over a wide range of capacitance readings, with a single setting of gain and phase. As the conductance increased, however, the capacitance values become artificially enlarged producing a high degree of inaccuracy for very low capacitances. The higher values of capacitance, however, were only seriously affected when the conductance was in the mU range, and even then the inaccuracy was below 20% the values always being too large. As the high capacitance region corresponds to the low film thickness values (< 2,000 Å) which were of most interest, the size and bias of these inaccuracies were seen to be very important. Additional, on the spot calibrations were carried out, therefore, whenever the conductance rose above 500 μU , and it is thought that in nearly every case the inaccuracies were kept well below the 20% value mentioned. Nevertheless, the error bars included in later results were estimated from the calibration curves of fig. 2.7, giving their maximum possible range.

2.5 Optical Interferometric System

Since the initial work of Cameron and Gohar (4) optical interferometry has developed into a versatile tool in lubrication research.

In this work a system which could measure oil film thicknesses from 10,000 Å down to the optical minimum of about 2,000 Å was needed. Other important requirements were a high sensitivity to small variations in film thickness, and a relatively large field of view. With these factors in mind a chromatic or 'white light' interferometric technique was adopted. Detailed discussions of the principles of optical interference utilised here are to be found in most optical text books, e.g. (5), (6).

2.5.1 Choice of 'White Light' System

In the case of monochromatic light of wavelength λ, that part of the beam reflected from the semi-reflecting chrome layers will be reinforced by the part reflected from the mercury surface if their path difference is some integral multiple of λ, This results in a bright fringe. Similarly, they will interfere destructively, producing a dark fringe, when the path difference is $(N+\frac{1}{2})\lambda$ where N is an integer. The white light spectrum consists of an infinite number of individual colours, each having a corresponding wavelength to which the above interference process applies. The overall effect, therefore, is a pattern of bright, differently coloured fringes, all the dark regions being obscured by bright fringes of different wavelength, except where the film thickness falls below the optical minimum of about 2,000 Å.

Several of the more distinct colours are chosen in this work. They have a fixed sequence which repeats itself as the path difference is increased, each repetition corresponding to a unit increase in the integer N, i.e. the 'order' of interference. The ad-

vantage of this is that a whole range of coloured fringes will cover a change in film thickness of around 3,000 Å, whereas monochromatic light would produce just the one fringe, i.e. the white light system is far more sensitive to small film thickness variations.

2.5.2 Reflecting Surfaces

The choice of chromatic light necessitates the use of two-beam interferometry as opposed to a multiple-beam method which, in this case, would add together so many beams of such a wide range of wavelengths that white light would be reformed. This dictates that, ideally, the reflecting surfaces should form two beams of similar intensity as they recombine and that any further reflections should be negligible.

The totally reflecting surface, in all cases, consisted of mercury, its actual reflectivity in oils being ~ 60%. The production of equal amplitude beams was, therefore, dependent on the nature of the semi-reflecting chrome capacitor plates. The thickness of these chromium layers could be regulated very accurately and therefore the required reflectivity achieved. In an ideal system the optimum thickness is 200 Å, giving a reflectivity of 18% and an absorptivity of 25%. If the beam incident in the glass is considered to have an amplitude of 100% then the two reflected beams will have 18% amplitudes, and further reflections will be less than 2%. In this apparatus, however, a further consideration in the thickness of the chromium layers was that their resistance should be no more than ~200 ohms, otherwise the capacitance readings would be seriously affected. This added constraint resulted in thicker layers each with a workable reflectivity of ~50% and ab-

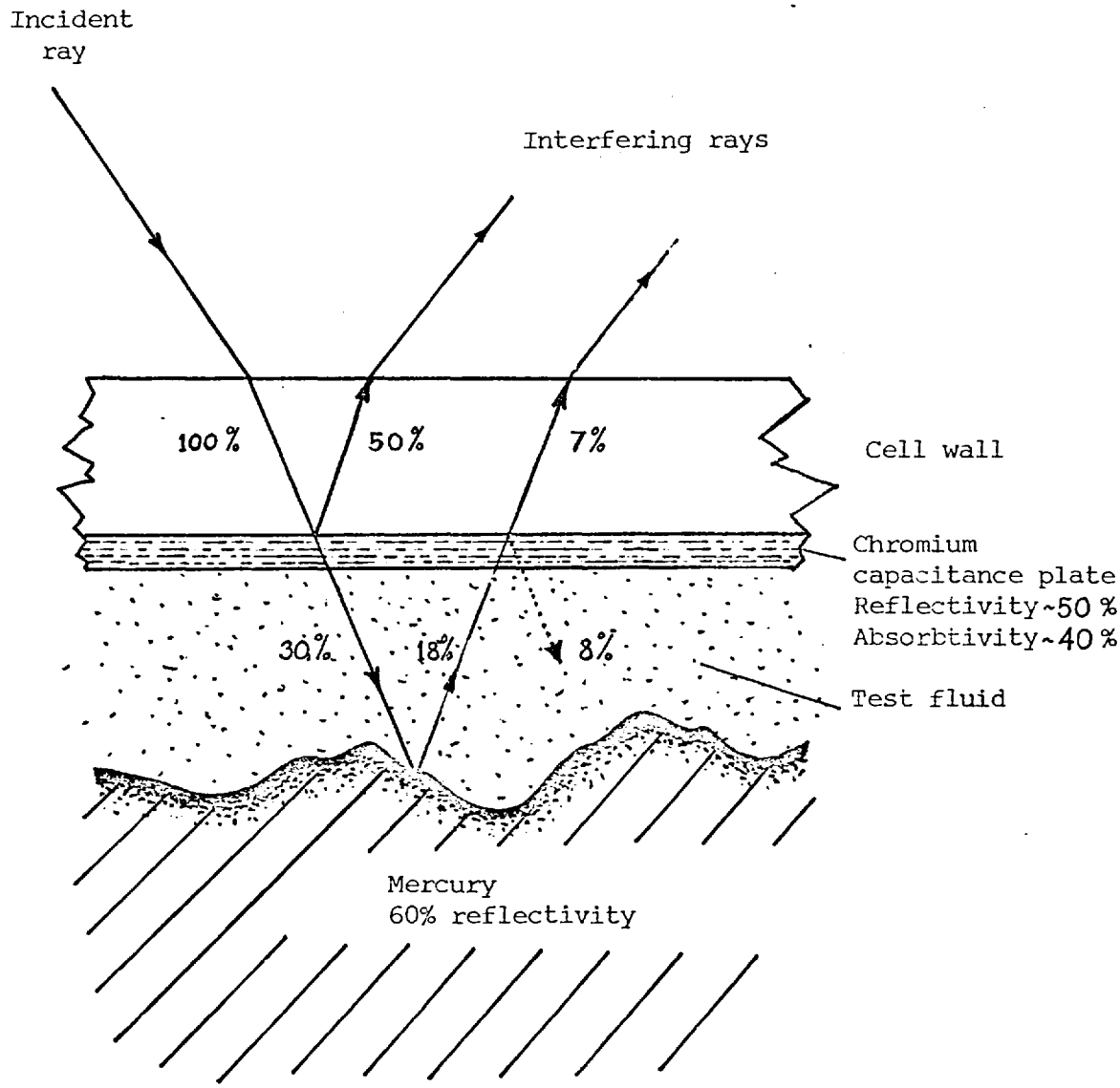


Fig. 2.8 Schematic representation of interferometric system

sorption of ~40% (see fig. 2.8). The interference fringe patterns produced were, therefore, superimposed on a very much brighter white background, making them faint and difficult to resolve. It must be stressed however that this in no way reduced the sensitivity of the system, but only caused the images produced to be very tiring to the eyes.

The most serious consequence of this, was that no satisfactory photographs of the interference patterns could be obtained. Although this was mainly due to the comparative faintness of the fringe colours superimposed on the bright white background the small size of the interference patterns accentuated the problem. The maximum magnification obtainable was x 160 and, as the features under observation were, at the most, between 10^{-3} and 10^{-4} cm. across, they remained very small in the field of view. For the patterns to be satisfactorily shown, therefore, the photographs had to be enlarged. This destroyed the already poor fringe definition on the photographs and also reduced the colour intensity even further. To overcome this deficiency diagrams made up of 'colour contours' taken direct from the field of view of the microscope are used in chapter 4.

2.5.3 Collimation

In general, the more closely collimated the light used the better defined are the interference patterns and the greater are the numbers of ordersof interference visible. The degree of collimation is a measure of how parallel a beam is.

To produce the required beam of collimated white light a stereoscopic microscope was used. Basically this microscope is a

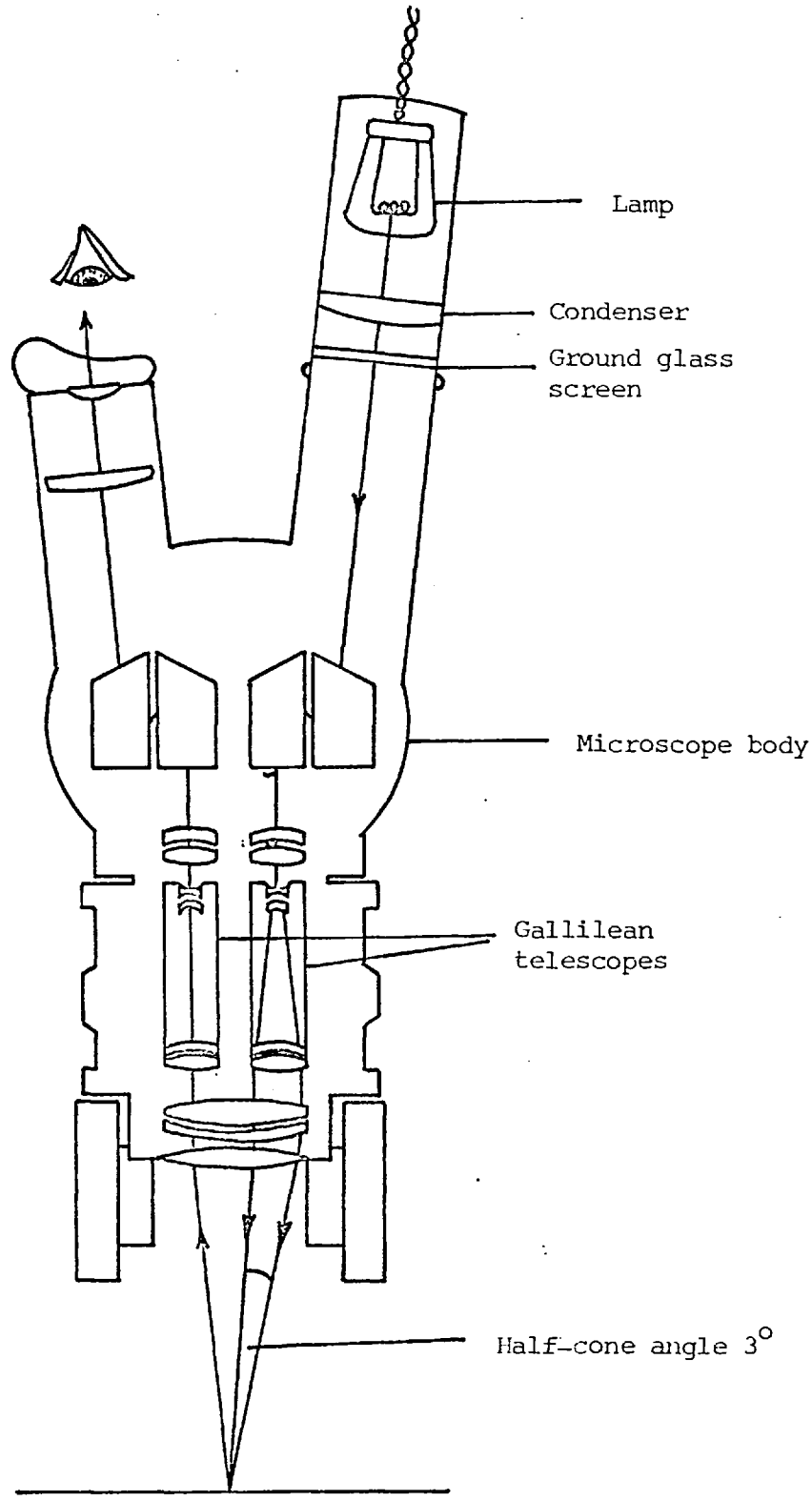


Fig. 2.9 Stereo Microscope showing illumination and collimation system

larger version of an ordinary one except that the need for an excessively long optical tube is eliminated by the use of a pair of Gallilean telescopes, see fig. 2.9. Light entering the objective from the viewing plane is formed into a wide parallel beam which passes into the two telescopes. Two narrow, parallel beams emerge and are observed at the eyepieces. If one of the eyepieces is removed and approximately parallel light is shone down the empty branch then, as the incident beam will traverse the reverse path, it will eventually focus at the viewing plane. The degree of collimation therefore depends mainly on the angle subtended at the viewing plane by the telescope aperture of width 1×10^{-2} metres and is approximately 6^{o}, resulting in an acceptable half-cone angle of approximately 3^{o}.

Other important qualities of this microscope, as a result of its overall larger properties, are a relatively large field of view and a long working distance (9.1 cms. for a 80x magnification).

2.5.4 Optical Calibration

There are two reasons why it is not possible to calculate film thickness from the optical expression:

$$\text{optical thickness} = \tfrac{1}{2} \times \text{path difference}$$

$$= \tfrac{1}{2} (N\lambda + \beta\lambda/2\pi).$$

Firstly, the use of chromatic light means no specific value of λ can be taken - the choice depends entirely on the observer. Secondly, the value of β, an anomolous phase change of the light resulting from reflections at the metal surfaces, is difficult to ascertain. Consequently the only accurate method of determining the film thicknesses must involve calibrating the interference colours chosen against some exactly known thicknesses.

An extremely accurate technique of this kind is described by Gentle (7). This method uses the precise Hertz's equation for the deformation of a loaded ball on plate contact, and eliminates the inaccuracies inherent in the simple Newton's rings measurements for a lens lightly touching a mirror. The separation of the surfaces in air outside the contact region, therefore, is precisely known at any radius from the centre of the contact and can be accurately compared with the corresponding diameter of each colour fringe. The use of this

Table 2.1 Optical Calibration

Fringe Order	Fringe Colour	Optical thickness in Angstroms (10^{-10} metres)
First	yellow	2,000 Å
	red	2,750 Å
	blue	3,400 Å
	green	4,250 Å
Second	yellow	4,700 Å
	red	5,600 Å
	blue	6,150 Å
	green	6,200 Å
Third	yellow	7,600 Å
	red	8,600 Å
	blue	9,000 Å
	green	9,600 Å

technique here involves the assumption that the phase change produced by reflection at the surface of a steel ball is very similar to that for mercury. The nature of the two metals makes this a reasonable assumption. The calibration produced is shown in table 2.1.

As the refractive index of air is virtually unity the optical and actual thicknesses correspond. The calibration of table 2.1, however, when applied to the test fluids must be used in conjunction with the expression:

Optical Thickness = Actual Thickness x Fluid Refractive Index.

The bulk refractive indices of the solutions were measured in an Abbe Refractometer.

2.6 Cleaning Techniques and Specification of Materials

The nature of this research makes both the cleanliness of the apparatus and the purity of the chemicals tested of prime importance.

2.6.1 Cleaning

As already mentioned, much of the apparatus used was made of glass. These sections were cleaned using hot chromic acid plus distilled water solutions. After a period of immersion of between five and ten minutes each part was thoroughly rinsed with distilled water followed by acetone and finally dried over a heating element.

Not all the apparatus was so easily cleaned, however, because of damage caused by the heat, chemical attack by the chromic acid, or both. These pieces, i.e. the cells, the silicone tubing, the ball apparatus and, later, the plate apparatus, were usually cleaned in an ultrasonic agitation bath. More rarely, however, the ball and the plate apparatus

were cleaned in an ionic bombardment device because of the resulting extreme cleanliness of their surfaces.

(a) The Ultrasonic Agitation Bath (wet cleaning process)

This involved several immersions of the apparatus in various solvents. First each piece was agitated for ten to fifteen minutes in an alkaline detergent solution (Ardrox 1618), then rinsed thoroughly in tap water followed by distilled water. This was followed by further agitation for a similar period in an emulsifier solution containing tetrachloro-perfluoro-ethane (Imperial Smelters Isceon 1135), and more thorough rinsing. The apparatus was then agitated for ten minutes in distilled water and rinsed in acetone. A final ten minute period of agitation in analar acetone followed, the pieces then being dried over a warm heating element.

The cell, ball apparatus and plate apparatus were always the last sections to be cleaned in their respective experiments. Once they were dry they were immediately used so that contamination of the metal surfaces by atmospheric impurities was reduced to a minimum. The silicone tubing was cleaned as described above with the periods of agitation reduced to five minutes in all solvents to prevent any substantial absorption of them by the silicone. It was also allowed a sixty minute final drying period. Over a period of several days the walls of the tubing could be seen to be discoloured by the mercury. Because of this new tubing was used for each experiment.

This cleaning process reliably yielded surfaces which could be completely wetted by distilled water. It could not, however, remove the oxide layer present on the metal substrates, nor would it prevent an

absorbed layer of water from remaining on these surfaces. Therefore it was designated the wet cleaning process. In later experiments surfaces free of both the oxide and water layers were required. A cleaning process capable of producing such 'dry' surfaces, the ionic bombardment technique, was used on these occasions.

(b) The Ionic Bombardment Apparatus (dry cleaning process)

Only the ball and plate apparatus were cleaned in this apparatus. The cleaning technique depends on the bombardment of the metal surface by medium energy ions and electrons in an evacuated chamber. By control of the ambient pressure and the potential across the discharge path it is possible to create a plasma in which the particles have enough energy to remove any absorbed and chemisorbed films from the surface. This process is also capable of eroding the metal surfaces (sputtering) and care was taken, therefore, not to damage the substrates. The optimum time for cleaning without damage was found to be approximately 25 to 30 seconds at the voltage used. Ideally, the clean surface should be immersed in the test fluid before air is allowed into the vacuum system. Smith (3) showed that as long as the period of exposure of the substrate to atmospheric oxygen and water vapour prior to immersion in the test fluid was kept short, i.e. of the order of 20 seconds, it was not a critical factor. The results discussed later in this thesis substantiate this.

Basically the apparatus consisted of a two stage, all glass system pumping out a small glass discharge chamber. The chamber was energised from a variable high voltage transformer capable of supplying 50 mA. at 5kV., see fig. 2.10.. A major feature in the design of this

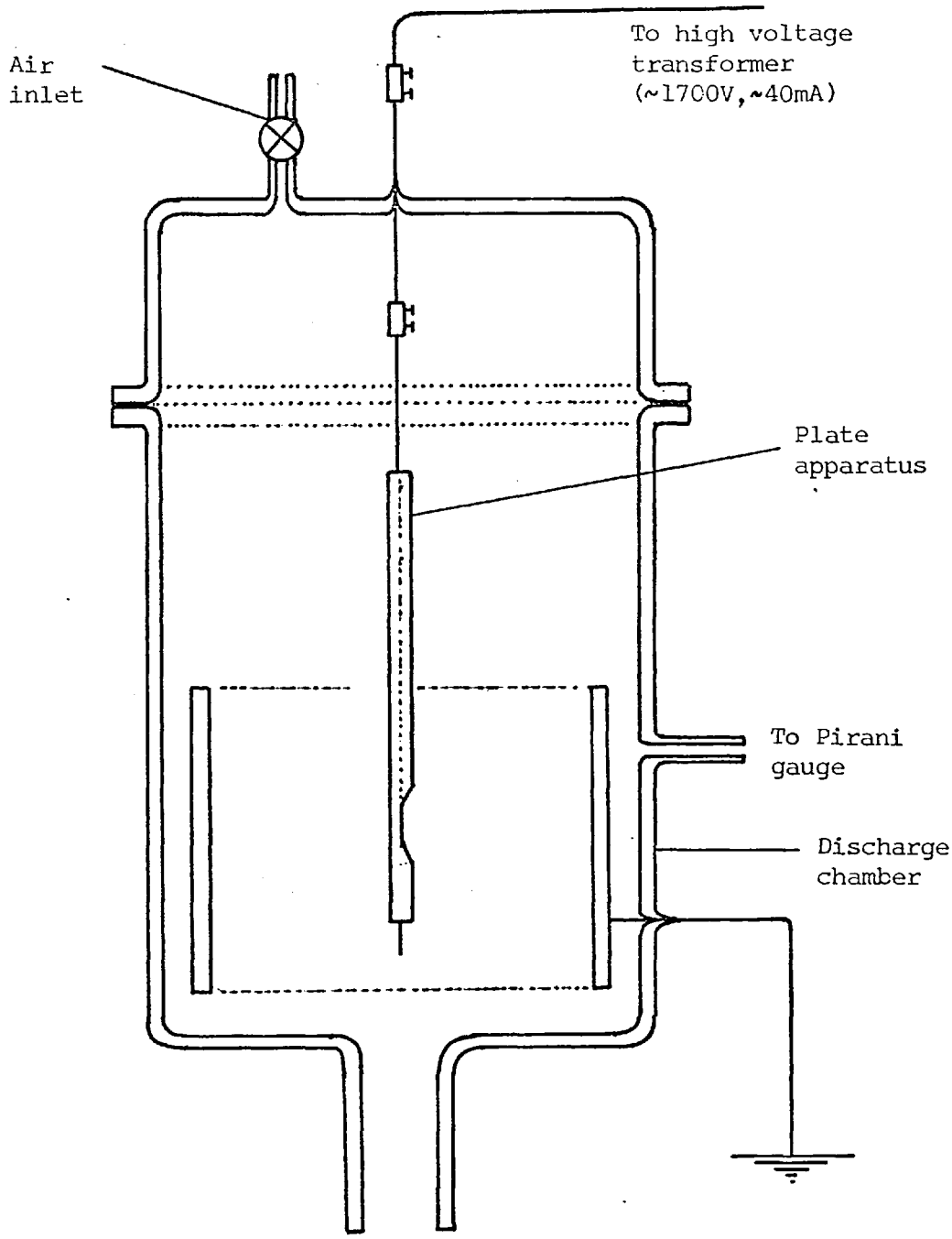


Fig. 2.10 Discharge chamber of Ionic Bombardment apparatus

system was to eliminate the possibility of contamination of the vacuum chamber by oil which could polymerize under the influence of high energy ions coating the metal substrate with a strongly adsorbed film. A more detailed description of this apparatus and its design are to be found in Smith's Ph.D. thesis (3). Adequate vacua for the necessary cleanliness in this research were achieved by the rotary pump alone without involving the diffusion pump as long as the metal substrate was initially cleaned by the ultrasonic agitation process.

The specimen to be cleaned was attached by its conducting wire to a spring clip on the tungsten high-voltage connector wire sealed into the chamber cover. The cover was carefully placed in position and the chamber evacuated to about 100 microns Hg. This vacuum was maintained for a short period and then a voltage of about 1,700 volts and a discharge current of 30 - 40 mA passed for the safe period. These quantities produced the best results, as was verified by the well developed cathode-glow discharge at the metal surface. Air was then readmitted to the chamber and the specimen quickly immersed in the test fluid.

2.6.2 Possible Contamination

The two materials used in the construction of the apparatus in this research which were unknown factors concerning possible contamination of the test fluids were the epoxy resin(s) and the silicone tubing. It has already been described how the likelihood of such contamination was reduced to a minimum in the design of the apparatus. Nevertheless, it was thought advisable to test for the existence of

any contamination by these materials under the working conditions. For this the ball apparatus (and later the similar plate apparatus) was used. The test fluid was hexadecane, purified by percolation over a column of silica gel. This fluid was chosen as it was to be used extensively as a base fluid and also because Smith has shown that extremely small concentrations of surfactant impurities markedly alter its thinning characteristics.

The experimental technique described fully in chapter 5 was used. The ball was left immersed in the hexadecane, above the mercury reservoir, for various growing periods. In each experiment a sample of one of the possible contaminants, i.e. epoxy resin, conducting epoxy resin (both thoroughly hardened), and wet cleaned silicone tubing after drying, was introduced into the hexadecane at the beginning of the growing period. These growing periods were varied from fifteen minutes to two days. The ball was then lowered into the mercury and the thinning of the hexadecane film with time measured. In no case was there any deviation in these thinning curves from the thinning spread of pure hexadecane alone. Most important, there was no evidence of any thick residual films in any of the tests. These experiments were repeated later with the more sensitive plate apparatus (chapter 7) and again no signs of surfactant contaminants were found.

2.6.3 Specification of Materials

The mercury used in all this work was trebly distilled in vacuo by the suppliers and stored in polythene bottles prior to the experiments. The two types of metal substrate used, i.e. stainless steel and chromium, have already been discussed. Two pure hydrocarbons were used as sol-

vents, i.e. hexadecane and hexamethyltetracosane (squalane). Both were of puriss grade as supplied by Koch Light and were always purified by percolation over columns of silica gel before use. Several polar materials were tested as additives in these solvents, others were tested pure, when possible. Again, they were of puriss grade and supplied by Koch Light.

The fluids supplied by N.A.S.A. were sometimes tested pure, and sometimes dissolved in hexadecane, depending on their viscosities. Although initially very pure, they were treated before testing to remove the products of oxidation and/or hydrolysis. The actual decontamination procedures were suited to the chemistry of the fluids in question. The fluids and their purification are described below.

(a) Hydrocarbons:

Hexamethyltetracosane (squalane),

Bicyclohexyl.

For these fluids the principal contaminants were the result of air oxidation. They were removed by storing the fluids over silica gel, in a dark, cool place. The fluids were passed over fresh columns of silica gel the day they were used.

(b) Esters:

Pentaerythritoltetavalerate,

Di (2-ethylhexyl) adipate,

Di (2-ethylhexyl) 3,3,4,4-tetramethyladipate,

1,1,7-Trihydroperfluoroheptylperfluoroglutarate.

For these esters there was the additional problem of hydrolysis back to acids and alcohols. It was decided to test how bad any such contamination was. By titrating for acid with phenol-phthalein before

and after the extraction of any acid from a small sample using 5% aqueous lye it was shown that there was no measurable impurity due to the hydrolysis. The purification procedure used for the hydrocarbons therefore was adopted for the esters.

Purification of the remaining N.A.S.A. fluids was not recommended, either because they were unlikely to decompose appreciably or because they were not expected to develop impurities which would alter their properties in any significant way.

CHAPTER 3

EARLY EXPERIMENTS WITH THE SHEAR APPARATUS

3.1 Introduction

This chapter deals with the initial work carried out with the shear apparatus, described fully in the previous chapter. The application of the mercury squeeze film technique used by Smith and Cameron (1),(2), to the needs of this research, however, proved to be more troublesome than expected. The major problems that arose are discussed together with the methods used to overcome them. Some preliminary results are also described.

3.2 Experimental Technique and Early Results

3.2.1 Original Experimental Technique

The early experiments were carried out solely with solutions of stearic acid in hexadecane. Once the apparatus had been thoroughly cleaned and assembled mercury was poured into the reservoir and then pumped up to the constant head device. The screw clip in the tubing from this to the cell was then opened slightly, and a measured amount of mercury allowed to flow into the cell which was tilted at an angle of approximately 45°. When the chrome capacitor plates could be seen to be covered by the mercury, the flow was stopped and the conductance between the dry metal and the mercury measured. This was to check that the electrical connections were functioning, and in later experiments was used to compare the conductance of the oil films with that for dry metal-mercury contact.

The cell was then inclined at approximately 20° to the horizontal, leaving the chrome plates free of mercury, and the test fluid introduced in enough quantity to cover completely these capacitors. The cell was left in this position for the required growing period, the time allowed for the additive to react with the metal substrates before thinning by hydrostatic

pressure was started. During this time final calibrations of the bridge circuit were carried out and any necessary corrections to the amplifier or attenuators made. More mercury was then allowed to flow gently into the cell until it was full, a stop watch being started as the mercury level rose above the capacitor plates. The variation of capacitance of the stearic acid solution with time was then recorded on log-log paper, from which the corresponding film thickness curves could be calculated.

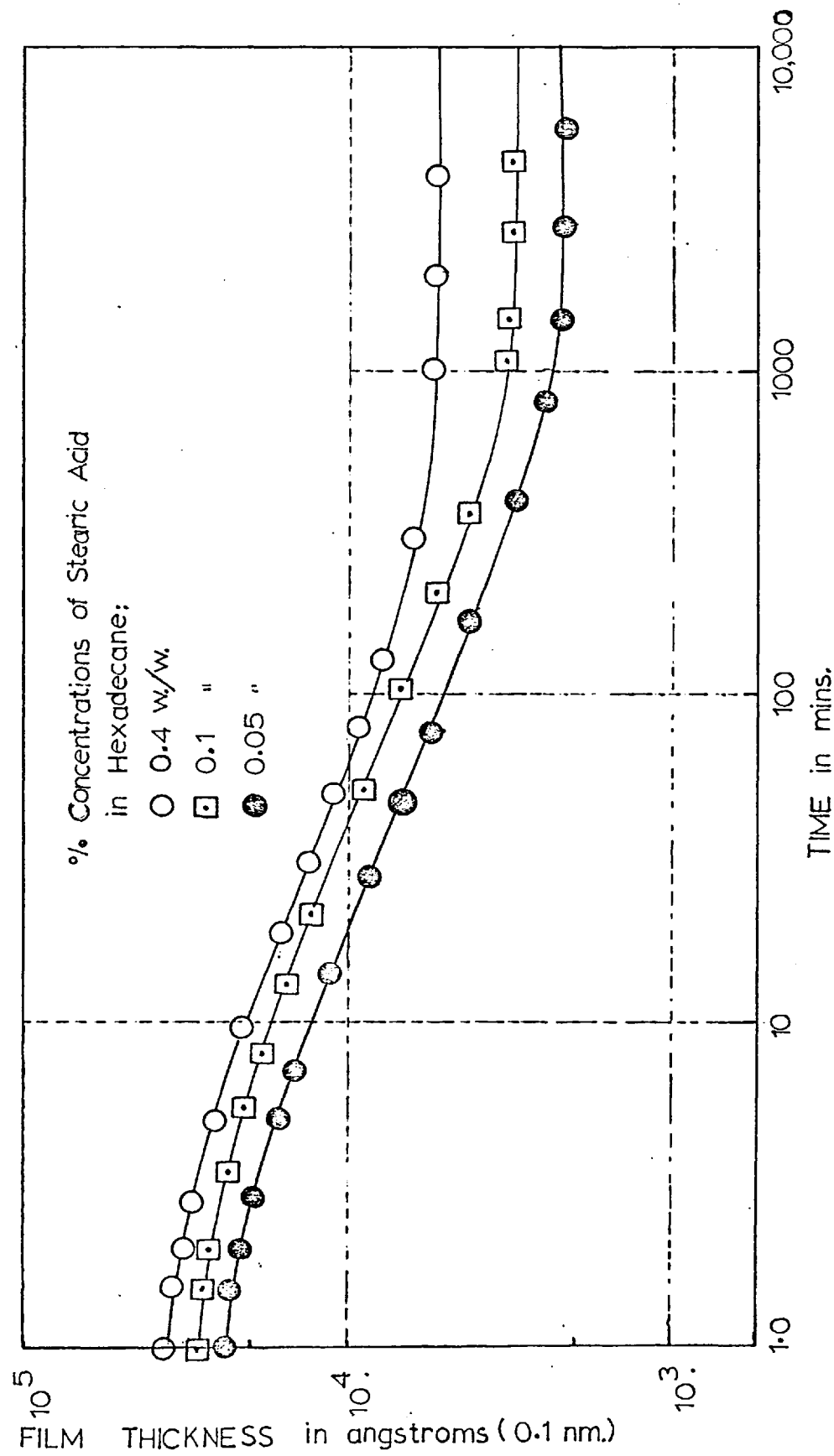
When these films had been left to thin for two days their capacitance curves showed that thinning had stopped leaving residual films of between, 2,500Å and 6,000Å, as recorded in the following section. These films were then exposed to shear by pumping the mercury past them at varying rates. The variation of the capacitance readings for each capacitor was measured at the bridge whilst the shear was being applied. The shear was calculated either from the rate of flow of mercury into the graduated flask or from the difference in height of mercury in the manometers at either end of the restricted channel,(see Chapter 2). From the capacitance measurements it was hoped to detect variations in the film thickness both with increasing applied shear and with the length of time of this application.

3.2.2 Results and Discussion

(i) Without Shear

Typical thinning curves of the stearic acid solutions being squeezed by the hydrostatic pressure of the mercury in the cell apparatus are shown in fig. 3.1. They show the variation of final residual film thickness with concentration of stearic acid in hexadecane. In each case the thinning curve is for the middle capacitor of the three in the cell. The curves for the other capacitors, for each concentration of stearic acid, only vary from this to any marked degree in the first thirty minutes. The

Fig. 3.1 Thinning curves for various concentrations of stearic acid in hexadecane



final film thicknesses on each capacitor were almost identical for each particular concentration. The thinning curves show, as might be expected, a positive relationship between the residual chemisorbed film thickness and the concentration by weight of stearic acid dissolved in hexadecane. The experiments with the ball apparatus, recorded in Chapter 5.3.1, showing the effect of increased growing time on the residual film thickness, were taken into account in these experiments. As the results showed that thicker residual films were produced after increased growing periods a constant growing time was necessary throughout these tests. It was set at 30 minutes.

If these results are compared with those of Chapter 5.3.1, the residual film on stainless steel produced by a 0·1% concentration of stearic acid in hexadecane is shown to be of approximately 4,000Å thickness, whereas the comparable residual film on the chrome surface is about 3,000Å thick. This indicates that of the two surfaces, chrome is less reactive than stainless steel under the experimental conditions.

The wet cleaning process leaves both oxygen and water available at the interface, and, amongst other workers, Lancaster (3) has shown that water is necessary for chemical reaction between metallic oxides and fatty acids (see Chapter 1). On the other hand, the chemical stability of chromium is known to be due to the presence on its surface of a coherent oxide film which normally presents a barrier to further attack. In the light of these two statements it appears that the necessity of the oxide layer for the formation of these thick chemisorbed films is counteracted, in the case of chromium, by the relatively unreactive properties of its oxide layer. The oxide layer on steel is made up of a combination of the oxides of the constituant metals present in the alloy which reduces the coherence of its structure. The resulting flaws, therefore, enhance the ability of the fatty acids to react with the oxides on the steel substrate.

It appears therefore that the thicker film on the steel surface corresponds to the enhanced rate of chemical reaction of the fatty acid due to its less coherent oxide layer. It does not follow, however, that this film is more strongly adsorbed than that on chrome, as this is largely governed by the polar attraction of the stearic acid to the metal. As chromium is, in fact, slightly more electro-positive than iron, it is possible that the thinner film on the chrome surface may well be slightly more strongly adsorbed. It seems reasonable therefore to compare quantitatively the results obtained in this research with those recorded by Fuks (4,5,6) on chilled steel. This is done in the next chapter.

(ii) Shear

The results obtained when shear was applied to these films were rather disturbing. The first cell used had a minimum separation of 5mm (5×10^{-3}m), which corresponded to a maximum obtainable shear of 100 dynes/cm^2 (~0·1gm/cm^2). The intention was to perfect the experimental procedure at these low rates of shear, and then work up to much higher values by reducing the minimum separation whilst increasing the rate of flow of the mercury.

The shear applied in the first experiments was ~25 dynes/cm^2 (0·025gms/cm^2). Within minutes of exerting this shear the conductivity of the films was seen to have increased suddenly from ~5μU to more than 1·0mU . In fact, the conductivity increased so rapidly throughout that the bridge could not be balanced and therefore no capacitance readings could be taken. A final value for the conductivity, similar to that obtained for the dry metal-mercury contact prior to the experiment, was reached within four minutes. The capacitance readings were of the order of the error predicted from the calibration curves of Chapter 2 for such high values of conductance, and therefore of little meaning.

The conclusion drawn from these results was that the bulk of the residual films had been removed from the chromium surface by this low shear. Further experiments were carried out with even lower applied shear, the minimum value achieved being 1 dyne/cm^2 (10^{-3}gms/cm^2). There was little variation in the above results, although in some cases the films appeared to remain for up to ten minutes before the conductivity suddenly rose to the dry metal-mercury value. During this period, however, the conductivity oscillated between 0 and 250μU so quickly that capacitance values were very difficult to read. Nevertheless, the film appeared to thin very little before final electrical breakdown occurred.

The possibility that the electric field produced by the bridge circuit across the oil film was somehow causing this electrical breakdown was considered unlikely. This was because the field achieved a maximum of only 2 volts/cm for a film 2,000Å thick. The work of Zoltoev (8) and Talmud and Bresler (7), amongst others, on the conductivity of microfilms of paraffins and mixed paraffin solutions indicated that the necessary field for dielectric breakdown of films 1,000Å thick was 56k volts/cm. Furthermore their fields were uni-directional. The unlikelihood of such breakdowns was substantiated by the fact that the films had thinned for two days previous to the application of shear, in which time they exhibited no electrical instability whatsoever. Nevertheless, the large discrepancy between the results of Fuks, questionable though their validity may be, and those obtained in this apparatus, suggested that some form of electrical breakdown was occurring whilst the oil film in fact remained physically intact. This possibility was investigated in two ways.

Firstly, the shear was applied to the film without the bridge circuit being closed. After a period of fifteen minutes the circuit was then switched on and the capacitance read. In some instances the film

appeared to be broken down electrically before the circuit was closed, in others breakdown did not occur for several minutes. These results were inconclusive so the experiments were repeated with the bridge switched off during the application of shear. Then, before the bridge circuit was closed and the capacitance measured the mercury flow was stopped and the pump switched off. In these experiments no breakdown occurred and the capacitance values indicated that the film had thinned hardly at all, whilst the conductance readings remained below the 50μU mark.

The second method for checking the behaviour of these residual films under shear was to utilize optical interference. A cell with semi-reflecting chrome capacitor plates was built so that the film thickness could be deduced from the colour fringes formed as described in Chapter 2.5.. These experiments confirmed that residual films of over 2,000Å remained whilst being exposed to a shear as high as 100 dynes/cm^2 ($\sim$0·1gm/cm^2), even though the autobalance bridge registered complete electrical breakdown. As will be described in Chapter 4.4, these interferometric observations were also used to examine the form of these residual films whilst undergoing shear, and to investigate the possibility of variation of the relative permittivity of the stearic acid solution after forming thick films.

It was apparent from these tests, therefore, that although the chemisorbed residual films were capable of physically sustaining the maximum shear applied so far, great care had to be taken to preserve their electrical stability. It appeared that the combination of the small electrical field due to the bridge potential across the film, and the motion of the mercury past the surface of the film, no matter how slight, somehow resulted in complete electrical breakdown of the film within a few minutes. The possible mechanisms of this breakdown are discussed in the next section.

3.3 Possible Mechanisms of Electrical Failure

The various means by which charge can be transferred from one electrode to another when separated by an apparently insulating liquid form substantial subjects in themselves. In his review of this topic Fiennes (9) sub-divides it into four main mechanisms of conduction. These are Bridging, Fritting, Cavity conduction and Ionic conduction. He stresses, however, that these sub-divisions are by no means mutually exclusive.

Before an analysis of the particular dielectric breakdown reported in this chapter is attempted, a brief description of the above conduction mechanisms is given.

3.3.1 Bridge Formation

The work of Kok (10) has shown that this form of dielectric breakdown centres on the presence of impurities in the liquid film. These may be particles of foreign matter or, more notable for this research, aggregates of constituent molecules of the liquid itself. Their nature dictates that these particles will have a different dielectric constant to the bulk fluid, and this in itself will cause field distortion and polarisation. If the field in which the particles are moving is inhomogeneous they will tend to drift to the region of maximum electric stress along the field lines - the process of dielectrophoresis. On contact with one electrode, a conducting particle will be charged accordingly causing field distortions that will impel it towards the opposite electrode. Non-conducting particles, when they come into contact with an electrode, have some of their surface polarisation charge neutralised producing a net charge of the opposite polarity and are then repelled. These particles will accumulate in the region of minimum potential energy, due to dipolar attractive forces. The stability of these congregations will increase as their number increases

since they will bind together in positions which minimise the total potential energy. Eventually they will stretch across the fluid film creating a "bridge" or region of enhanced conductivity. The film then breaks down electrically, often accompanied by physical rupture.

3.3.2 Fritting

This is a form of bridging, found in very thin insulating layers, where the actual material of one, or both of the electrodes is drawn out towards the opposite electrode. Pearson (11) proposed that high field emission produces a local softening of the electrodes around surface irregularities. Holm (12) covers this subject extensively. For the film thicknesses found in this research, fritting only usually occurs where at least one of the electrode materials melts and is drawn into the dielectric fluid by electrostatic forces. The necessary field strength for fritting to occur is quoted as 10^6 - 10^7 volts/cm.

3.3.3 Cavity Breakdown

There is a considerable amount of evidence (see Fiennes (9)) to show that the ultimate dielectric strength of a liquid is limited by the tendency to form cavities under the influence of an applied field. These cavities allegedly form around impurities, dissolved microscopic bubbles of gas, or vapour. It is also proposed that "cavity fluctuations" exist on a statistical basis, especially for fluids of low cohesion forces, such as hydrocarbons. These cavities grow when the electrostatic pressure caused by the field exceeds the sum of the hydrostatic pressure and surface tension forces. They can accelerate ionisation processes in the liquid and dissociation of the liquid molecules. The vapour or gas in the cavity is likely to have a lower intrinsic breakdown strength than the liquid. The bubble can also distort in the field direction, bridging

the electrodes and causing effective dielectric breakdown of the fluid film. The field magnitude necessary to initiate this breakdown in the context of this research is about 10^5 volts/cm, although this value may be significantly reduced if cavities of some kind are already present.

3.3.4 Ionic Conduction

This centres around the mobilities of ions, or ionized regions, present in the fluid film. These molecular and/or macroscopic ions drift in the applied field, the resulting linear charge motion constituting a form of conduction. Jachym (13), working on a liquid hydrocarbon, showed that the necessary activation energy decreased with applied field to a constant minimum of 0·4eV at about 2,000V/cm. The mobility of ionized long chain hydrocarbons is markedly less than that of ionized oxygen and water, probably present to some small degree in the fluids used here. Although these oxygen and water ions would reduce the necessary applied field for conduction it is thought that their mobility and concentrations would never rise to the level necessary for conduction of the sudden nature experienced in this experimental system.

3.3.5 Proposed Mechanism

The field applied across the fluid films in this research fluctuates at 1,000cycles/sec. The maximum voltage applied, producing it, is 40μV (40×10^{-6} volts) peak to peak. The film thicknesses, derived from the capacitance measurements and therefore only average values, at which breakdown occurred in these experiments, were of the order of 2,000Å (at the least). The maximum field these films experienced due to this applied voltage alone, therefore, was 2 volts/cm, oscillating at 1000 cycles/sec. On the strength of these values compared with the minimum fields necessary in each of the four possible breakdown mechanisms the

stability of these films seems assured. It is necessary to postulate, therefore, how the local film thickness and/or the field strength may be varied, by the motion of the mercury, to allow any of these mechanisms to take place.

The electron photomicrographs produced by Smith (1) coupled with the interferometric topology shown in Chapter 4, fig.10, indicate the large degree of heterogeneity of these films. The diagrams of fig.4.10 also indicate that these irregularities in the chemisorbed film are largely reduced as the shear is increased. A few small regions of below-average film thickness, seen as grey-blue specks in the microscope, remain, however, even with increased shear. The film thickness at these points cannot be measured, but, as no interference fringes are produced, they are well below 2,000Å thick. These weak spots in the film are thought to be the cause of these electrical breakdowns. A model of the variation of the mercury-oil film interface at one of these weak spots with applied shear is shown in fig. 3.2.

In the absence of shear (fig. 3.2a) the surface tension of the mercury will prevent it from fully penetrating the gap in the film. As many results have shown these films exhibit a high degree of electrical stability, even for thicknesses of 1,000Å or less, as long as no shear is applied whilst the field is present.

When the mercury is set in motion, however, the film becomes more ordered. This, coupled with the increased pressure in the mercury as shear is applied, causes much deeper penetration of the gap, fig. 3.2b. Not only will this decrease the local film thickness, possibly down to 400Å or less, but the large outcrop in the mercury surface will increase the field concentration at this point. In these circumstances the field could possibly approach the order necessary for the conduction mechanisms to take place.

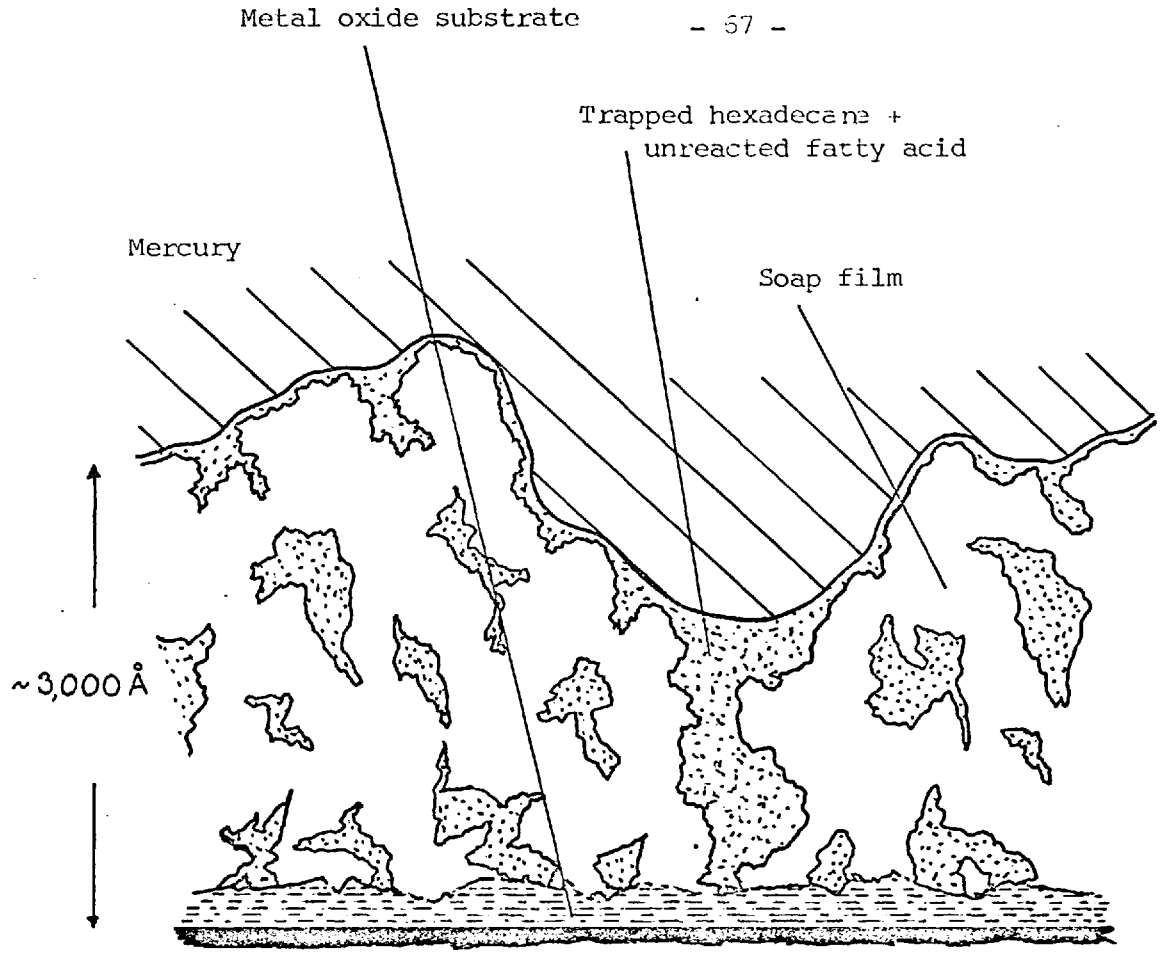


Fig. 3.2a Cross section of thick film prior to application of shear

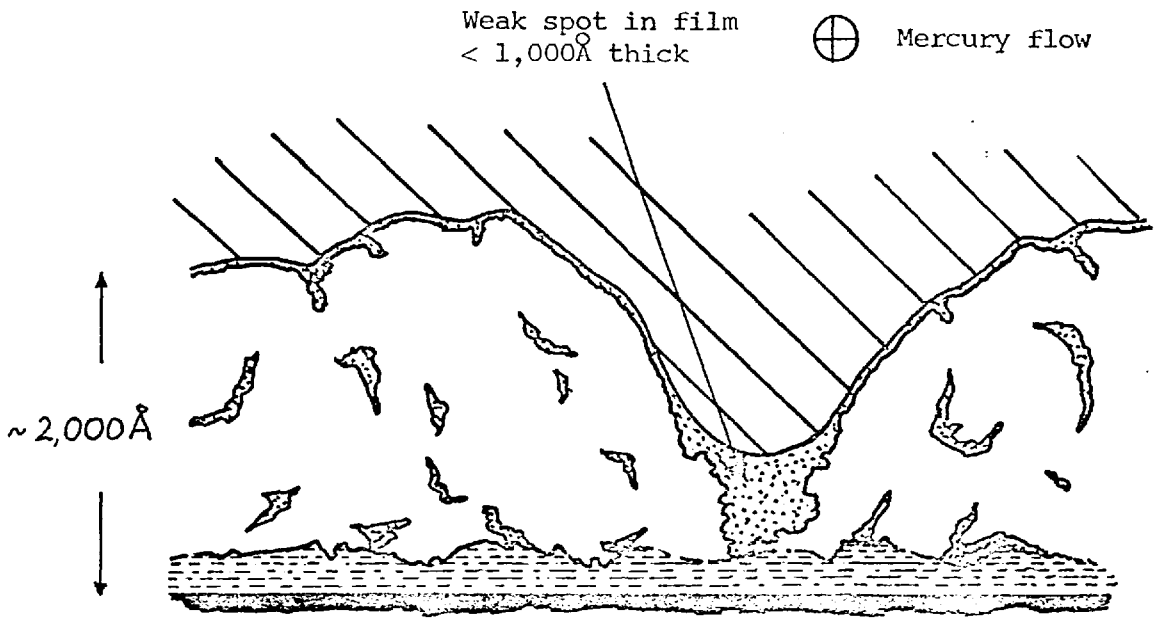


Fig. 3.2b Compression of the above film during shearing

Of these mechanisms ionic conduction has already been discounted due to the field oscillation and dimensions. Cavity breakdown also seems unlikely in these circumstances as an increase in pressure will reduce the likelihood of cavity formation whilst increasing the necessary field strength, already of an unattainable magnitude.

Bridging and fritting, on the other hand, seem much more likely under these conditions. The large field enhancement at the weak spots would attract any free acid ions and polar groups, oxygen and water ions, or particle impurities as described. This would be an accumulative process, increasing the field strength which, in turn, would increase the number and stability of the various particles. Simultaneously, the increasing electrostatic forces would overcome the surface tension of the mercury, drawing a column of it further into the gap. This process could accelerate until dielectric breakdown occurred. The rapid increase in conducitivity followed by sudden complete dielectric breakdown predicted in the above model resemble the actual experimental results very closely.

3.3.6 Experimental Comparison

The actual breakdown will occur either when the gap between the mercury and chrome oxide, coupled with the semiconducting bridge inbetween, has decreased enough for a spark to jump the gap, or when the extruded mercury actually makes metal-metal oxide contact. In either case the field will be instantly reduced causing the gap to widen and/or the contacting mercury to break away in a globule. The conductivity should, therefore, decrease until the same process builds up again. This is not observed experimentally. Once breakdown occurred there were no cases of dielectric recovery. It is thought that this could have been due to debris being present after the initial breakdown, forming a highly conducting bridge through the oil film. The conducting debris might be vapourised

mercury, or particles of chrome and chrome oxide formed when the sudden conduction, or spark, produced local heating on the two surfaces. Any globules of mercury present would have a similar effect in forming a bridge.

The permanence of this conducting bridge, indicating both dielectric and physical breakdown, was illustrated by leaving the field off for several days, after which time no change was observed when the circuit was again closed. In later experiments, when these breakdown mechanisms were more fully understood, removal of the conducting bridge was attempted by applying shear with the field switched off. It was supposed that the extra energy imparted by the motion of the mercury would cause the now free particles constituting the bridge to dissociate by random motion. Surprisingly, there was only one case where a partial dielectric recovery was observed. Even then, the recovery lasted only ten seconds once the field was applied in the absence of shear.

There are two possible reasons for these results:

(i) The residual chemisorbed film is so solid and coherent that once the bridge has formed in the weak spot it is virtually sealed into position.

(ii) In the absence of the applied field some form of electrostatic field exists, both when the mercury is stationary or in motion, such that the bridge, once formed, remains stable.

The first possibility is contrary to the original formation of the bridge. It is also not compatible with the known chemical structure and observed form of the films.

The second possibility concurs with the work and hypotheses of Deryagin et al (14,15). It is also a forerunner of results described later in this thesis, where the whole effect will be discussed more fully.

3.4 Conclusions

Thick films, as described by Smith (1), have been shown to exist for various concentrations of stearic acid in hexadecane. The thickness of these films has been correlated with the variation of reactivity of the oxidised metal substrates.

Capacitance measurements of the resistance to shear of these films could not be obtained with the technique described due to dielectric instabilities at "weak spots" in the chemisorbed layer. Bridging and fritting, advanced to explain this dielectric breakdown, suggest the existence of a permanent electrostatic field, possibly as an inherent property of these thick films.

The capacitance measurement technique (aided by the preliminary use of optical interferometry) showed the thick films were little affected by a tangential shear of 100 dynes/cm^2 (0·1 gms/cm^2). Further experiments utilizing these two techniques could now be carried out applying much larger maximum shear stresses. These experiments are described in the following chapter.

CHAPTER 4

MECHANICAL PROPERTIES OF THICK FILMS

4.1 Introduction

In this chapter some of the mechanical properties of the thick residual films formed by a range of aliphatic acid solutions are investigated. Similar work has been carried out by Needs (1) and more extensively by Fuks (2,3) using a loaded disc. As described earlier, these results are in doubt due to possible contamination of their systems, more especially by dirt particles. Nevertheless a brief review of their findings is given here before the results of this chapter are described, so that comparisons may be made.

4.1.1 Previous Studies of Thick Film Properties

The more impressive results were obtained by Fuks (2). He performed many experiments with apparatus very similar to Needs'. Two small flat discs were submerged in the test fluid with normal loading and the variation of film thickness with time was observed. The film thicknesses were calculated from measurements of the capacitance between two remotely located discs, one of which was attached to one test plate. For thicknesses of approximately 200Å and above he claimed an accuracy of ± 100Å.

Fuks found that the addition of a 0·1% of stearic acid to MS-20 oil ("a chromatographically separated naphthene-paraffin fraction") increased the residual film thickness by about 1,500Å. It is notable that the MS-20 oil alone produced a 2,000Å film. Lower molecular weight hydrocarbons such as benzene, hexane, cyclohexane, iso-octane and decane were extruded from between the surfaces in about one hour leaving no residual film. This means that solid contaminants larger than 200Å dimensions must have been excluded from these experiments.

Using a 0·1% solution of palmatic acid in MS-20 oil Fuks showed that the residual films thinned very little beyond contact pressures of 100 psi. The film thinned to approximately 1,000Å for pressures up to 100 psi, whereas further increments to 300 psi reduced the film by only a further 400Å. Needs also observed such a response to normal loading for stresses up to 800 psi with five different oils. Again, beyond a stress of about 100 psi, little extra thinning occurred.

Fuks found that when the applied normal stress was relaxed the residual films thickened, or recovered, fig. 4.1.a. For a load of 6.4 psi the thick film stabilised at 2,700Å, but on reducing the stress to 3.2 psi the film thickens to about 3,200Å. The trend was revealed for different load variations and fluids, the recovery apparently needing around one hour for completion. He tested several fatty acids dissolved in various solvents on steel, aluminium oxide and quartz plates. The thickest films were produced on steel, decreasing with diminishing surface energy in the order steel, Al_2O_3 and quartz. These films were from 100Å to 200Å thinner on Al_2O_3 than on steel and decreased a further 100Å to 400Å on quartz. For each fatty acid he found that the residual films increased slightly when the hydrocarbon chain length of the solvent was increased. Also, the thick films were enhanced with increasing fatty acid concentration, up to Fuks' maximum of 0·2% by weight.

Fuks also performed a series of experiments in which the static shear strength of the thick films was measured. He found that the shear strength of an iso-octane-palmitic acid solution was three times greater on steel surfaces than on quartz for a film thickness of 600Å. The shear resistance of a benzene-stearic acid solution was markedly lower than the comparable iso-octane solution at the same film thickness. For really thick films, i.e. above 2,500Å, he showed that the shear strength increased with decreasing fatty acid concentration, i.e. 7 gm/cm^2 for a 0·1% solution

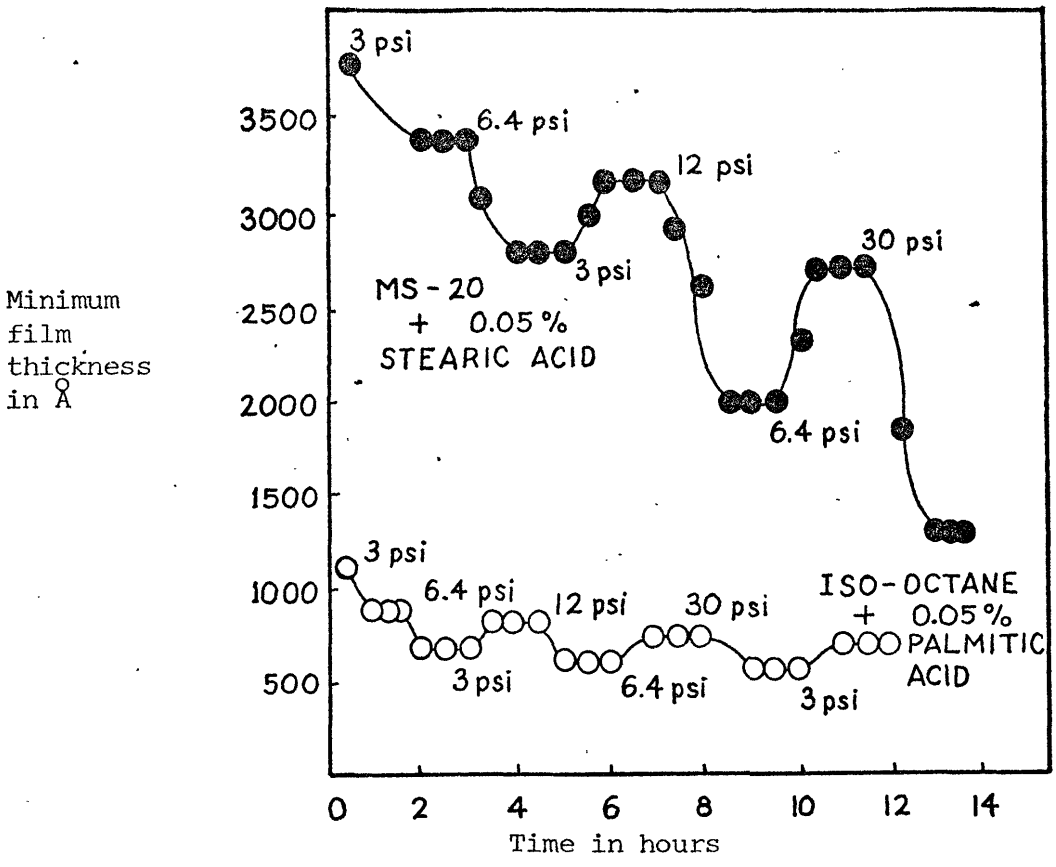


Fig. 4.1a Effect of normal stress on film thickness, showing recovery properties (from Fuks (2))

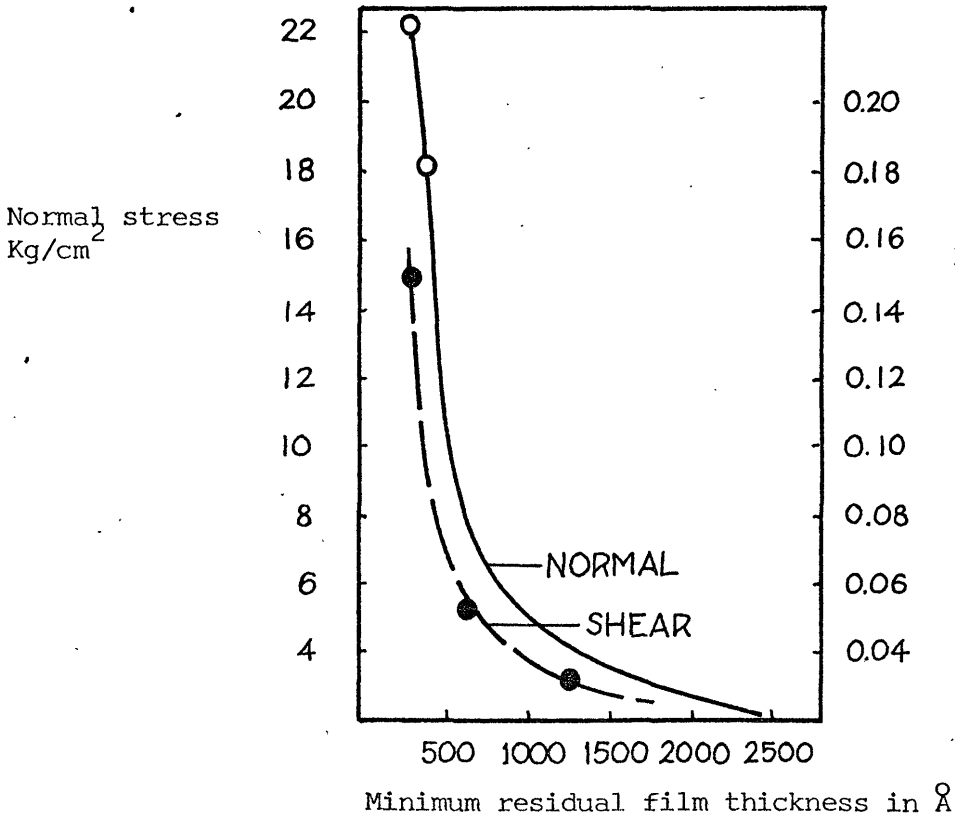


Fig. 4.1b Residual Film thickness related to applied stress for a 0.01% soln. of Palmitic Acid in MS-20 (from Fuks (3))

compared with 40 gm/cm^2 for a 0·005% solution. The increase in concentration decreased the time necessary to reach the stable residual film and constant shear resistance.

Needs also carried out tests on the shear resistance of his thick films with similar results to Fuks. He discovered that the static shear resistance of olive oil was some 7 to 9 times the kinetic resistance. Further, the kinetic shear resistance dropped to its low level in about 20 minutes but needed about 3 hours to regain the static shear resistance value once relative motion between the steel flats was stopped. Needs concluded that the bulk viscosity of the fluid and, at the same time, the viscosity in the normal direction approached infinity. Terzaghi (4) observed similar behaviour with clay-water solutions which he attributed to molecular reorientation and long time recovery.

Fuks provided more data on thick film shear strength in his recent work (3). He also derived a friction formula for boundary lubrication which related the role played by intimate contact between asperities of the solid surfaces, the shear resistance offered by the adsorbed monolayer and the shear resistance of the thick (multimolecular) film. He stated that the coefficient of friction for unlubricated surfaces lies within a range of 0·5 to 7; for adsorbed monolayers 0·1 to 0·2 and for thick films from 0·01 to 0·02. In hydrodynamic lubrication these coefficients lie between 0·001 and 0·006.

At 20°C on steel surfaces Fuks found that the thick film produced by a turbine oil (of unknown constitution) decreased from 1,200Å to 800Å when shear is induced under a normal load of 8·5 psi. With the addition of 0·1% palmitic acid the static film increased to 1,900Å, dropping to 1,200Å when tangential shear was applied. These and other results are given in Table 1 of Appendix B. When the normal load was increased to 25 psi the thick film, initially 1,200Å thick, fell to 900Å with shear.

It followed that the shear stress was related directly to the film thickness, in most cases, see fig. 4.1.b. The shear stress generally appeared to be about two orders of magnitude below the normal stress, for any particular film thickness. Generally, the shear stress increased with decreasing film thickness and increasing normal shear (or load).

Fuks also found that the coefficient of static friction became greater with increasing fatty acid and hydrocarbon chain length. The static shear stress, however, remained constant for constant film thicknesses and was independent of these chain lengths. He revealed that when the solvent chain length greatly exceeded that of the fatty acid, the static coefficient of friction ceased to be a linear function of chain length. Such a linear relationship was exhibited by various fatty acid solutions in both benzene and iso-octane. These results are shown in fig. 4.2. The relationship, revealed by Fuks, between normal stress and shear stress as a function of chain length of the solvent is given in Table 2 of Appendix B. The films were produced by 0·05% solutions of stearic acid and were 600Å thick in all cases.

Finally, Fuks carried out some sliding "four-ball" experiments at a contact stress of 200,000 psi. In these tests he observed the same relationship between the coefficient of friction and the fatty acid chain length described above. An important practical finding therefore is that the effects observed at low contact stresses still occurred at high contact stresses, i.e. under similar conditions to those experienced in most lubrication conditions.

Fuks did not attempt a comprehensive analysis of all his results, but provided several interesting interpretations. He attributed the effect of substrate composition to the strength of the chemisorbed monolayer. He believed that shear in the thick films took place in localised planes "passing through the terminal hydrocarbon radical of the oriented surface active molecules". Further, he thought that the length of the molecule established the residual film thickness, hence setting the separation of

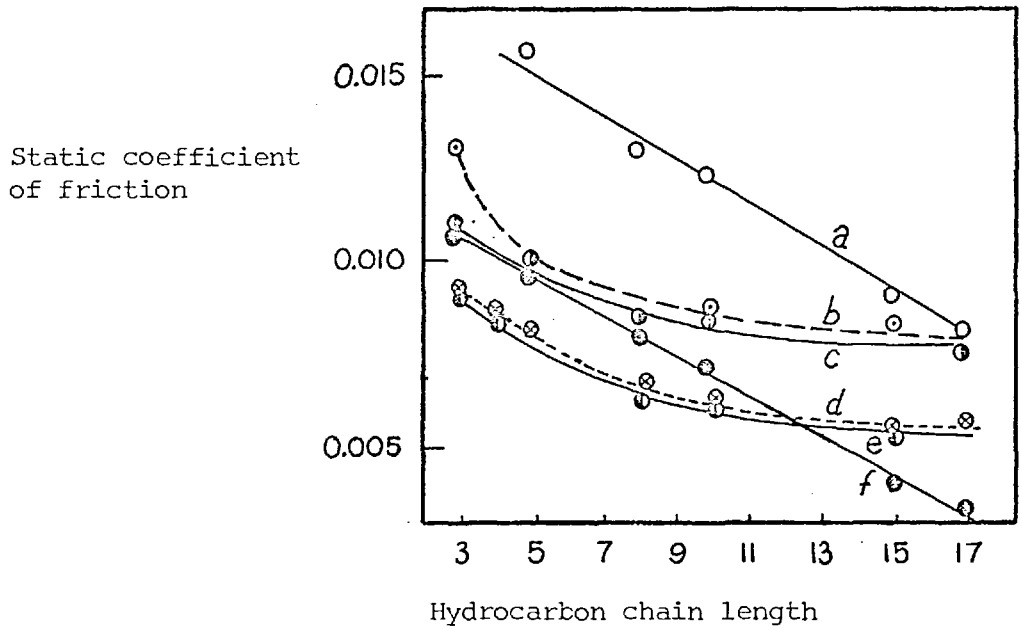


Fig. 4.2 Static coefficient of friction of 'Polymolecular' films v. fatty acid carbon chain length (3).

(a) Normal stress = 22 kg/cm^2, 0.05% fatty acid in benzene

(b) Normal stress = 22 kg/cm^2, 0.1% fatty acid in PPF

(c) Normal stress = 14 kg/cm^2, 0.1% fatty acid in PPF

(d) Normal stress = 4 kg/cm^2, 0.1% fatty acid in PPF

(e) Normal stress = 6 kg/cm^2, 0.1% fatty acid in PPF

(f) Normal stress = 4 kg/cm^2, 0.1% fatty acid in iso-octane.

the slip planes and the solid surface - "chemical activity of the molecule is of no significance here". Generally, Fuks attributed the observed behaviour of the thick films to adsorption coupled with an unspecified interaction of solvent and fatty acid molecules.

4.1.2 Proposed Experiments

Not all of Fuks' results are reviewed because of the limitations of the apparatus used in this research. Most notably, the temperature effects could not be studied due to the cell construction and the risk of mercury poisoning. Several interesting variables were explored, however, namely:

a. Variation of film thickness with concentration.

b. Variation of film thickness with substrate.

c. Variation of film thickness with growing time.

d. Effect on resistance to shear of thick films of several combinations of a. and c.

e. Variations in resistance to shear and film thickness of residual films produced by fatty acids of different chain lengths.

f. Recovery properties of residual films on cessation of tangential shear.

Of these, a. and b. are covered in the previous chapter and c. in Chapter 5.3.1. The remaining effects are studied both electrically and interferrometrically and described in this chapter. The results are compared with those of Fuks and any correlations discussed.

4.2 Revised Experimental Technique and Discussion

In order that the residual films should remain electrically stable whilst undergoing shear the technique developed in Chapter 3.3.2 was expanded. This circumvented the problem of electrical breakdown during shear by never having the bridge circuit closed whilst the mercury was in motion. Up to the point where the thick films had been produced in the

cell the procedure was exactly the same as in section 3.3.1.

Before the mercury was set in motion to produce shear, the bridge circuit was opened. The pump motor was then switched on and the screw clip adjusted to give the required flow rate, i.e. shear. This shear was applied for two minutes and then the screw clip was closed and the pump stopped. The bridge was immediately switched on and the values of capacitance and conductance read for each of the three capacitor plates. This procedure was repeated, either at the same shear, or for an increased value, until the maximum possible shear for the particular cell was reached. As described in Chapter 2.3.3, this maximum value depended on the separation of the restricted section of the cell where the chrome plates are situated.

The two minute duration for the application of shear was chosen for two reasons. Firstly it was long enough to show variations in the capacitance readings for any increase in the shear. Secondly it was short enough to be repeated several times at a constant value of shear to show the variation of film thickness at that shear over a prolonged period of application.

All the experiments conducted in this revised manner used cells with semi-reflecting chromium layers as capacitor plates. The thickness of the residual films could thus be observed both optically and electrically at any time. At first the colour interference patterns were used to check the presence of these films and corroborate the value of thickness calculated from the capacitance readings. These fringes were also very useful, however, for studying the three dimensional form of these chemisorbed layers, and also for investigating variations in their structure whilst actually undergoing shear, when no capacitance readings could be taken.

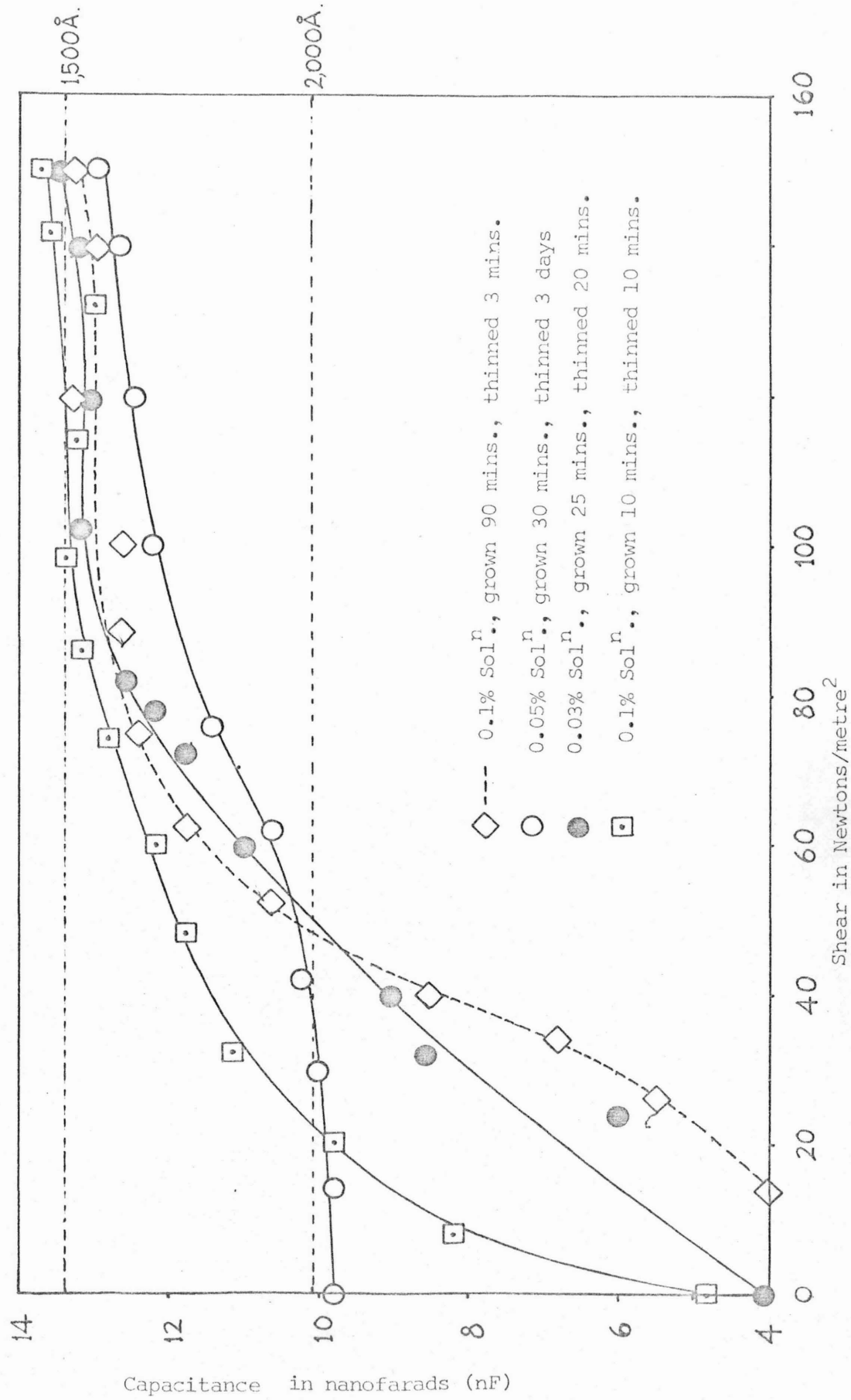
4.3 Results and Discussions

4.3.1 Effect of Various Initial Conditions

The results catalogued earlier in section 3.3.2 and those obtained with the ball apparatus described in Chapter 5.3.1 show marked changes of residual film thicknesses both with variations of stearic acid concentrations and with the growing period allowed. Experiments were carried out, therefore, to check whether these relationships remained important once the films were exposed to shear, and if so, to what extent. These tests were again carried out on concentrations by weight of stearic acid in hexadecane. The tests using the original technique involved allowing the fatty acid solutions to thin under the hydrostatic pressure of the mercury until only the residual chemisorbed films remained. As this was a very lengthy process its importance was investigated by applying shear at varying periods, from three minutes to three days, after thinning had been initiated. A range of experiments were carried out, where the growing period, the fatty acid concentration, and the time allocated for the film to thin before shear was applied were all varied systematically. The results from the most representative of these experiments are shown in fig. 4.3.

The large differences in the starting conditions for these experiments are mirrored in the varied range of thinning curves produced for the lower regions of shear. These differences are mainly self-explanatory, although the curve for the 0·03% concentration of stearic acid, having a 25 minute growing period and a 20 minute period of hydrostatic thinning prior to the application of shear, merits further discussion. This is because of its comparatively discontinuous thinning curve in this low shear region. The 0·03% concentration was the lowest used and coupled with the comparatively short growing period of 20 minutes the resultant chemisorbed film was almost certainly less coherent than usual. This would result in local large differences in the thickness of the residual layer and, as the capacitance is a measure of the average film thickness, such

Fig. 4.3 Thinning under shear of various concentrations of stearic acid-alkane solutions with different starting conditions



discontinuities in this average could well to expected for this case. An experiment carried out for this concentration where only ten minutes were allowed for growing and a further ten minutes for hydrostatic thinning produced more marked discontinuities in its thinning curve against shear. A more important fact was that the conductivity in this test rose well above the 50 μU value, whereas in all the other tests this margin was never reached. This, again, indicates an incompletely formed, or incoherent, residual film. In this one test the residual film thinned to a minimum value of approximately 1,000Å under the maximum shear of 150 newtons/metre^2 and the conductivity remained at the high value of approximately 300 μU throughout the experiment. This was the only case where this residual film thickness fell significantly below 1,500Å.

In all the other experiments, as fig. 4.3 shows, the final residual film thicknesses left after the maximum applicable shear of 150 newtons/metre^2 were very closely centred around the 1,500Å mark. In all these tests the maximum shear was applied for 60 minutes, but no further significant reduction in these film thicknesses occurred. In fact, in some cases the residual films appeared to increase slightly in thickness during this lengthy period of shear.

From these results it appears that, apart from the one exception, the many different starting conditions had very little effect on the behaviour of these chemisorbed films above a shear of 100 newtons/metre^2. The exception indicates that there must be enough fatty acid and enough reaction time for a coherent chemisorbed film to be produced on the metal surface. It is very interesting to note, however, that once the minimum levels for these criterea have been achieved the behaviour of the resulting residual films under shear is virtually independent of their initial thickness, period of existance or fatty acid concentration.

Although these results have been obtained solely for various solutions of stearic acid in hexadecane it seems reasonable to assume that similar effects would be exhibited by most solutions of fatty acids in hydrocarbon solvents on the understanding that they produced a residual film. This assumption is based on the fact that these films are of a predominantly chemical nature. A further assumption is that the time necessary for a well established coherent film to be produced by all the fatty acids tested will be of the same order as that for stearic acid.

4.3.2 Residual Films of Various Fatty Acids

In these experiments fatty acids of increasing hydrocarbon chain length were dissolved in 0·1% solutions by weight in hexadecane. There was one exception, that of caproic acid, where a 0·25% by weight solution was used. This, as explained later, was in order that a sufficiently enduraible residual film was formed. The results in the previous section showed that the behaviour of these residual films under shear was largely independent of the initial conditions experienced by the solutions. It was decided, however, that the conditions should be standardised for these experiments to simplify comparisons of the results. To this purpose all the test fluids were allowed a thirty minute growing period and then a twenty minute duration of hydrostatic thinning before shear was applied.

The errors in these results were calculated from two major factors.

1. Capacitance readings taken for high values of conductivity contained an inherant error tabulated in the calibration curves of Chapter 2, fig. 2.7.

2. The three capacitors present in each cell were of the same area and, to a relatively high degree of accuracy, experienced equal amounts of shear. They should, therefore, exhibit residual films of equal thickness, i.e. equal capacitance. From any variations in these three values of capacitance, therefore, the standard deviation was calculated.

In the few cases where both these errors occurred simultaneously it was decided to add the two calculated values to give the total error.

The error calculated from case 2 above was not included in any of the results for low shear. This was because the three capacitors invariably exhibited an increase in residual film thickness along the line of shear after a few two minute periods of low shear had been applied. This was almost certainly due to surplus fluid which had been trapped in the enmeshed fibrillar structure of these films being squeezed out and carried along to the next capacitor, which would thus give a slightly enhanced value of film thickness. Interferometric observations corroborated this as apparently hemispherical globules of fluid were seen to be forced from the first capacitor to the second, and so on. The diameter of the base of these globules was of the order of 10^{-5} metres or less. In all experiments, after the third or fourth two-minute-period of shear had been applied, (i.e. for shears of no greater than 40 newtons/metre^2) these globules could not be observed, indicating their complete removal by shearing.

The thinning curves of the residual films of the various fatty acids with shear are shown in fig. 4.4. These may be compared with the stearic acid curves of fig. 4.3. The curves tend to fall into two categories:

i. Those that exhibit continuous thinning with increased shear coupled with a varying degree of electrical instability. These are for solutions of Lauric acid, Behenic acid and Caproic acid.

ii. Those that stabilise to a constant residual film thickness with increased shear, namely for solutions of Myristic acid, Stearic acid and Palmitic acid.

The three fatty acid solutions in the first category thin to relatively low final film thicknesses. The Lauric acid thins to $\sim$ 920Å, the Behenic acid to $\sim$ 780Å and the Caproic acid to a mean 470Å. It is

Fig. 4.4 Thinning under shear of various fatty acid solutions in hexadecane

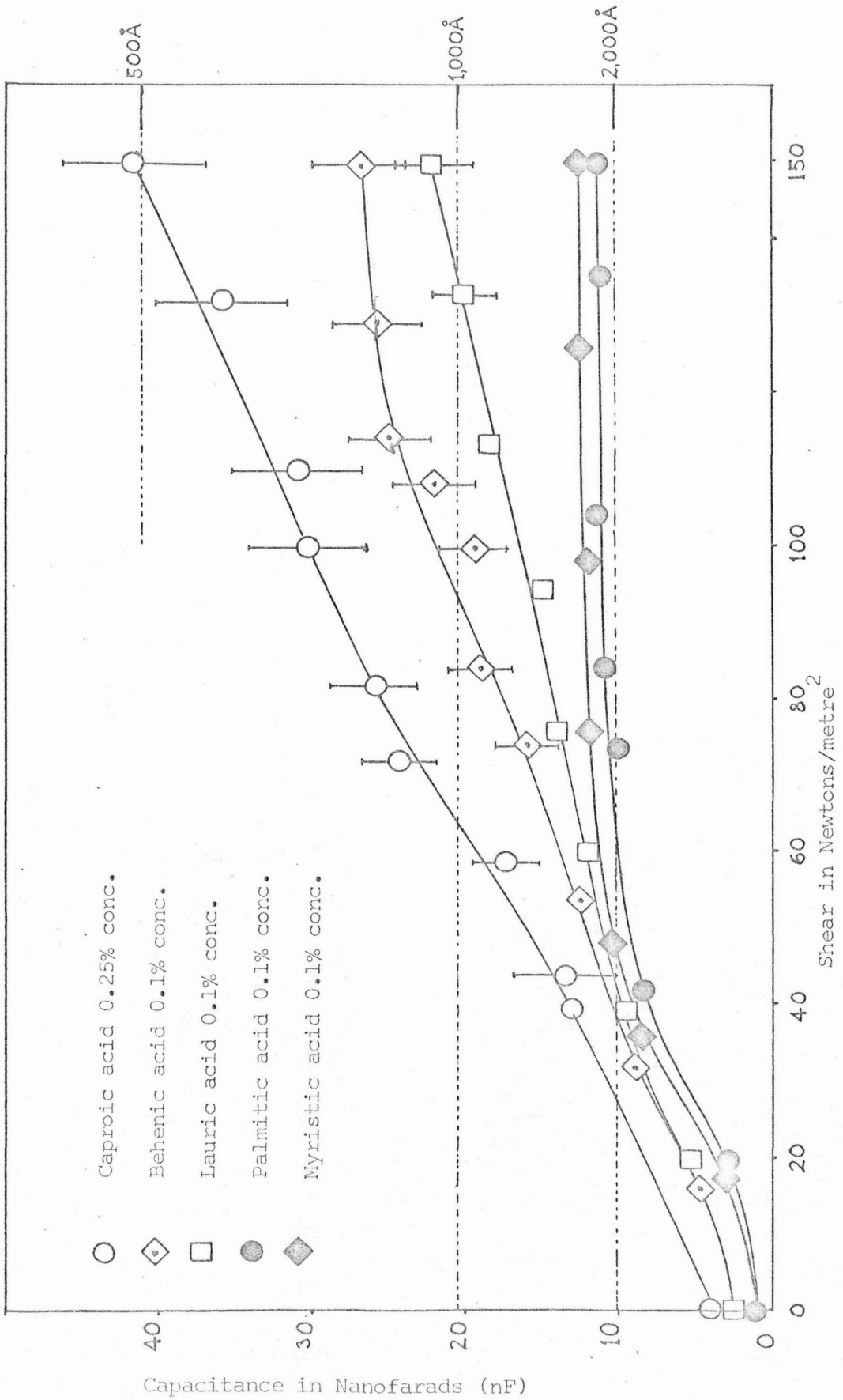
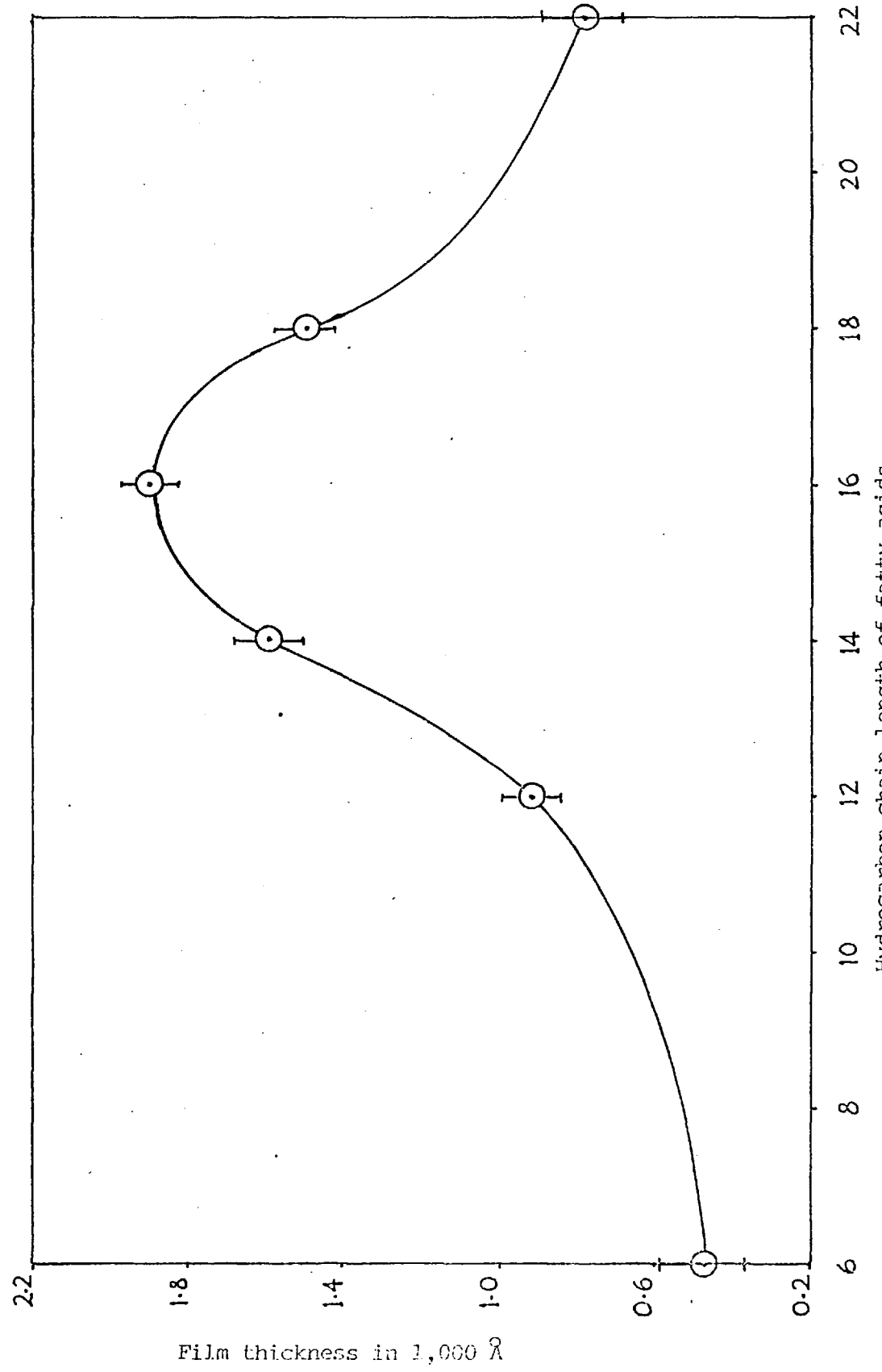


Fig. 4.5 Final film thicknesses after shear of 150 newtons/metre^2 v. fatty acid chain length



important to note, however, that although these films exhibited a much lower resistance to shear by their continued thinning than those in the second category, their final residual thicknesses underwent 60 minutes of continuous maximum shear (i.e. 150 newtons/metre^2) with no further thinning. In other words, these thinner films remained stable for this degree of shear.

The three fluids in the second category produce markedly thicker residual films able to withstand 60 minutes of the maximum applicable shear. The Myristic acid thins to 1,600Å, the stearic acid to 1,500Å and the palmitic acid to 1,800Å.

The constant film thicknesses were reached for values of shear between 40 and 60 newtons/sq. metre. This early period, as already mentioned, saw the removal of surplus fluid from the chemisorbed film structure. It appears, therefore, that once this surplus fluid had been squeezed from the films in the second category, little further thinning took place. This was corroborated by the interferometric observations of these films.

These final film thicknesses are plotted against the number of carbon atoms in the fatty acid molecule, i.e. hydrocarbon chain length, in fig. 4.5. The curve shows a marked peak for palmitic acid which has 16 carbon atoms in its hydrocarbon chain. As the name implies this is also the number of carbon atoms in the hexadecane molecule. This effect is known as chain matching, and is discussed fully at the end of this chapter.

4.3.3 Conductivity of the Various Residual Films

The conductivity of these residual films, unlike their capacitance, bears no direct relationship to their thickness. Nevertheless, it does give a qualitative measure of how well formed and coherent these films are. Again these results can be split into two categories, each containing the same fatty acids as in the previous section. The curves for the myristic, palmitic and stearic acids are shown in fig. 4.6, and those for

the lauric, behenic and caproic acids in fig. 4.7. The errors in these results are taken as the standard deviation of the spread of the conductivity readings for the three capacitor plates in each cell.

The curves for the acids in the first category (fig. 4.6) are very similar. The conductivity readings remain practically constant, below 15 μU , up to a shear of 80 newtons/metre^2, and then appear to increase reasonably linearly, with similar gradients, until the maximum shear is reached. The final values of conductivity, i.e. 62 μU ; 55 μU and 40 μU for the stearic, myristic and palmitic acids respectively, are so low that they introduce virtually no errors in capacitance readings above 2 nanofarads. This level is well below the values of capacitance equivalent to the relevant film thicknesses. It appears, therefore, that these three solutions produce residual layers of comparatively high electrical stability, the palmitic acid film evidently being the most stable.

The residual layers produced by the fatty acids in the second category exhibit much larger conductivity increases with shear. The lauric and behenic acids show comparatively slight increases for shears below 80 newtons/sq. metre. After this the two films' conductivities increase more rapidly, with similar gradients, to values of 280 μU and 540 μU respectively. Although these values are comparatively high, the calibration chart of Chapter2. shows that the equivalent capacitance readings will be only slightly affected. There is, however, a marked decrease in the electrical stability of these layers compared with those in the first category.

The caproic acid film exhibits large conductivity increases with shear even in the range below 80 newtons/metre^2. The slackening of this conducitivity increase in the higher shear range is certainly due to saturation in the amplifier of the bridge circuit. The final conductivity readings of approximately 940 μU are within 50% of the dry metal-mercury contact for these capacitors and under these conditions the results are

Fig. 4.6 Conductance against shear for the chain matching fatty acid, hexadecane solutions

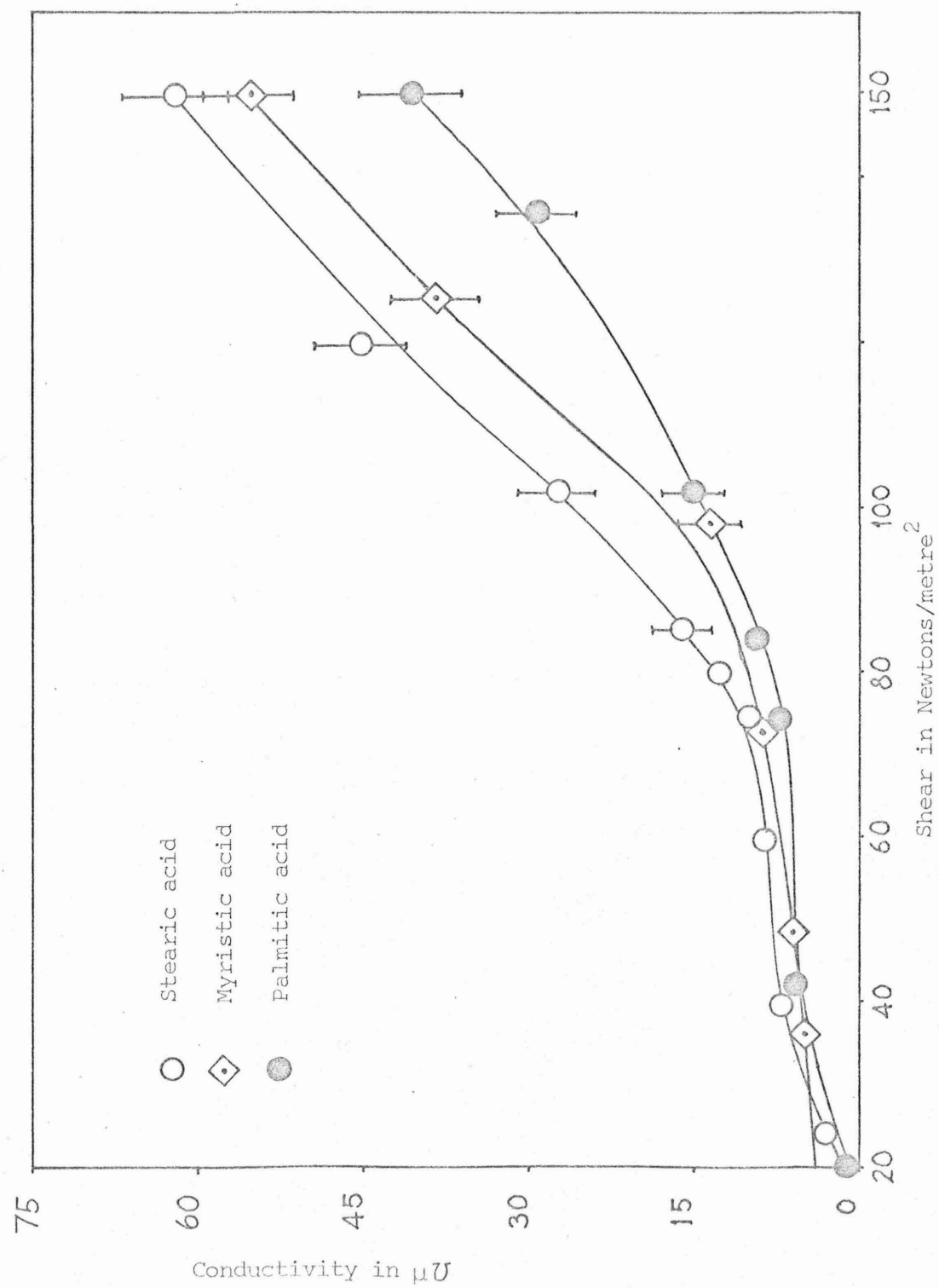


Fig. 4.7 Conductance against shear for the non-chain matching fatty acid - hexadecane solutions

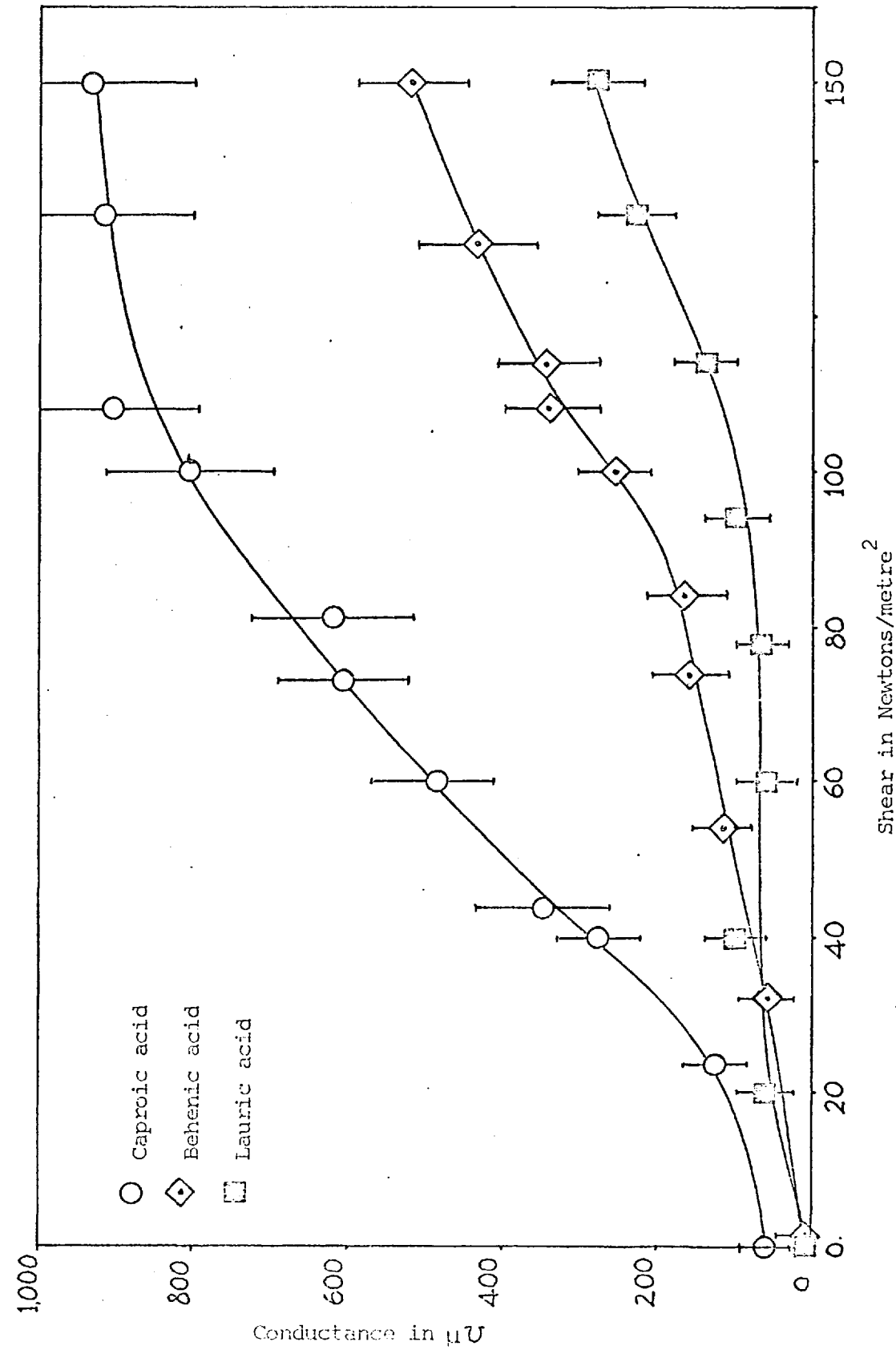
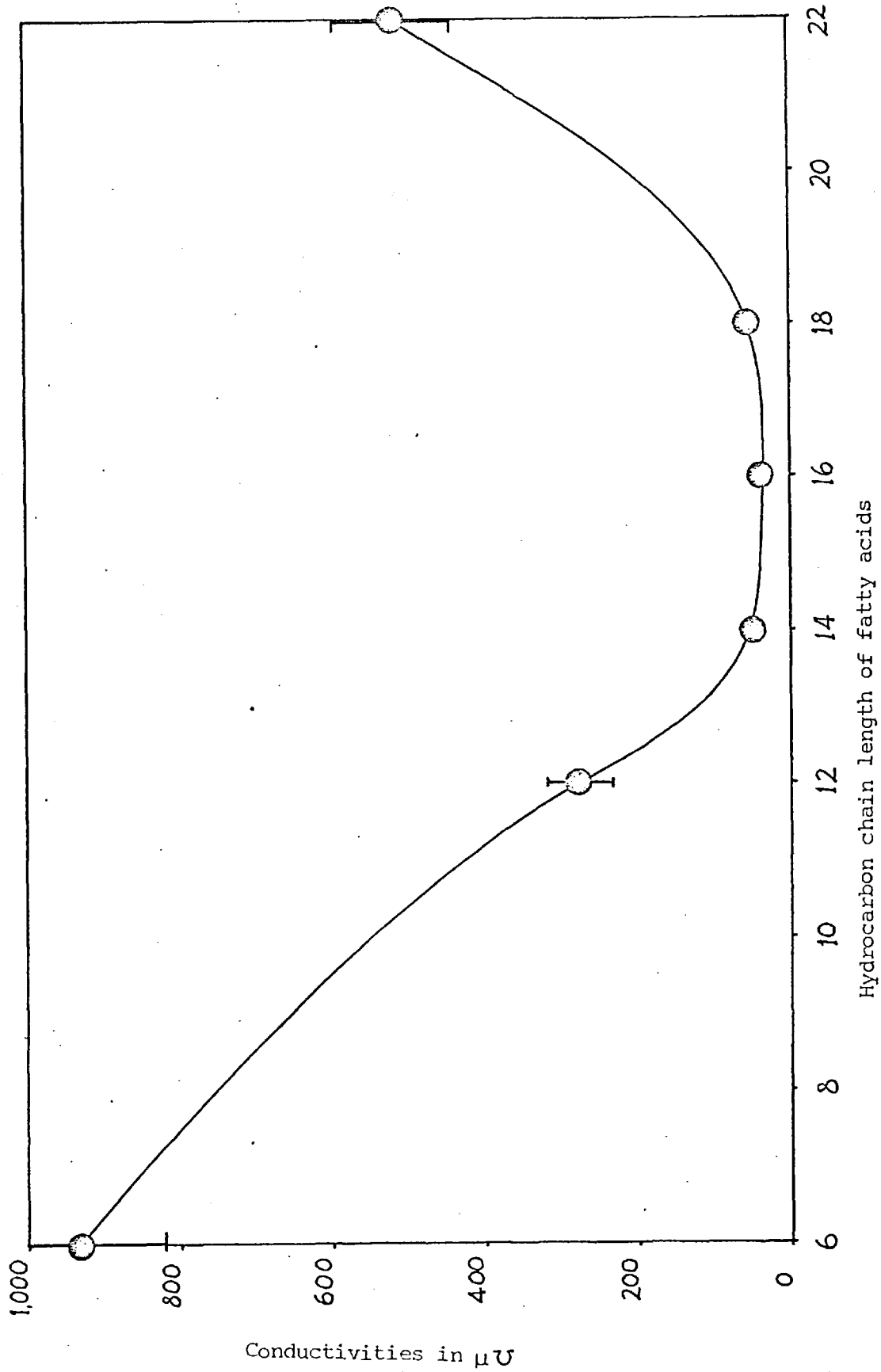


Fig. 4.8 Conductance after shear of 150 newtons/metre^2 v. fatty acid chain length



considered to be more qualitative than quantitative. Saturation in the amplifier results in the readings of both conductance and capacitance shown by the bridge being markedly lower than their actual values. The final residual film thickness of ~500Å calculated for this acid, therefore, is certainly too high, possibly by as much as 500%. This value of 500% was arrived at by simulation of the above results using various known capacitors and resistors in parallel, as for the original calibration, with additional resistors in series to allow for the overall resistance of the cell. These results clearly indicate that the residual film formed by caproic acid has been removed to a large extent from the chromium substrate by a tangential shear of 150 newtons/metre^2. Interferometric observations, described fully in section 4.4 of this chapter, also give the impression that the caproic acid thick film had physically broken down. As mentioned earlier, the concentration of this acid in hexadecane was 0·25% by weight as opposed to 0·1% for the other cases. This was because experiments carried out at the lower concentration were almost impossible to record accurately. The conductivity readings were high, even during the hydrostatic thinning, and as soon as shear was applied the conductivity became large enough to saturate the amplifier. This indicated that a coherent residual layer had not formed fully in the time allowed, hence the concentration was increased.

The final conductivity values were plotted against the acid chain lengths, as shown in fig. 4.8. This graph shows even more dramatically than fig. 4.5 the chain matching effect demonstrated by the myristic acid, stearic acid, and especially the palmitic acid solutions in hexadecane.

4.3.4 Thick Film Recovery

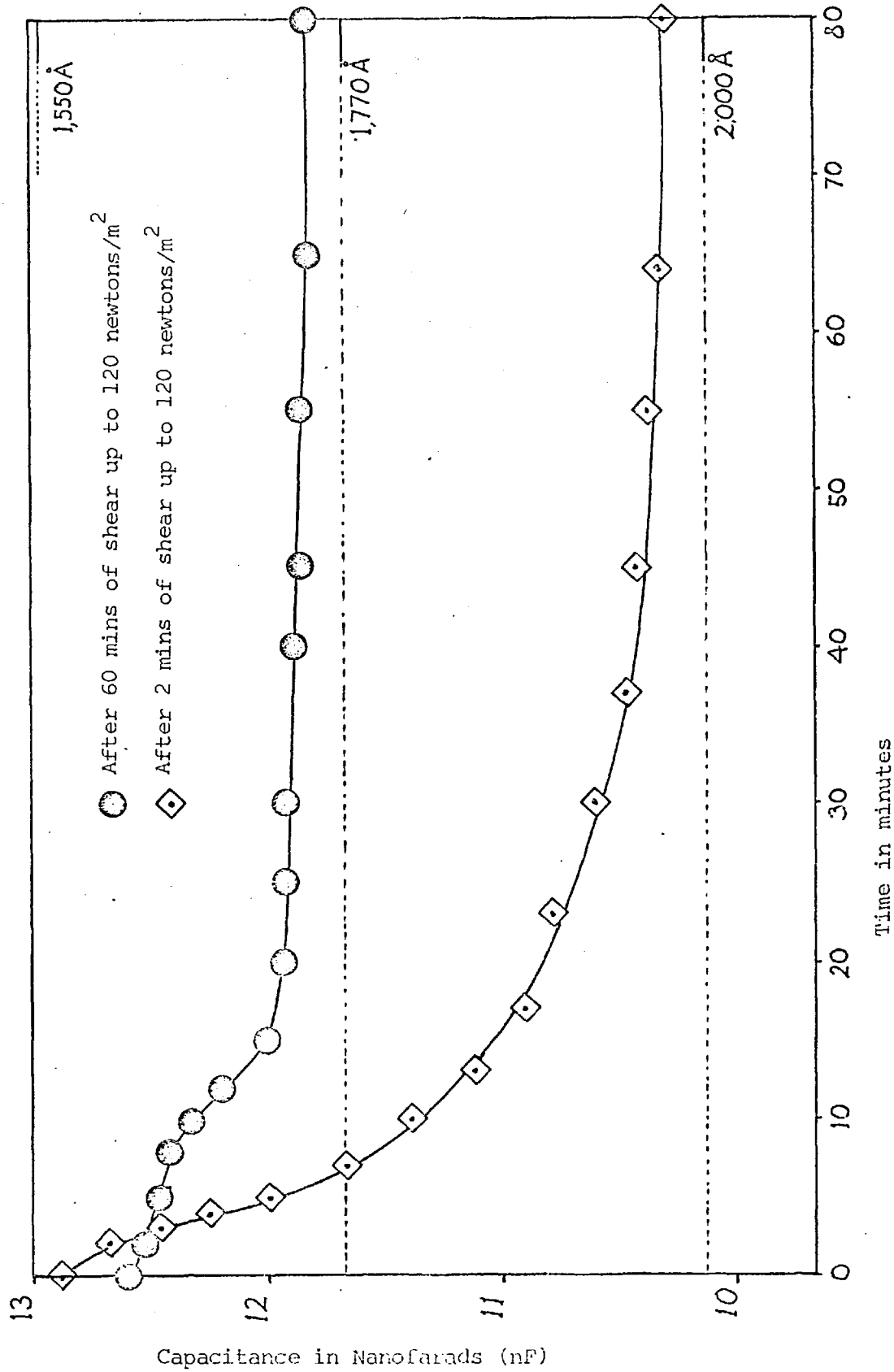
Here the behaviour of the residual films immediately after they had undergone varying periods of shear was investigated. 0·1% solutions of stearic acid in hexadecane were used. These solutions were again allowed

a thirty minute growing period followed by twenty minutes of hydrostatic thinning before shear was applied. They were then subjected to five two-minute periods of shear below 50 newtons/sq. metre to remove all the obvious surplus fluid as described in section 4.3.1. After this the test shear of 120 newtons/metre^2 was applied for periods varying from two minutes to sixty minutes. Immediately this shear was stopped a stop watch was started and any variations in the capacitance of the films observed.

The resulting curves are shown in fig. 4.9. Only the curves for the two extremes of duration of shear are plotted because the other results, for 15 minute and 40 minute periods, are almost duplicates of those for the 60 minute period. As can be seen, both curves show some recovery of the residual film thicknesses. The film that undergoes a mere two minutes of this shear recovers from 1,550Å to nearly 2,000Å, most of this growth being over the first 30 minutes. The films that experience the longer periods of shear, however, recover by less than 150Å to ~1,700Å in all cases. They increase to this thickness within 20 minutes.

The very large recovery shown by the film sheared for just two minutes is almost certainly due in the main to the remnants of the surplus fluid the bulk of which was removed by the earlier relatively low shear. This fluid, although more securely enmeshed in the fibrillar structure of the thick film, cannot be considered as a constituent part of the film as it is removed by prolonged shearing. Again, this is supported by interferometric observations. Hemispherical globules, of one or two orders of magnitude smaller than those described earlier, were seen to form and grow. They appeared firmly fixed until they reached a critical size, apparently determined by the local geometry of the film surface, when quite suddenly they would move off along the surface of the film in the direction of the mercury flow. After approximately 5 minutes of continuous shearing no remaining globules could be observed. It must be stressed that the poor

Fig. 4.9 Recovery of thick films of stearic acid after various periods of shear



interferometric conditions and the small size of these globules made them difficult to detect, more so than the larger ones mentioned earlier. They were not observed, therefore, until such phenomena were specifically looked for.

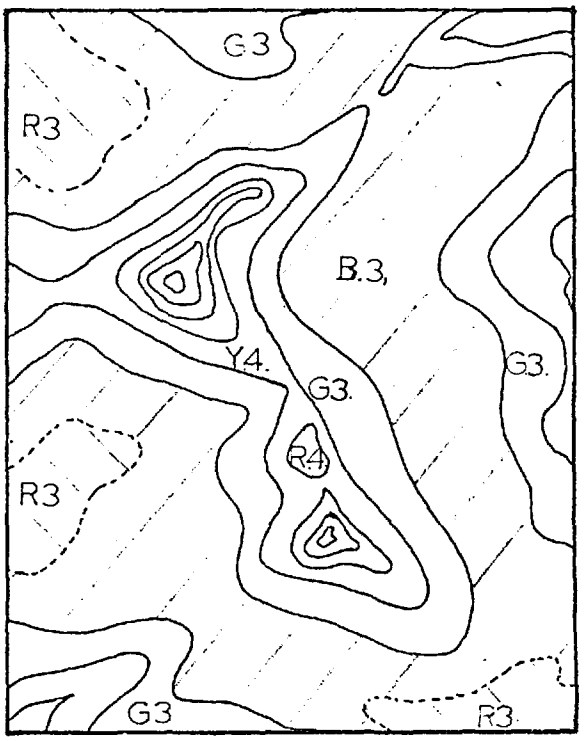
The fact that similar recovery curves were produced by the films thinned for longer, but varied, periods of shear suggests that all traces of surplus fluid had been removed. This duplicated curve can be considered, therefore, as showing the true recovery properties of the residual films produced by stearic acid.

4.4 Interferometric Results and Discussion

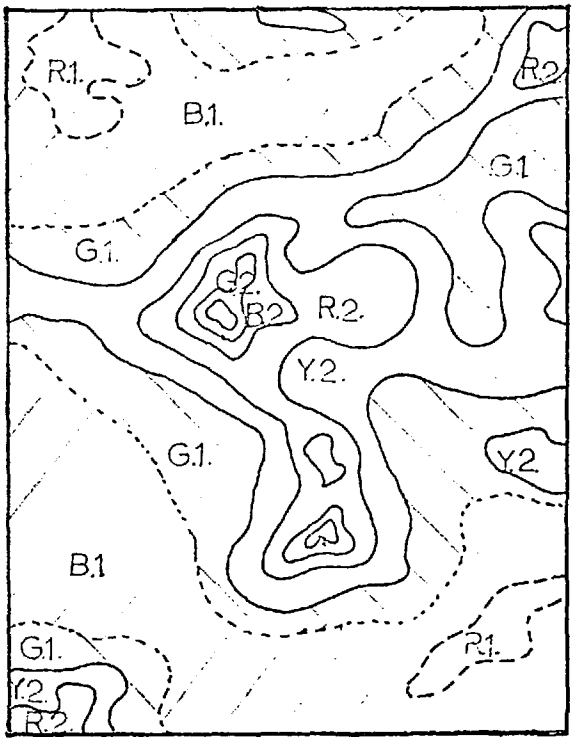
As mentioned above the thick films were originally studied optically in order to verify their existence. It became apparent that the interferometric technique could be used to observe the behaviour of the residual layers whilst undergoing shear and to corroborate the film thicknesses deduced from the capacitance measurements. Several of these observations have been mentioned already, and are discussed together with further optical results below.

4.4.1 Topography of the Thick Films

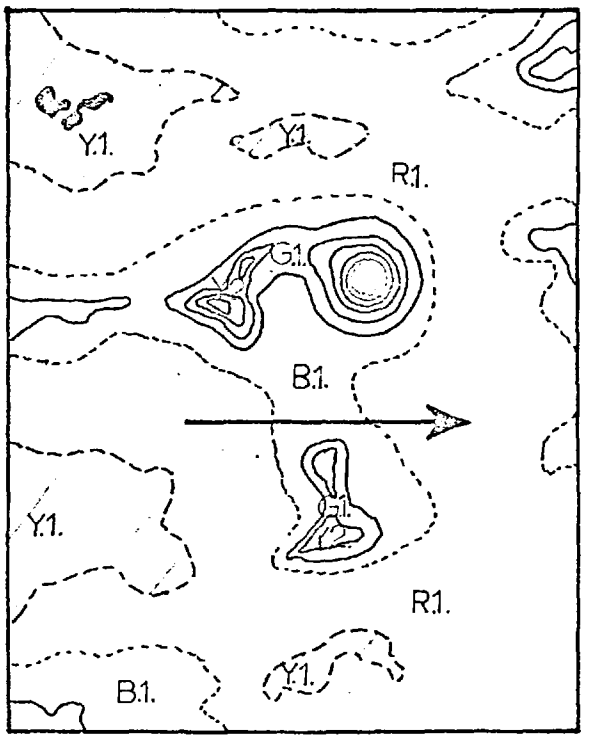
The diagrams of fig. 4.10 represent typical interferometric patterns produced by a thick film in various stages of thinning. The film was chemisorbed from a 0·1% stearic acid-hexadecane solution after a 30 minute growing period. At the beginning of the hydrostatic thinning process no fringes could be observed through the microscope the film being too thick. After 30 minutes, however, discernable interference patterns appeared and the microscope was centred on one of the most interesting of these and fixed for the rest of the experiment. Fig. 4.10, therefore, shows four aspects of the same feature in the thick film. Although the maximum magnification of the microscope was X160, the copying process included a



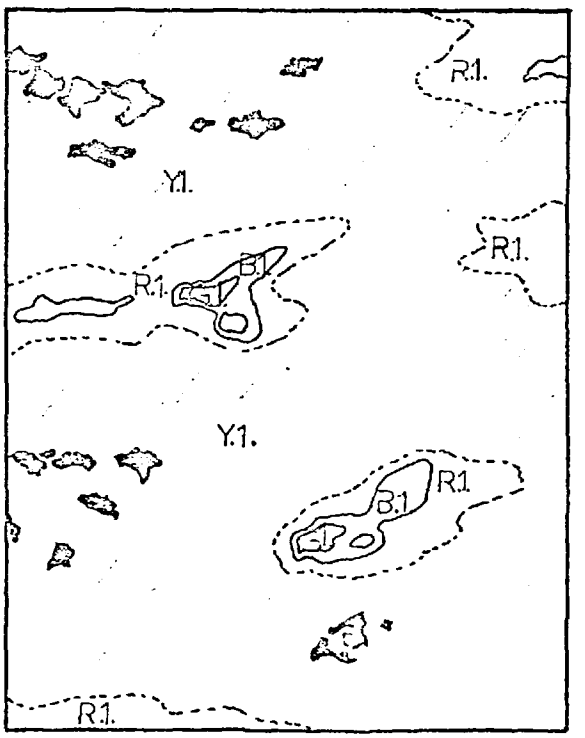
(a) After 70 minutes of hydrostatic thinning



(b) Thick film after 2 days of hydrostatic thinning



(c) Film undergoing shear of 40 Newtons/metre^2



(d) Final residual film after shearing of 150 Newtons/metre^2

Fig. 4.10 Interferometric topography of stearic acid thick film

further approximate magnification of X12, resulting in an overall magnification for the diagrams of about X2000. In each figure the shaded areas correspond to the thinner regions of the films.

Fig. 4.10.a shows the interferometric pattern after about 70 minutes of thinning due to the hydrostatic pressure of mercury. At this stage the movement of the fringes, corresponding to the thinning of the film, was very slight but just detectable over a period of minutes. The fringe colours were also very faint at this stage. The capacitance at this time was read as 3·1 nanofarads. This corresponds to an average film thickness of ~ 6,500Å, assuming a dielectric constant of 2·2 for the film. Even at this early stage the film was not uniform but can be seen to have consisted of 'hills' and 'valleys', varying as much as 4,000Å in depth.

The residual film pattern, after two days of thinning, is shown in fig. 4.10.b. The capacitance was 8·0 nanofarads corresponding to an average film thickness of 2,500Å. The fringes were now much clearer and the colours more distinct. The major features appear in the same position as in the previous diagram, their shapes chaging very little. The height of the outcrops has decreased to the order of 5,000Å, whereas the majoritory of the film appears between 2,000Å and 3,000Å thick.

Fig. 4.10.c shows this thick film whilst undergoing a shear of 40 newtons/metre^2, the arrow indicating the direction of the mercury flow. The film had already experienced two 2 minute periods of low shear, and the third period was elongated so that the interference pattern could be copied accurately. The outcrops are still similarly positioned although their shapes have changed quite markedly. They are now about 4,000Å high, whereas the bulk of the film appears generally more uniform at around 1,500Å to 2,000Å thick. The capacitance could not be measured whilst the mercury was in motion, but once stopped it was read as 11·2 nanofarads.

Two interesting features have appeared in this diagram. Firstly, one of the "hemispherical globules" mentioned earlier has grown near the

centre of the figure. It is not possible to estimate the height of this feature accurately as the fringes overlap near the middle. It is unlikely, however, that it would be more than 6,000Å deep at the most. The base measures over 1 cm. in the diagram, which is equivalent to more than 50,000Å across. It appears, therefore, that the globules are not perfectly hemispherical, but are squashed flat by the applied pressure. It is interesting to note that the globule has grown in the 'shadow' of one of the outcrops, i.e. directly behind it in the line of shear. The globule moved off in an E.N.E. direction shortly before the shear was arrested. These observations coupled with the symmetry and sudden appearance of the globule under increased pressure seem to comply with the theory that they consist of surplus base fluid (hexadecane) squeezed from the film structure.

The other new feature was the appearance of the dark regions (grey-blue in colour) in the top left hand corner. These correspond to film thicknesses below 1,300Å, and, almost certainly, to the 'weak spots' mentioned in Chapter 3 in connection with the electrical breakdown of the thick films under shear. It cannot be deduced how much thinner than 1,300Å the film is in this region. An interesting point, however, is that when the mercury flow was stopped these dark grey-blue areas disappeared almost immediately, being superimposed by the first order yellow fringe.

The fourth diagram, fig. 4.10.d, shows the thick film after it has experienced 60 minutes of the maximum applicable shear (150 newtons/metre^2). The film now appears as predominately first order yellow, and the outcrops have become aligned in the direction of shear, the lower one apparently having moved in that direction. They barely exceed 3,000Å in height, whilst the vast majority of the film is about 1,500Å thick. The capacitance was measured at 13·4 nanofarads. The dark grey-blue regions have increased in number and no longer disappear when the shear ceases, although some of them decrease in size. The interference patterns now appear identical both

when the film is undergoing shear and when the mercury is stationary. In fact the film was left for several days with no further variations in these patterns.

Although the results described were obtained with stearic acid, very similar interference patterns and trends were observed for the myristic and palmitic acids. The films produced by the 0·1% solutions of lauric acid and beheric acid in hexadecane gave patterns that were initially quite like those above, but, under shear, showed much larger regions of dark grey-blue. No hemispherical globules were observed when the thick films of these acids first experienced shearing. When the film produced by caproic acid was exposed to shear large regions of dark grey-blue appeared almost immediately. They were seen to enlarge and combine as the shear was increased until in many positions they filled the field of view of the microscope. The magnification, therefore, was reduced so that most of one chromium plate could be observed. Above a shear of 120 newtons/metre^2 these dark grey-blue areas combined to produce a region with no colour fringes at all across the middle of the chromium plate in the direction of shear. This area could be described as a wear track where any chemisorbed film along it had been completely removed by shearing, at least down to the order of a monolayer. Interference patterns remained at either side of this track, indicating the existance of a thick film surviving in the regions of lower shear.

4.4.2 Variation of Thick Film Dielectric Constant

The possibility of variation of the relative permittivity of a thick film was studied by calculating the film thickness from simultaneous interferometric and capacitance measurements. If the two values are similar it seems reasonable to conclude that the dielectric constant has not altered. The liklihood of the dielectric constant and refractive index of the film varying identically so that similar film thicknesses would still be obtained is very slight and may be neglected.

The film thicknesses corresponding to the colours listed in the interferometric calibration table of Chapter 2.5.4 are for a medium with refractive index of 1·0. The actual film thicknesses are obtained by dividing by the refractive index of the medium concerned. In this case a 0·1% stearic acid-hexadecane solution was used, their respective refractive indeces being almost identical at 1·433 and 1·434. The thicknesses corresponding to each calibration colour for this solution are set down in Table 4.1. The dielectric constants of the hexadecane and stearic acid at the bridge frequency are again very close, being 2·03 and 2·29 respectively. As these films have been shown to contain a large proportion of reaction product, the dielectric constant of the metal soap of stearic acid should be considered. Smith (5) measured this at 2·28 although there was no guarantee that the substance this value was obtained for would resemble the composition and structure of that produced in the thick films. Nevertheless, the reduction in polarity of the acid molecules on formation of the soap makes it unlikely that the dielectric constant would vary to any significant degree. An average value of 2·2, therefore, is used in these calculations.

In the diagrams of fig. 4.10 a large spread of colours is evident for cases a, b and c. As the region shown represents only a very small proportion of the whole capacitor plate it is apparent that in these cases it would be extemely difficult to accurately assess the average film thickness from optical measurements. This is not so for fig. 4.10.d, where 80% of the whole capacitor plate showed a first order yellow fringe. ~15% showed outcrops varying through first order red, blue and green and the other 5% consisted of the dark grey-blue regions of unknown thickness. Using the thicknesses deduced from these colours the film may be considered as a set of capacitors in parallel, the total capacitance being the sum of the constituent values, calculated in Table 4.2 using E = 2·2:

Table 4.1 Colour-thickness calibration

Colour	Actual Film thickness in Å (10^{-10} m).			
	1st order	2nd order	3rd order	4th order
Yellow	1,400	3,280	5,300	7,330
Red	1,880	3,000	6,000	8,000
Blue	2,370	4,250	6,300	8,700
Green	3,000	4,670	6,200	

Table 4.2 Colour-capacitance calibration

Colour	Percentage Area	Optical Thickness (Å)	Corresponding Capacitance/cm^2
Dark grey-blue	$\sim$ 5%	$<$ 1,200 Å	$\sim$ 20nF/cm^2=C_1
1st order Yellow	$\sim$ 80%	1,400 Å	14.3nF/cm^2=C_2
Ist order red - green	$\sim$ 15%	$\sim$ 2,500 Å	$\sim$ 8.0nF/cm^2=C_3

This gives a value for the total capacitance of

$$C = 5\% \times C_1 + 80\% \times C_2 + 15\% \times C_3$$

$$= 13.64 nF/cm^2$$

This compares with the capacitance measured in this case for the 1 square cm. chrome plates of 13.4nF. Although several quantities in the above calculation are only vaguely assessed the similarity of these two values indicate that there is no significant variation in the dielectric constant of the thick film constituents. Comparable calculations were carried for other films produced by palmitic acid, myristic acid and lauric acid with similar results. It seems reasonable to conclude, therefore, that in these experiments the relative permittivity of the soap films retain constant values of between 2·2 and 2·3.

4.5 General Discussion and Conclusions

4.5.1 Summary of Results

The results of both Chapters 3 and 4 provide strong evidence that the thick films adsorbed on metal substrates from fatty acid-hydrocarbon solutions are of a predominantly chemical nature. The interferometric patterns produced by these films concur with the electronphotomicrographs obtained by Smith (5) showing the reaction product to be of an enmeshed fibrillar structure.

The fibrils of these soap films are substantially aligned under tangential shear in the direction of flow producing a comparatively uniform film. The thickness of the resulting films is almost independent of their initial conditions, being mainly related to the chain lengths of the fatty acid and solvent hydrocarbon. Where chain matching occurred the resistance to shear and coherence of the thick films were markedly enhanced.

Only the caproic acid film was broken down physically, above a shear of 120 Newtons/metre^2 ($\sim$ 1·2 gm/cm^2). The greater endurance of the behenic

acid film indicates that the shear strength of thick films generally increases with fatty acid chain length regardless of the molecular structure of the solvent.

The films exhibit properties of recovery on cessation of tangential shearing, suggesting some form of elastic deformation of their structure under shear.

4.5.2 Discussion and Conclusions

Before comparing any of the results described above with those reported by Fuks, some differences between the two types of apparatus used should be mentioned. The most important variation is that the thick films produced in Fuks' apparatus underwent shearing and compression within a reservoir of test fluid. Repair of his thick films by the surplus surfactant fatty acid additive, therefore, was possible throughout his experiments. It has been shown that in this work the shearing method removes surplus test fluid very early in the shearing process. The thick films experience starvation conditions and their ability to repair themselves is greatly impaired. It seems reasonable to expect, therefore, that the thick film shear strength measured here should be below that measured by Fuks for the same acid. The less marked recovery capabilities reported above may also be accounted for in this way. Another difference is that thick films would be expected to form on each surface of the two discs used in Fuks' experiments. As a result the applied shear would be dissipated by deformations in both films. In this work only one thick film is present. The absence of a solid oxide layer on the mercury prevents any thick film formation on it. The applied shear must therefore be taken up by the one film. Also, the shearing in Fuks' work is predominantly static, whereas in this research it is dynamic. The added possible complication of turbulence must therefore be taken into account, as discussed in Appendix A.

Although these facts undermine the value of quantitative comparisons between the two sets of results there are some marked similarities. The effects of acid chain length and various solvents detected by Fuks, shown in fig. 4.2, indicate a similar interrelationship to that found in this work, figs. 4.5 and 4.8. Decreasing coefficients of static friction, presumably equivalent to increasing film thicknesses, occur for increasing fatty acid chain length. Fuks did not test any chain matching solutions and so, understandably, the effect does not show in his results. He also found similar increases in shear resistance for decreasing film thickness, comparing figs. 4.1.b with 4.3 and 4.4. Nevertheless, the actual values of shear strength vary. He found that a 1,500Å thick film from a 0·05% stearic acid in iso-octane solution had a shear strength of ~ 15 gm/cm^2. In this research the final residual film of a 0·1% stearic acid-hexadecane solution, also 1,500Å thick, was produced at a shear of 150 Newtons/metre^2, i.e. $\sim 1{\cdot}5$ gm/cm^2. This difference of an order of magnitude is probably explained by the difference in apparatus. Lastly, he also detected recovery in the thick films on decreasing the normal load. It has already been described in this chapter how the presence of a comparatively small amount of surplus test fluid produced a much larger effect than that due to the thick film alone, see fig. 4.9. The large recovery effects, shown in fig. 4.1.a, reported by Fuks are almost certainly due mostly to the large amount of surplus fluid present in his experiments. Nevertheless, a thick film structure is necessary for any recovery to occur, and there is a similarity between the periods of recovery in the two sets of results.

The proximity of these results produced on two very different types of apparatus suggest that Fuks' research should be regarded as being generally correct. On the other hand, his theory that the shear properties of the thick films are largely independent of the chemical properties of the surfactant molecules is almost certainly wrong, as the films are actually

produced by chemical reaction.

The relevance of the thick films to most lubrication systems remains uncertain. On the one hand Fuks observed that they reduced the coefficients of friction at 200,000 psi in a sliding four ball machine to values similar to those found at low pressures. Conflicting results were produced by Gentle (6) using an optical ball on disc apparatus to test a fluid, shown to form a thick film in the ball apparatus. He found no reduction in the coefficient of friction nor increase in the elastohydrodynamic film thickness at both high and relatively low contact pressures. It is possible that surface roughness plays an important role in the retention of the thick films, once formed. Reasonably, the films may be expected to be retained in the valleys between the larger asperities on which they would be reduced to a monolayer, or completely removed. In this way they could keep such asperity contacts down to a minimum, resulting in a comparatively low coefficient of friction. On an extremely smooth surface, however, there would be no asperities to retain the films when subjected to shear in excess of their shear strength. The fact that Gentle used a highly polished ball (better than 1 μ inch c.l.a.) in his work to produce good interference fringes may, therefore, account for the difference between his results and those of Fuks, if surface roughness is an important factor.

The interferometric results described above, coupled with the electronphotomicrographs produced by Smith (5) are very strong evidence of the fibrillar structure of the thick films. The actual structure of the individual fibrils should now be considered in relation to their measured shear strength. Akhmatov (7) discussed in some length the findings of Bowden and Tabor (8) that soap films were capable of withstanding considerable deformations without rupture owing to their high lateral cohesion. Akhmatov did not accept this explanation, arguing that the relevant London-Vander Waal dispersion forces are too weak to produce such a large increase in strength.

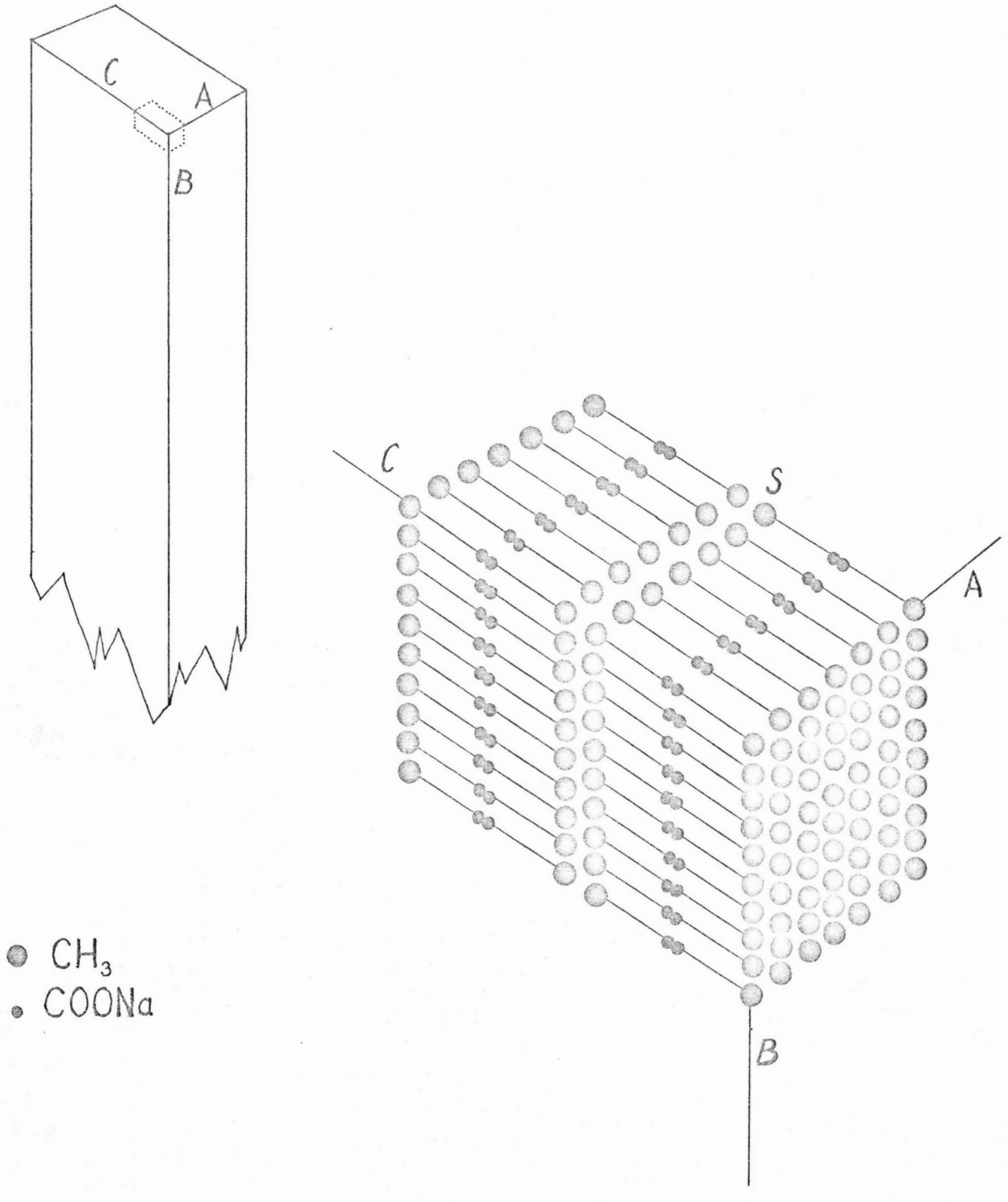


Fig. 4.11 Scheme of Structure of a soap fibril. Carbon chains of the soap molecules $CH_3 - (CH_2)_n - COONa$ are perpendicular to the fibril length, B. The planes of easy slip, S, are parallel to the length of the fibril (according to Thiessen (9)).

He invoked the presence of a long range force field due to the metal substrate to explain the effect.

Thiessen (9) studied the fibrillar structure of soaps, showing that the carbon chains are oriented roughly perpendicularly to the length of the soap filaments, see fig. 4.11. Akhmatov assumed that these fibrils would be arranged normal to the metal surface and, therefore, that the chains were aligned in the direction of flow. He then argued that sliding would occur between the methylene (CH_2) groups, the weak London dispersion forces producing very little resistance to shear. The results described above and by Smith, however, indicate that the fibrils are oriented somewhat randomly between the normal and horizontal. Their behaviour during shear further indicates that they are strongly adsorbed at one end with the other end free to become aligned approximately in the direction of flow. It seems very unlikely, therefore, that the carbon chains could be similarly aligned, giving a low shear strength. The important factors in the shear resistance of these fibrils, therefore, would be the elastic strength of their overall crystalline structure and the strength of the chemisorption bond at the metal oxide interface. Of the two, the former is generally weaker.

The observed importance of chain matching of acid and solvent molecules to the thickness and shear strength of these films can be explained best also by considering a randomly oriented crystalline fibril structure. The lattice strength of crystals is known to decrease markedly with increasing numbers of lattice defects, or discontinuities. In the formation of the soap fibrils it seems reasonable that a large number of solvent molecules would be trapped in the fibril crystalline structure. The lateral cohesion of the pure hydrocarbon would be similar to that of the carbon chains of the soap molecules. Only in the plane of the dipole-dipole interactions would the lack of a polar end group slightly reduce the strength

of the crystal lattice. When the hydrocarbon is of dissimilar length to the soap molecules, discontinuities in the lattice at the loci of the hydrocarbons are almost certain to result, producing a larger decrease in lattice strength. If, however, the chain lengths match, then these defects would be reduced to a minimum, the resulting increase in lattice strength being generally larger than the decrease due to the lack of polar end groups in the hydrocarbons included in the close packed structure. A review of the important research showing the existence of chain matching is included in Smith's Ph.D. Thesis (5), but only Smith himself and Askwith, Cameron and Crouch (10) considered systems where thick films and/or polymolecular layers may be produced.

CHAPTER 5

EXPERIMENTS WITH THE BALL APPARATUS

5.1 Introduction

The ball apparatus, used extensively by Smith (1), was included in this research to test fluids of unknown or complex chemical nature for any thick films. Those fluids producing thick films could then be investigated further in the cell apparatus. This process proved a great time saver, the ball apparatus being much quicker and simpler to clean and operate than the cell apparatus. During the course of these preliminary tests other anomolous effects appeared which were not exclusive to those fluids producing thick, chemisorbed films. Further experiments were carried out, therefore, in an attempt to isolate these effects and throw some light on their cause. It became clear that the apparatus in its present state was not sensitive enough for these more specialised experiments.

5.2 Experimental Procedure

Whichever cleansing method was used the freshly cleaned ball was quickly plunged into the test fluid, above the mercury in the test tube. After it had been left fully immersed in the lubricant for the required period the ball was lowered gently into the mercury until completely covered, a clock being started simultaneously. The variation of the capacitance of the system with time was noted, and from this a thinning curve for the oil film plotted on log-log paper.

In some cases the dry metal-mercury contact was checked before an experiment. For this the ball was cleaned as before and immersed in a test tube containing only mercury. The conductance between the mercury and specimen was then measured by the bridge. The test fluid was poured onto the surface of the mercury, the ball raised until completely covered by the oil and the process then continued as before.

5.3 Results (& Discussions)

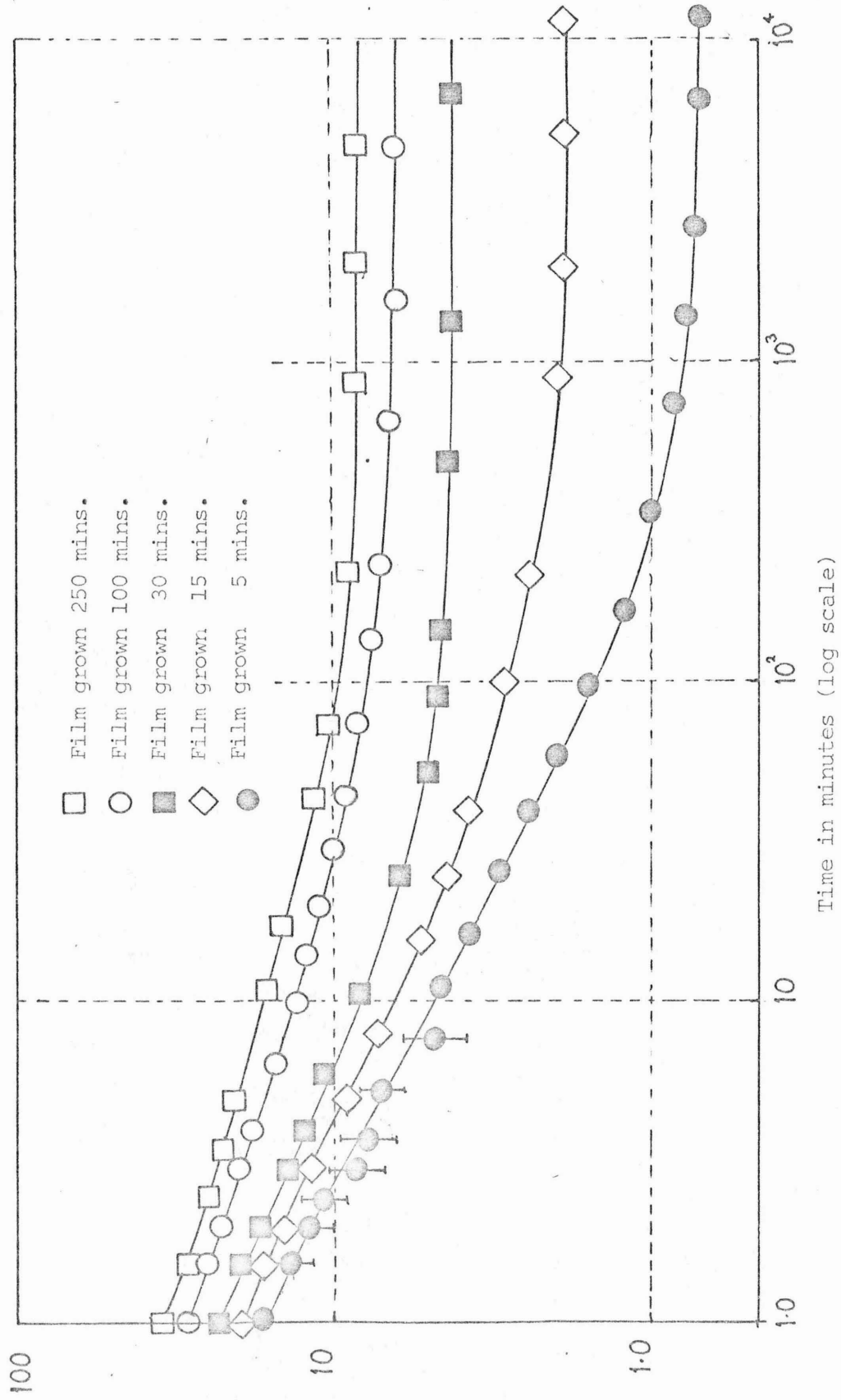
5.3.1 0·1% Stearic Acid in Hexadecane

Work described in Chapter 3 demonstrated a positive relationship between the final residual film thickness on the chrome substrates of the cell apparatus and the concentration of stearic acid solutions in hexadecane. In this section the variation of the final film thickness with the time of immersion of the metal surface in the test fluid prior to thinning (the growing period) was investigated. The aim was to establish experimentally the optimum time necessary to grow a coherent chemisorbed film.

The experiments were carried out for growing periods increasing from 5 minutes to ten hours, at ambient temperature (i.e. 20°C - 22°C). As justified optically in the previous chapter, the relative permittivity of the solution was taken as being $\sim 2{\cdot}2$. The film thicknesses were calculated from the capacitance readings using this value.

The thinning curves of the fluids are shown in fig. 5.1. They demonstrate that the longer the growing period the slower the rate of thinning and the thicker the final residual film. It is interesting that for the solution grown for only five minutes the early region of the thinning curve is affected by electrical instability. This is shown by the error bars introduced because the conductance in the oil film had risen enough to affect the capacitance readings, albeit only slightly, as demonstrated in the calibration curves of Chapter 2, fig. 2.7. This instability indicates that a coherent chemisorbed film had not had time to form and completely cover the ball surface resulting in regions of electrical weakness in the film. Possibly these were situated around asperities on the ball surface. After ten minutes, the conductance fell from $\sim 200\,\mu\mho$ back to a value of less than $10\,\mu\mho$. In all the other thinning curves the conductivity never rose above this $10\,\mu\mho$ region. It appears, therefore, that the residual film continued to form over the entire surface of the

Fig. 5.1 Residual film thickness v. growing time for 0.1% stearic acid in hexadecane solutions



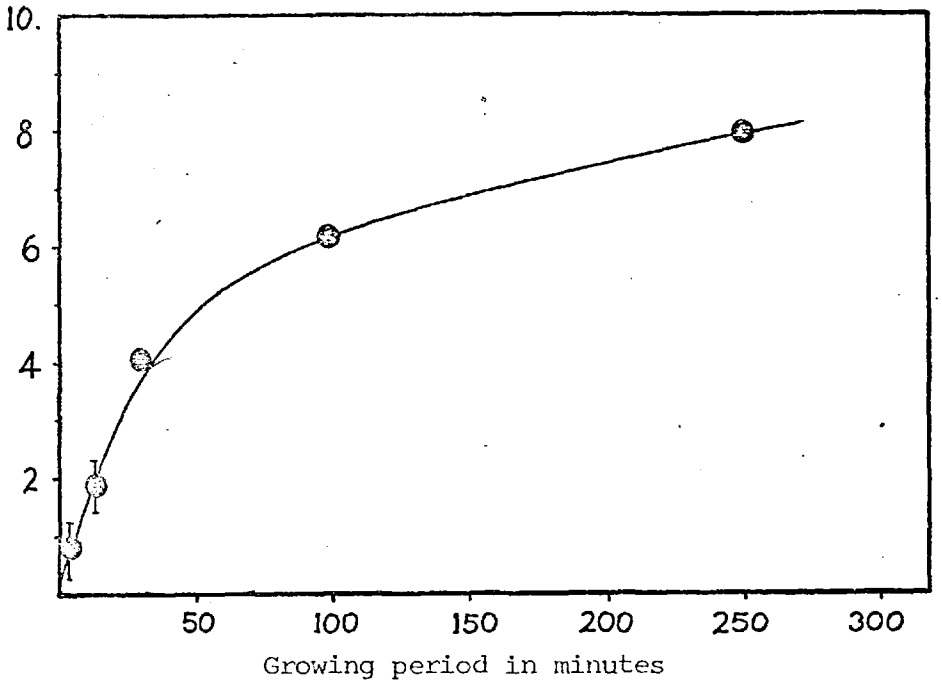


Fig. 5.2a Growing period v. final film thickness for 0.1% stearic acid in hexadecane solutions on stainless steel

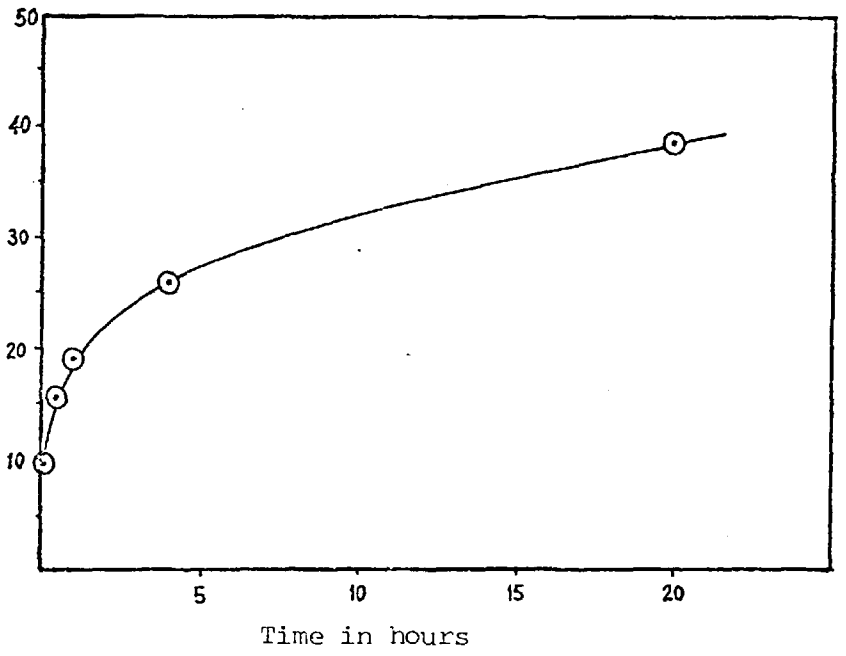


Fig. 5.2b Adsorption of stearic acid on copper powder at 23°C (from Bowden and Tabor (2))

ball whilst undergoing squeezing by the mercury.

The final residual film thicknesses are plotted against growing period in fig. 5.2.a. Initially the final film thickness increases rapidly, but for the growing periods above 30 minutes this tendency quickly declines. The errors in the first two points on the graph are twice the mean deviation calculated from the spread of results taken for repeated experiments at each growing period. This was the method used throughout this chapter to estimate errors, unless the conductivity had risen above the critical level given in the calibration curves of Chapter 2 fig. 2.7. These deviations are too small to show on the other points on the graph.

By varying the temperature in similar experiments with the ball apparatus Smith (1) showed that, below 100°C, 0·1% solutions of stearic acid in hexadecane followed Arrhenius' Law, i.e.

$$U = Ae^{-E/RT}$$

where U is the chemical reaction rate, E and A are constants depending on the reacting agents, (E is the activation energy) & R is the gas constant,

and T is the absolute temperature.

He quotes this as being further evidence of the chemical nature of thick films, the film thickness being a direct measure of the degree to which reaction has proceeded. Using this relationship there is a marked similarity between the graph of fig. 5.2.a and that produced by Bowden and Tabor (2) for the adsorption of stearic acid on copper powder, fig. 5.2.b. They interpreted the difference between the isotherms produced by the acid and octadecyl alcohol as indicating continuous chemical reaction between the copper and the fatty acid producing a multilayer, whereas the alcohol produced a close packed physically adsorbed monolayer. They also mentioned the appearance of a pale blue colouration of the solution after some hours, suggesting that some of the copper stearate reaction product had dissolved in the solution. This may account for the apparent difference

in the multilayer thicknesses in the two graphs.

These curves cannot be interpretted in terms of simple first, second or third order chemical reactions. Reactions at a surface, however, can usually be broken into the following steps, according to Moore (3)

(i) Diffusion of reactant(s) to surface.

(ii) Adsorption of reactant(s) at surface.

(iii) Chemical reaction on the surface.

(iv) Desorption of reaction products from surface.

(v) Diffusion of products away from surface.

These are consecutive steps, and if any one is much slower than all the others it becomes rate determining. Usually step (iii) is slowest and rate determining, but as there was no obvious reaction order, this does not appear to be the case here. Diffusion, as in steps (i) and (v), is normally a rapid process. It appears, therefore, that step (iv) is the rate slowing process, i.e. the desorption of the reaction product from the surface is very slow. This corroborates the results of Chapter 4 where the thick films were shown to consist of strongly adsorbed fibrils consisting mainly of the crystalline and semi-crystalline reaction product (i.e. metal soap). Although some of the soap molecules and macro-molecules must desorb to produce the observed fibrils it is apparent that the available number of adsorption sites in the oxide layer will decrease rapidly once a monolayer has formed. Further reactions probably occur at the relatively few new sites made available from swelling and disintegration of the oxide layer caused by the penetration of soap molecules.

The period necessary for a coherent multilayer to form probably corresponds to the knee in the graph occurring between 25 and 40 minutes. In most of this work, therefore, a growing period of 30 minutes was used, producing, for 0·1% stearic acid-hexadecane solutions, thick films between 4,000Å and 5,000Å with a high degree of reliability.

5.3.2 The Fluids Supplied by N.A.S.A.

These fluids were supplied to be tested for their capabilities of giving thick residual films before the mechanisms of such films were fully understood. Because of this they cover a wide range of chemical properties and viscosities which are given in Table 5.1. The dielectric constants of some of these fluids were known. The values for the remaining fluids were deduced using a hollow cylindrical capacitor of known separation. The fluid concerned was introduced into the gap between the parallel plates and the capacitance measured. Using the equation stated in Chapter 2 the bulk relative permittivity of each fluid was then calculated.

Amongst these fluids there are two distinct groups, the esters and the hydrocarbons. The remaining fluids are grouped together for the sake of convenience.

a. The Esters

Four of the fluids supplied were esters and their thinning curves are shown in fig. 5.3. None of them gave any signs of residual films and so, initially, were thought to be of little interest. On reexamination, however, several points became apparent.

The first is that three of the four fluids thin with a gradient of about $-\frac{1}{2}$ in the latter half of their curves. This is equivalent to a relationship for the film thickness of

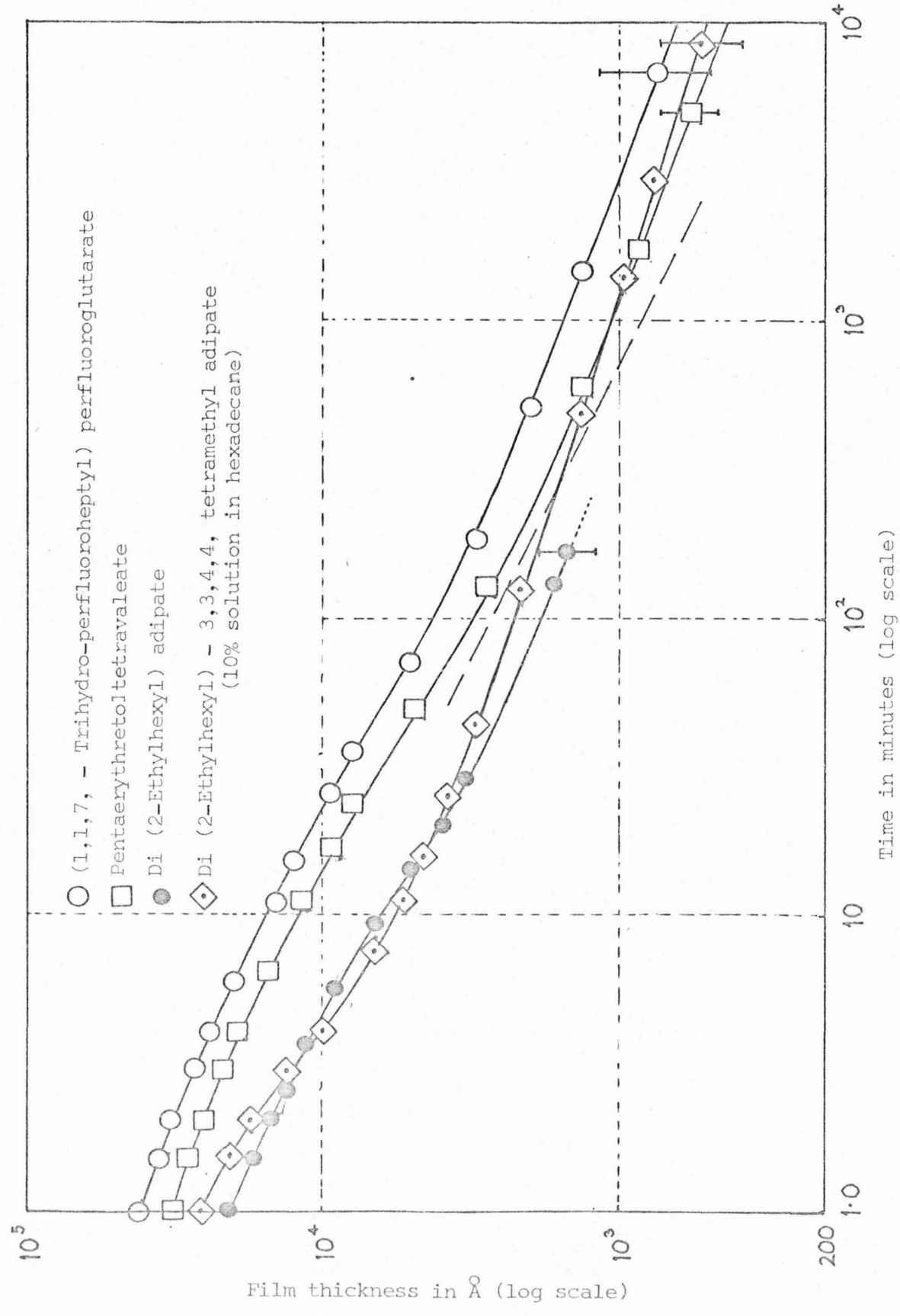
$h \propto (t)^{-\frac{1}{2}}$ where t is the time of thinning.

Earlier workers in this field (4,5,6) using loaded parallel metal plates to squeeze the test fluid from between them also found such a relationship. As the Stefan-Reynolds equation covered the kinetics of these systems such a relationship would be expected if the behaviour of the test fluid were Newtonian, i.e. its viscosity remained constant. It may reasonably be expected, therefore, that the fluids in the ball apparatus should also fit this relationship, especially when the oil films are thin so that small areas of the ball and mercury surfaces may be approximated to parallel metal

Table 5.1 Density and kinematic viscosity of test fluids at room temperature (21°C)

Test Fluid	Density (g/cm^3)	Kinematic viscosity (c.stokes)
Pentaerythritol-tetravalerate	1.015	26.98
Polyethyleneglycol (UCON-LB165)	0.981	61.62
Squalane	0.807	32.55
Di(2-ethylhexyl)-adipate	0.922	12.18
Di(2-ethylhexyl)-3,3,4,4-tetramethyladi - pate	0.951	39.75
Bicyclohexyl	0.883	3.96
3,3'-Dichlorodiphenyl-ether	1.281	6.07
1,1,7-trihydroperfluoro-heptylperfluoroglutorate	1.802	32.83
Dimethylsilicone (1000 c.stokes)	0.972	1028.5
Oleic acid	0.885	32.48

Fig. 5.3 Thinning curves of various esters



plates. Any variations in the thinning curves of fluids in the later stages from this relationship may therefore be interpreted as possible variations in the fluid viscosity. For the purpose of comparisons the theoretical gradient of $-\frac{1}{2}$ is shown on all the results of this chapter by dotted lines.

Bearing this in mind it can be seen that all four fluids diverge slightly from this gradient near the ends of their curves, i.e. from thicknesses of 2,000Å downwards. Although these variations are small they occur where the fluids should most fit the theory, i.e. when a large time has elapsed, and are therefore all the more interesting. If this effect were due to random factors, such as surface asperities or dirt particles coming into play, then one would expect these gradients to vary randomly about the mean of $-\frac{1}{2}$. As they do not vary randomly but uniformly, it suggests that some common property of the esters is being revealed. By far the largest variation is for the Di(2-ethylhexyl)-3,3,44, Tetramethyl-adipate which was dissolved in hexadecane in a 10% weight for weight concentration. This was simply to bring down the rather high viscosity of this fluid and hence speed up the rate of thinning. The bulk viscosity of the solution should be little more than that for pure hexadecane, yet if its thinning plot is compared with those for the hydrocarbon, see fig. 5.4, it is apparent that the former is always thicker, i.e. it is thinning more slowly. This effect becomes more pronounced as the film thins and can be explained as an increase in concentration of the ester in this region. This, in turn, suggests preferential attraction of the ester to the metal surface, i.e. some form of physical adsorption.

As one would expect, these curves show that the larger the viscosity of a fluid the slower it thinned. If the values of the viscosities for the three fluids not dissolved in hexadecane are compared with the separation of their curves at any particular time, however, no simple mathematical relationship can be fitted. It appears, therefore, that such viscosity differences are only shown qualitatively in this apparatus.

Lastly, the Di(2-ethylhexyl) adipate curve is shorter than the others, ending at the relatively large thickness of 1,500Å. This is because electrical breakdown occurred and no further capacitance readings could be taken. With most fluids this electrical breakdown occurred at thicknesses between 400Å and 1,000Å and was thought to be due to the surface roughness of the ball, its largest asperities being in the order of 250Å to 400Å. As mentioned in Chapter 3, field concentrations will build up at these asperities causing a greater electrical stress on the fluid film which will also, probably, be thinner at these points. Nevertheless, it is difficult to explain the early electrical breakdown of the Di (2-ethylhexyl) adipate in this way, especially as the fluid was tested several times and never thinned below 1,500Å before breaking down electrically. It appears, therefore, that the fluid behaves in a somewhat different manner near the metal surface resulting in a decrease in its electrical stability.

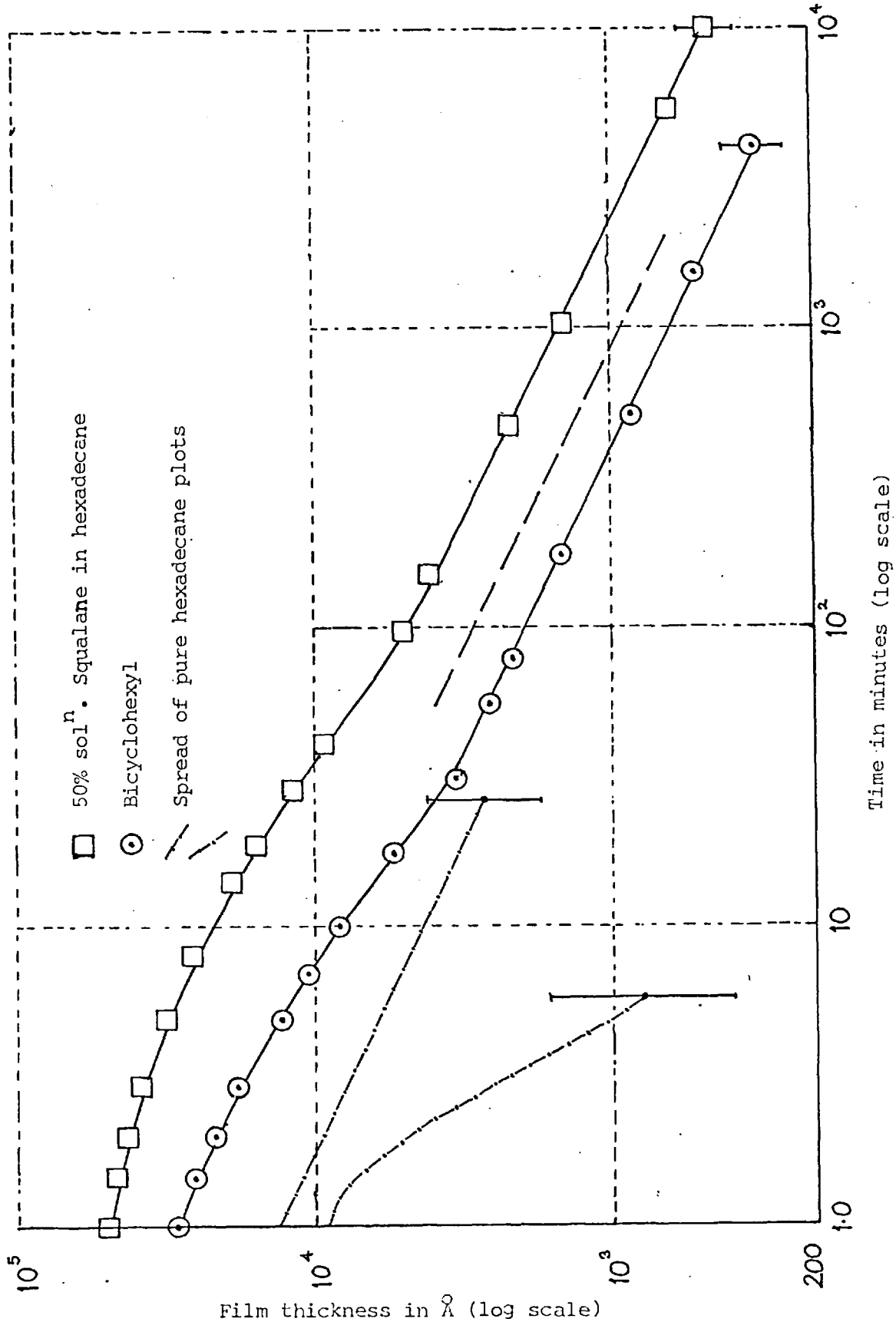
b. The Hydrocarbons

The three hydrocarbons tested were squalane (hexamethyl-tetracosane), bicyclohexyl, and hexadecane. Of these the squalane was much more viscous and therefore dissolved in hexadecane to give a 50% concentration by weight, thus increasing its rate of thinning.

In fig. 5.4 the squalane and bicyclohexyl appear to behave as model fluids. Both thin with gradients of exactly $-\frac{1}{2}$. The more viscous squalane thins slower than the bicyclohexyl down to thicknesses of between 400Å and 500Å where electrical breakdown occurs. The behaviour of hexadecane, however, is very different.

Many tests were carried out with this fluid, but the results varied quite markedly. No single curve can be plotted to represent these experiments and so the dotted lines are used instead to show the total spread of the results. As the viscosity of hexadecane is only marginally less than that of bicyclohexyl one would expect it to produce a thinning curve similar

Fig. 5.4 Thinning curves of some hydrocarbons



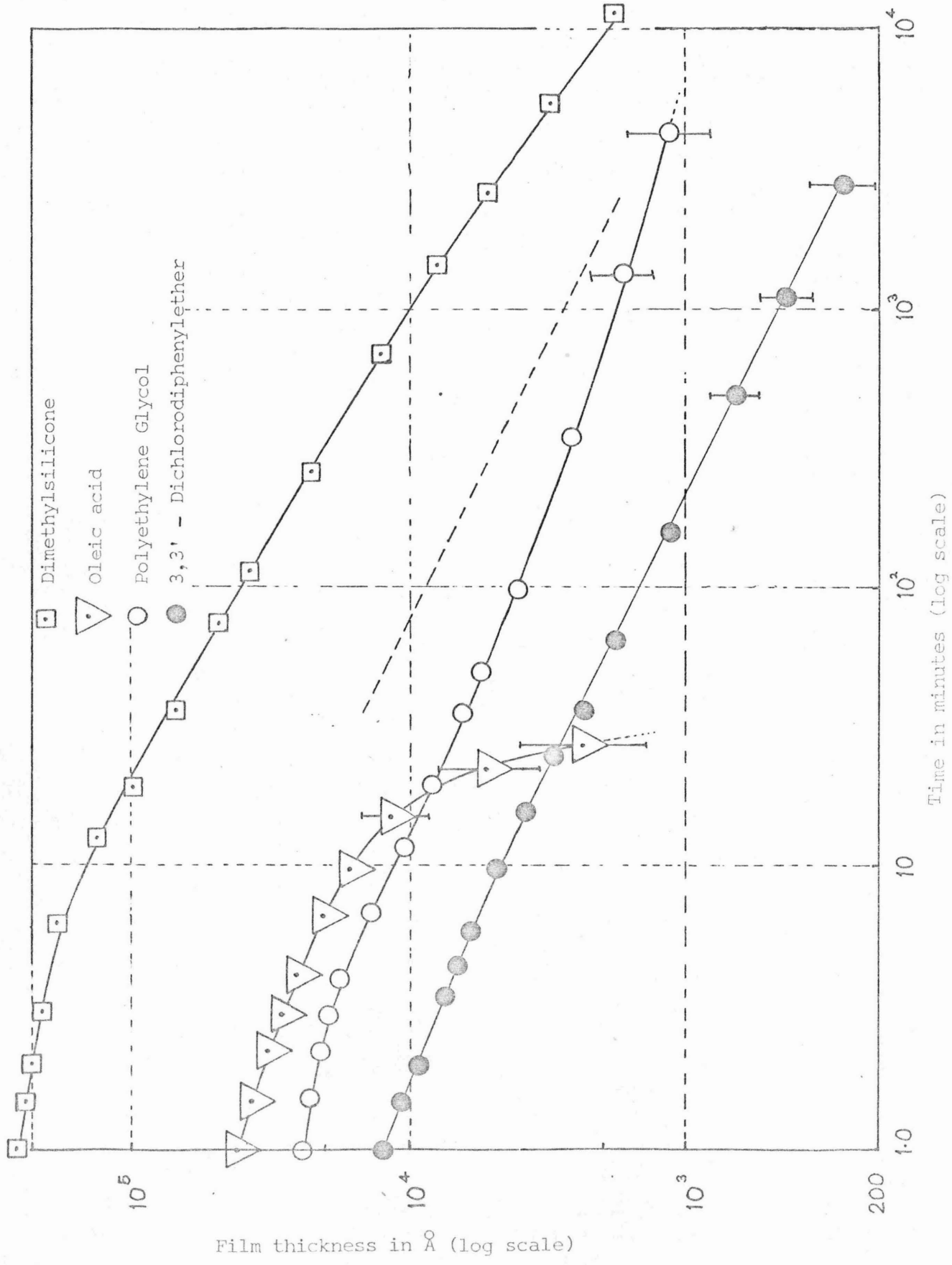
to and just below the latter's. The upper dotted line would fit this model if it were extrapolated past 100 minutes, but the lower line would not. In all the tests with the hexadecane the conductivity was unusually high, over 100 μU , even after only two to three minutes of thinning, which corresponds to film thicknesses around 10,000Å! This increased rapidly with thinning and, usually within 15 minutes, the conductance was so high that the film was considered electrically broken down. The errors introduced into the capacitance readings by the high conductivity (shown by the calibration curve of fig. 2.7 Chapter 2) account for the large variation in these results. The cause of the high conductivity, however, was not understood.

It was thought that the electric field created by the potential applied across the film by the bridge terminals, although very small ($\sim$ 0·4 volts/cm at the relvant film thickness), might be causing this effect. To check this three tests were carried out on the hexadecane. It was left to thin for ten, twenty and thirty minutes respectively before the bridge terminals were connected, producing the field, and any readings taken. In the first case the film was already highly conducting, in the order of 800 μU , whereas in the second and third tests the films had already broken down electrically before the field was applied. It appears, therefore, that this effect was caused solely by some property of the fluid possibly enhanced by the proximity of the metal surface. It was thought, however, that the surface roughness of the ball may well have promoted this electrical instability.

c. The Remaining N.A.S.A. Fluids

These consisted of Dimethylsilicone, Oleic acid, 3,3^1-Dichlorodiphenylether and Polyethyleneglycol, which was dissolved in hexadecane to give a 10% solution by weight. Their thinning curves are shown in fig. 5.5.

Fig. 5.5 Thinning curves of some N.A.S.A. fluids



The 3,3^1-dichlorodiphenylether, like the hydrocarbons, thinned in a model fashion. Its curve has a gradient of exactly $-\frac{1}{2}$ and it thinned down to 300Å before electrical breakdown occurred. The line is slightly higher than that for bicyclohexyl which is to be expected, as its viscosity is 7·7 c.stokes, compared with 4 for the hydrocarbon at ambient temperature.

The dimethylsilicone fluid, thinned very much slower than the other fluids, having a viscosity of ~1,020 c.stokes. At first the gradient of its thinning curve is almost exactly $-\frac{1}{2}$, but as the film thins below 20,000Å its apparent rate of thinning increases. At about 1,500Å, i.e. after the fluid had been thinning for 14 days, the film's conductivity increased quite suddenly, with an accompanying large increase in capacitance. Within thirty minutes the film had completely broken down electrically. This sudden increase in the conductivity of the film after fourteen days of stability indicates a variation of some kind in the dielectric properties of the fluid in the region up to 1,500Å from the metal surface.

The oleic acid result was very unexpected. Instead of giving a thick residual film like the fatty acid solutions in hexadecane described earlier, it broke down electrically within thirty minutes of the start of its thinning. As a marked dependence on the growing period was exhibited by the other acids the oleic acid was tested again after being left to react with the steel surface of the ball for an increased period of two hours. The resulting curve was almost identical with the original one shown in the graph. It appears, therefore, that the oleic acid was behaving in a similar way to the dimethylsilicone, though at a far greater film thickness of approximately 15,000Å. The early results with the cell apparatus recorded in Chapter 3 showed that complete electrical breakdown of the oil film does not negate the possibility of a chemisorbed thick residual film existing, only that it cannot be measured by capacitance techniques. It seems likely, therefore, that the oleic acid may form such a residual film, but that changes in its electrical properties below 15,000Å prevent its detection by

means of capacitance.

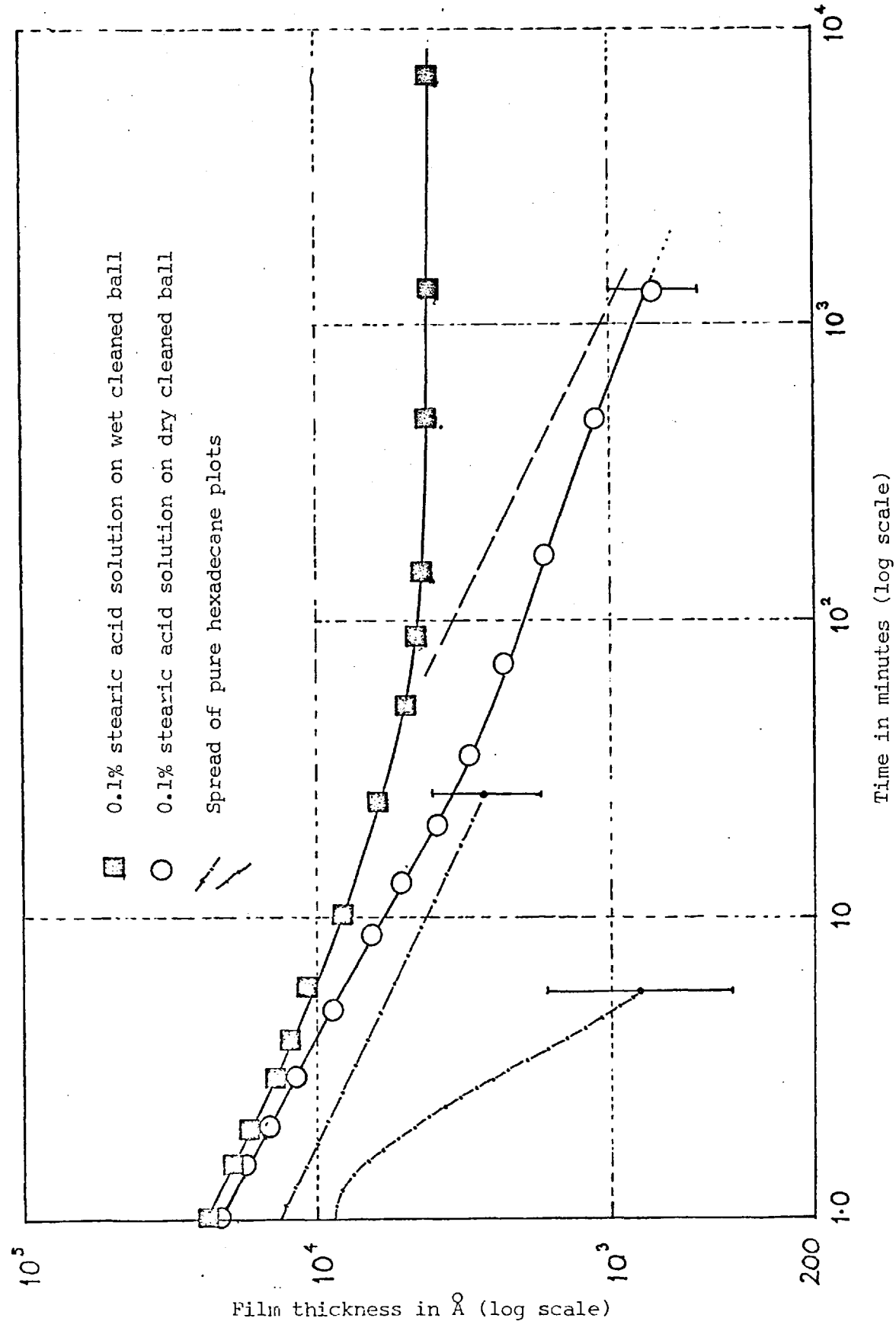
The polyethyleneglycol, having a viscosity of 62 c.stokes, was dissolved in hexadecane to increase its rate of thinning. It should, therefore, only have increased the bulk viscosity of the solution by a small amount giving a value of 6-8 c.stokes. It can be seen to have thinned much slower than the 3,3^1- dichlorodiphenylether which has such a viscosity of approximately 8 c.stokes. Coupled with the fact that in the later stages of its thinning curve the gradient is less than $-\frac{1}{2}$ it suggests that, as with the ester dissolved in hexadecane, this fluid is being preferentially adsorbed at the metal surface, the effect becoming more marked as the film thins. Below 2,500Å the conductivity of the film increased producing errors in the capacitance readings, but complete electrical breakdown did not occur until the film was 1,200Å thick. Nevertheless, this electrical instability may not be explainable by the effects of asperities alone.

5.3.3 Comparison of Wet- and Dry-cleaned Surfaces

These results, shown in fig. 5.6, compare the effect of the different cleaning processes on the thinning of 0·1% stearic acid solutions in hexadecane. In these tests each fluid was allowed a thirty minute growing period. The two methods of cleaning the ball used were the wet cleaning process of the ultrasonic agitation bath, and the dry cleaning process utilising the ionic bombardment technique. The wet cleaning process is so called because it removed all contaminants from the metal surface with a very high degree of reliability but left the oxide and hydroxide layers which are present on most metals exposed to atmospheric conditions. The dry cleaning process, however, removes even these layers resulting in surfaces which were both highly oleophobic and hydrophobic.

On the wet cleaned ball the stearic acid solution produced a residual film 4,000Å thick, whereas no residual film at all was detected on the dry cleaned surface. This is very strong evidence that the residual

Fig. 5.6 Thinning curves of 0.1% stearic acid in hexadecane solutions on wet and dry cleaned metal substrates



films formed are of a chemical nature. The fatty acids alone are not capable of detaching atoms from the pure metal surface to form the metal soap. The layers of metallic oxide and/or hydroxide, however, contain metal ions already removed from the pure metal substrate enabling the above reaction to take place and producing a chemisorbed residual film.

It has been established, therefore, that a dry cleaned surface prevents any chemical reaction taking place between the metal and stearic acid in hexadecane solution. The difference between the thinning curve of this solution on a dry cleaned ball and the spread of results given by pure hexadecane alone is therefore very interesting. The stearic acid appears to be able to prevent the electrical instability of the hexadecane causing electrical breakdown of the film. This suggests either that the mere presence of the acid retards the mechanism which caused such a change in the dielectric properties of the hexadecane or that the stearic acid is present in a much higher proportion than the bulk value of 0·1% w/w near the metal surface. It is also noticeable that in the later stages of its thinning curve this solution thinned more slowly, i.e. its gradient is less than $-\frac{1}{2}$, indicating an apparent increase in viscosity of the film below 3,000Å. These results suggest that some kind of adsorption of the stearic acid from the hexadecane solution onto the metal surface is still taking place, and, as the dry cleaning process has been used, this adsorption can only be of a physical nature.

5.3.4 Synthetic Paraffin With and Without Antiwear Additive

These fluids were tested after interesting results were reported by Parker and Kannel (7) on their X-ray Disk Machine. This apparatus operates in the regime of elastohydrodynamic lubrication, and experiments were carried out between 150°F & 600°F . Some of their results that are of particular relevance to this research are quoted below:

"One unique result observed in using the additive-containing lubricant... was the formation of a very obvious surface film on the disks. This film exhibited very pronounced dielectric properties when the disks were loaded together statically. This film was not present after tests with the lubricant without the additive." These results are very similar to some reported earlier in this work. The fluids were therefore tested in the ball apparatus with the aid of a temperature bath, at 73°F, 200°F and 300°F. The antiwear additive used in the synthetic paraffinic oil was described as an organic phosphonate. Although the fluids had a viscosity of nearly 500 c.stokes at ambient temperature it was decided not to complicate matters by dissolving them in solutions of hexadecane. The usual growing period of 30 minutes was allowed in all cases.

The results of these experiments are soon to be published in a paper by Gentle and the Author (8) and will therefore be dealt with comparatively briefly here. The six thinning curves, two at each temperature, are shown in fig. 5.7.

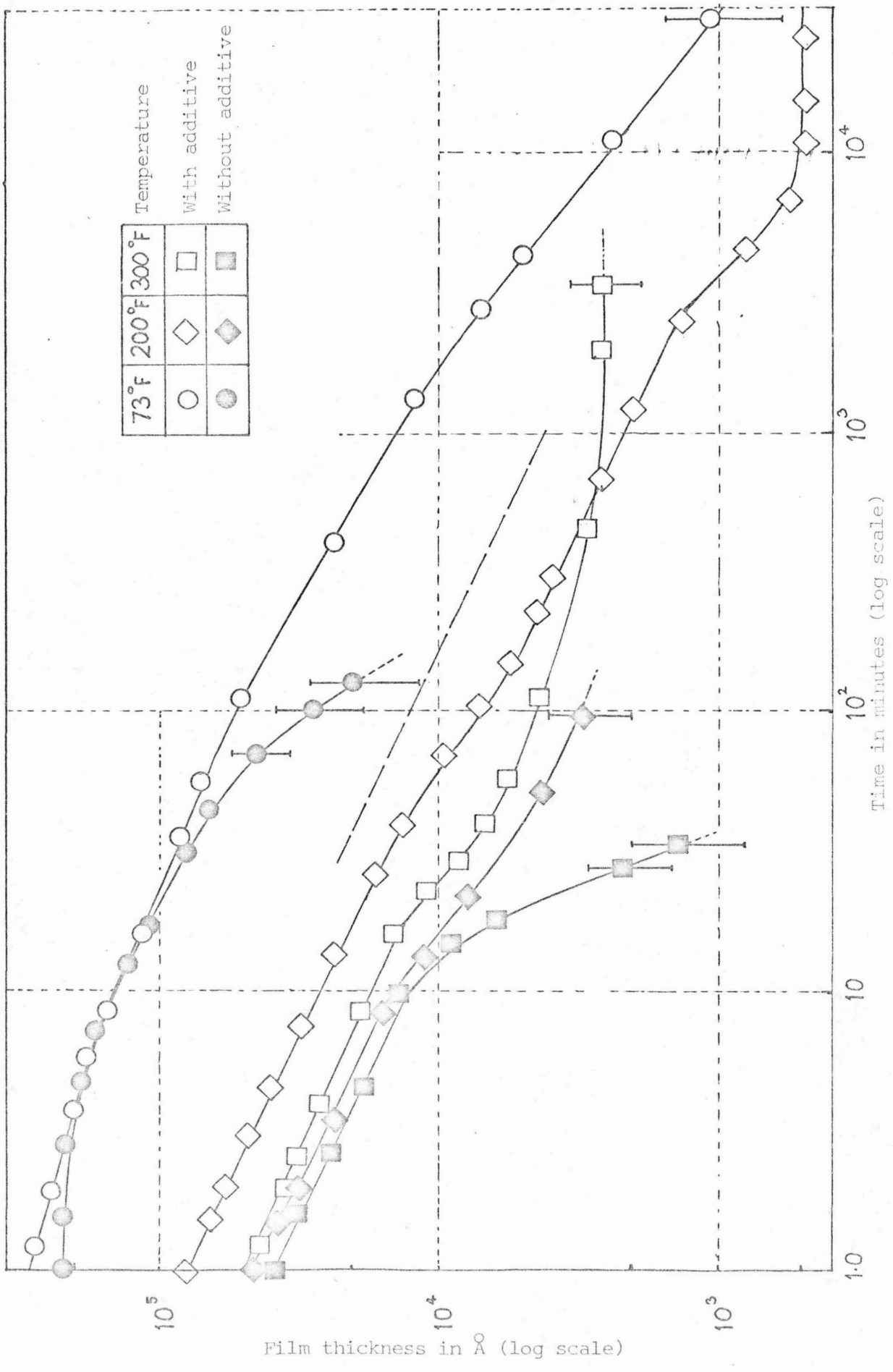
a. At 73°F

Both fluids thinned almost identically over the first thirty minutes. After this time the conductivity of the film of the synthetic paraffin alone increased steadily until complete electrical breakdown occurred before 150 minutes had passed. The synthetic paraffin with antiwear additive, however, exhibited a very high degree of electrical stability, continuing to thin for more than twenty days before the conducitivity rose to approximately 350 $\mu\mho$ at a film thickness of about 1,000Å. It also appears that this film thinned faster than predicted theoretically, by comparing its thinning gradient with that of $-\frac{1}{2}$ (shown by the dotted line on the graph).

b. At 200°F

At this temperature the synthetic paraffin alone thinned more quickly than with the additive, again breaking down electrically before

Fig. 5.7 Thinning curves of synthetic paraffin with and without additives at various temperatures



100 minutes had passed. The fluid with the additive retained electrical stability throughout, thinning after seven days to a residual film apparently 500Å thick. The conductivity in this case remained below 50 μU, even after 20 days had passed. This curve shows two distinct regions where the gradient increases from the theoretical value of $-\frac{1}{2}$, one at ~10,000Å and the second around 1,000Å prior to the residual film thickness being reached.

c. At 300°F

The same pattern shown in cases a. and b. emerges at this temperature. The base fluid alone thinned more quickly, this rate increasing after 10 minutes until electrical breakdown occurred before 50 minutes had passed. The fluid with the additive thinned to a residual film approximately 3,000Å thick after one day. At this temperature, however, this fluid exhibited less electrical stability, the residual film breaking down after two days. Again this curve exhibited an apparent increase in the rate of thinning around a thickness of 10,000Å.

Several interesting points are evident in these results.

(i) The films produced by the base fluid, i.e. the synthetic paraffinic oil, were electrically very unstable at all temperatures.

(ii) The addition of the organic phosphonate greatly improved this stability at all temperatures, and produced residual films at 200°F and 300°F.

(iii) The thickness of these residual films increased with temperature. This is to be expected if the films are of a chemical nature, as discussed earlier. It is also notable that, in all cases, the films took longer to thin the lower the temperature. This is in accordance with the accepted relationship between viscosity and temperature.

(iv) The apparent increases in the rate of thinning of the fluid with additive occurred at all three temperatures, most notably around film thicknesses of 10,000Å. In the equation relating film thickness to capa-

citance given in Chapter 2, the dielectric constant of the oil is assumed to be constant. As an alternative to the films thinning more quickly, therefore, it could be postulated that the dielectric constant of the oil film increased at these points. It will be demonstrated in the next chapter that an increase in the thinning rate is physically very unlikely, involving a marked decrease in the fluid viscosity. The possibility of increases in the relative permittivity of these thin fluid films, compared with their bulk values, should therefore be taken very seriously. The fact that Parker and Kannel also detected "pronounced dielectric properties" in these residual films, using a different experimental technique, adds more weight to this interpretation of the results.

(v) If these dielectric constant increases do, in fact, occur, then the actual film thicknesses will be greater than those shown in fig. 5.7. The residual film at 200°F will be 1,000Å in thickness, as opposed to 500Å; and the film at 300°F will increase from 3,000Å to ~4,500Å in thickness. The film at 73°F will have thinned only to ~3,000Å in twenty days, not to the 1,000Å shown, and may, therefore, still produce a residual film.

5.4 Summary

Because of the large volume of results listed in this chapter a brief summary is given below. The data of Section 5.3.1, i.e. the variation of residual film thicknesses produced by 0·1% stearic acid-hexadecane solutions with growing time, have been fully discussed. The trends described below all stem from the assumption that Newtonian Fluids thin with the relationship

$$h \propto (t)^{-\frac{1}{2}}$$

in the mercury squeeze film apparatus.

Apart from the synthetic paraffin plus antiwear additive the only fluids producing residual thick films were fatty acid-hexadecane solutions. The history of the synthetic paraffins is unknown and it is very likely

that the organic phosphonate additive (an ester) could have hydrolyzed to some degree producing the corresponding acid. No attempt was made to remove such polar contaminants either with silica gel or alumina as Kannel and Parker had not done so. As already mentioned, the experiments were carried cut for comparison with the results of these workers. In the light of the results of this and earlier chapters it seems almost certain that some acid was present to a small extent causing the thick films.

The most interesting results of this chapter are the anomolous variations in the gradients of some fluid thinning curves. These results may be split into three sections, those with gradients of $-\frac{1}{2}$, those above and those below.

a. Fluids Producing Gradients of $-\frac{1}{2}$

These are remarkably few in number, i.e. two pure hydrocarbons, bicyclohexyl and squalane (hexamethyl tetracosane), and the $3,3^{1}$-dichlorodiphenylether. These all consist of non-polar molecules, are chemically very unreactive, and may be considered approximately Newtonian.

b. Fluids Producing Gradients above $-\frac{1}{2}$

These fluids thinned more slowly than it is proposed they should and were therefore considered to be showing anomolous viscosity increments, preferential adsorption on the metal substrate or a combination of both. They include all the esters, the polyethylene glycol (in hexadecane) an alcohol, and the 0·1% stearic acid-hexadecane solution, which was tested on a 'dry' cleaned ball. There was little possibility of chemical reaction in any case. All these fluids contain markedly polar molecules so it seems reasonable to propose that some kind of physical interactions between molecules and metal substrate and/or molecules and molecules were occurring as far out as 3,000Å into the fluid.

c. Fluids Producing Gradients below $-\frac{1}{2}$

There are two possible interpretations of this effect. Either the fluids were thinning more quickly than expected, i.e. their viscosity was

decreasing from the bulk value, or their relative permittivity was increasing. Fluids that exhibited this behaviour were: the dimethylsilicone fluid, oleic acid, the synthetic paraffin both with and without the antiwear additive and, more variably, pure hexadecane. Overall these fluids do not possess any common properties, either physical or chemical. It is unlikely, therefore, that one particular process can account for these results. The diverse range (from 1,000Å up to 10^5Å) at which the effect was first observed corroborates this reasoning . . A thorough analysis of similar results is given at the end of Chapter 7, but, as a precursor to this, two fluids bear further discussion here.

(i) Oleic Acid

It has a similar number of carbon atoms as stearic acid, but, due to differences in the hydrocarbon chain structure, is somewhat shorter (~18Å). Nevertheless it is chemically very similar and should have produced a thick film. It has been described how it is possible for such a film not to be detected in this apparatus. If the effect is interpreted as merely a decrease in the bulk viscosity of the acid, then this falls from 32.5 c.stokes to the order of 2 c.stokes in a period of 20 minutes. It is much easier to accept, even before the mechanisms of such a viscosity drop are considered (Chapter 7) that there is an alternative cause, i.e. a dielectric constant increment. As such an increase would mask the detection of any thick film produced then this interpretation seems all the more likely.

(ii) Synthetic Paraffin plus Organic Phosphonate

Instead of an overall large increase in the rate of thinning, followed by dielectric breakdown, this solution exhibited several short lived increments, remaining electrically stable down to 1,000Å or less. These 'steps' occurred at about 10,000Å and 1,000Å and were more clearly defined at higher temperatures. It has been mentioned that a long chain acid is almost certainly present in the solutions, although only in low concentrations. This acid increased the electrical stability of the synthetic

paraffin as well as producing thick films, an effect also exhibited by the stearic acid-hexadecane solutions. As the general behaviour of the viscosity in these acid-hydrocarbon solutions is to increase from the bulk value of the base fluid to infinity for the rigid thick film it is hard to believe that the viscosity will decrease during this process. The fact that the dimensions of the 'steps' were not reduced by increased temperature also contradicts the possibility of viscosity decrease. It seems likely, therefore, that small dielectric constant increments were taking place as the concentration of phosphonate and acid near the surface increased with diminishing film thickness. It also appears that the ability of long chain acids to produce dielectric increments varies markedly, increasing from stearic acid (and the others tested in Chapter 4) through the phosphonic acid to oleic acid. The fact that the first two cases were for low concentrations of acid whereas oleic acid, being liquid at room temperature, was tested in bulk must also be taken into account.

5.5 Conclusions

Several anomalous variations in the bulk properties of the fluids tested near the metal substrate have been observed. Apart from the formation of thick chemisorbed films the possible anomalies are:

a. Viscosity increments below 3,000Å.

b. Viscosity decrements below 10,000Å.

c. Increments in the relative permittivity as far as 50,000Å into the fluid.

The possibility of dielectric constants decreasing in value has been checked in Chapter 4 and seems very unlikely.

These effects appear to be basically physical. The viscosity increases occur for long chain polar molecules that, for various reasons, are not able to react chemically.

The dielectric increments have been observed for long chain acids. The possibility of viscosity decrements seems highest for the synthetic

paraffin and, more especially, hexadecane.

Before these effects can be investigated more thoroughly the assumption that $h \propto t^{-\frac{1}{2}}$ must be checked for the system used. The nature of flow of long chain molecules, both polar and nonpolar, in such a system must also be considered. On the practical side, an improved apparatus in which the problems of surface roughness and field concentrations are reduced as much as possible is necessary. A range of experiments on simpler systems of fatty acids, esters, alcohols, amines and pure hydrocarbons may then be carried out to identify and possibly isolate the anomalies observed.

CHAPTER 6

THEORY OF FLUID THINNING PROCESS

6.1 Introduction

In the previous chapter several anomolous effects, most notably viscosity variations, were detected in the fluids near the metal substrate. So that these variations could be assessed more quantitatively a theory of the fluid flow under the particular experimental conditions was derived, as shown below. The aim was to be able to predict the oil film thickness after any particular time of thinning and at any particular depth below the mercury surface. Previous workers in this field who displaced test fluids between loaded metal discs compared their results with the Stefan-Reynolds equation which states

$$t \propto \left(\frac{1}{h_1^2} - \frac{1}{h_2^2} \right)$$

where t is a given period of time,

h_1 is the film thickness after this time,

h_2 is the film thickness before this time.

In his Ph.D. thesis, Smith (1) derived an approximate equation for the kinetics of the thinning of a liquid film in the ball apparatus, producing a similar relationship between film thickness and time. Some of his assumptions, however, were too sweeping to allow this derivation to be used here.

The theory below was derived for the simpler case of the flat metal capacitor plates which were used later in this research.

6.2 Derivation of theory

A schematic representation of the metal-test fluid-mercury system for the plate apparatus is shown in fig. 6.1.a. The problem is basically two-dimensional since there are no forces to cause motion in the Z-direction for laminar flow in a container of uniform geometry. As the fluid

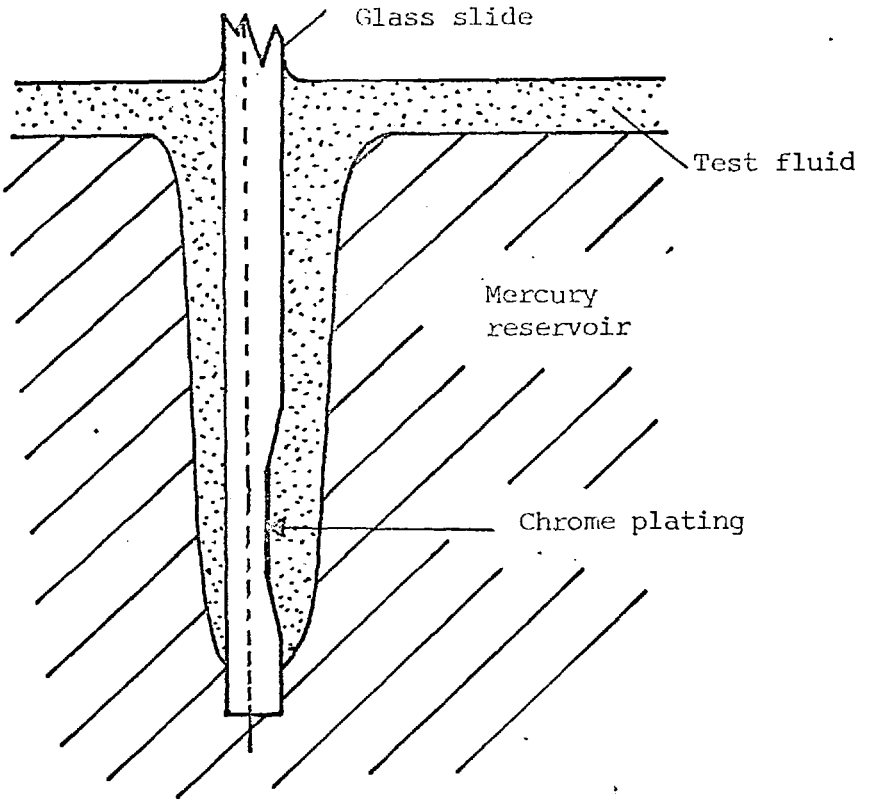


Fig. 6.1a Schematic representation of the metal-test fluid-mercury system

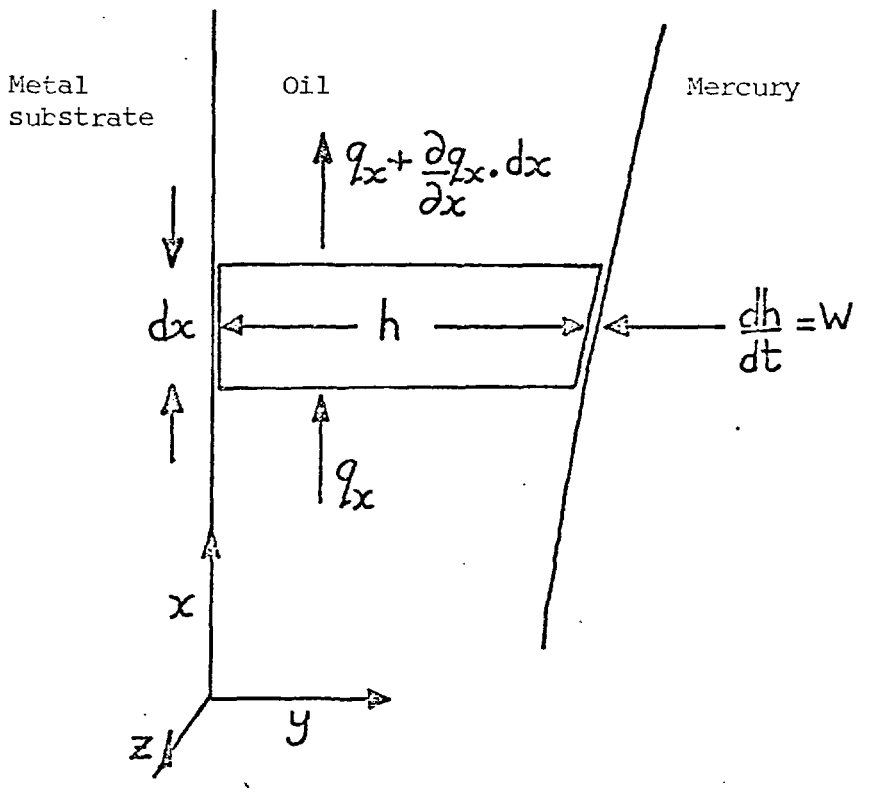


Fig. 6.1b Flow through a segment of oil film

velocity is always small the Reynolds Number is very low and the flow is laminar.

The Navier-Stokes equation of motion for incompressible flow is, in two dimensions:

$$\frac{\partial u}{\partial t} + u\frac{\partial u}{\partial x} + w\frac{\partial u}{\partial y} = -g - \frac{1}{\rho_o}\frac{\partial p}{\partial x} + \nu_o\left(\frac{\partial^2 u}{\partial x^2} + \frac{\partial^2 u}{\partial y^2}\right)$$

where the direction of motion is vertically upwards (i.e. positive x direction)

and u is the velocity in the x direction,

w is the velocity in the y direction,

p is the pressure,

$-g$ is the acceleration due to gravity (i.e. the external force on the system),

ρ_o is the density of the fluid,

and ν_o is the kinematic viscosity of the fluid.

If, in this problem, a mobile, parallel wall replaced the mercury (similar to the parallel plate viscometers) then steady motion would quickly be established. If this were the case the velocity upwards, u, would be constant for all x at any particular y, and the partial differentials with respect to x would be zero. In fact, the fluid properties of mercury prevent such a steady state being completely established until all motion stops. Nevertheless, the very slowness of the thinning and its similarity to the parallel plate case make it reasonable to neglect all differentials of the upward velocity, u, with respect to x, apart from the first order, i.e. $\frac{\partial u}{\partial x}$. The rate of change of u with time is also neglected, for the moment.

The Navier-Stokes equation then becomes:

$$u\frac{\partial u}{\partial x} + w\frac{\partial u}{\partial y} = -g - \frac{1}{\rho_o}\frac{\partial p}{\partial x} + \nu_o\left(\frac{\partial^2 u}{\partial y^2}\right) \qquad \ldots\ldots\ldots 6.1.$$

Integrating this expression with respect to y across the full depth of the fluid film at any particular value of x gives:

$$\int_0^h u\frac{\partial u}{\partial x}.dy + \int_0^h \omega\frac{\partial u}{\partial y}.dy = -gh - \frac{1}{\rho_o}\int_0^h \frac{\partial p}{\partial x}.dy + \nu_o\left[\left(\frac{\partial u}{\partial y}\right)_{y=h} - \left(\frac{\partial u}{\partial y}\right)_{y=0}\right]$$

The pressure at any point in the test fluid will be that exerted by the mercury, i.e. $g\rho_m l$

where ρ_m is the density of mercury,

l is the depth below the mercury surface.

For fluids in equilibrium the pressure gradient is constant at

$$\frac{dp}{dx} = -g\rho_m$$

and, as the thinning process is very slow the relationship is valid for this problem.

$$\therefore \frac{1}{\rho_o}\int_0^h \frac{\partial p}{\partial x}\,dy = -\frac{g\rho_m.h}{\rho_o}$$

The general continuity equation gives:

$$\frac{\partial \omega}{\partial y} = -\frac{\partial u}{\partial x} \qquad \text{everywhere}$$

and, therefore

$$\int_0^h \omega\frac{\partial u}{\partial y}.dy = [\omega u]_o^h - \int_0^h \frac{\partial \omega}{\partial y}u\,dy = [\omega u]_o^h + \int_0^h u\frac{\partial u}{\partial x}.dy$$

Now

$$\int_0^h u\frac{\partial u}{\partial x}.dy = \left[\frac{\partial u}{\partial x}\int u\,dy - \int\frac{\partial^2 u}{\partial x\partial y}.\int u\,dy.dy\right]_o^h$$

As explained earlier, the higher derivates of u are negligible,

thus, $$\int_0^h u\frac{\partial u}{\partial x}.dy = \left[\frac{\partial u}{\partial x}\int u\,dy\right]_o^h = \left(\frac{\partial u}{\partial x}\right)_{y=h}.\int_0^h u.dy$$

as $\frac{\partial u}{\partial x} = 0$ at $y = 0$, where $u = 0$

The original integral may then be written:

$$[\omega u]_o^h + 2\left(\frac{\partial u}{\partial x}\right)_{y=h}.\int_0^h u\,dy = gh\left(\frac{\rho_m}{\rho_o} - 1\right) + \nu_o\left[\left(\frac{\partial u}{\partial y}\right)_{y=h} - \left(\frac{\partial u}{\partial y}\right)_{y=0}\right]$$

By including the boundary conditions:

at $y = 0$, $u = \omega = 0$

and at $y = h$, $u = U$ &. $\omega = W = \frac{dh}{dt}$

the integral becomes

$$WU + 2\left(\frac{\partial u}{\partial x}\right)_{y=h} \cdot \int_0^h u\,dy = gh\left(\frac{\rho_m}{\rho_o} - 1\right) + \nu_o\left[\left(\frac{\partial u}{\partial y}\right)_{y=h} - \left(\frac{\partial u}{\partial y}\right)_{y=0}\right] \quad \ldots 6.2.$$

Integrating equation 6.1 twice with respect to y across the oil film gives: $W\int_0^h u\,dy + 3\int_0^h \frac{\partial u}{\partial x}\cdot\int u\,dy\,dy = \frac{gh^2}{2}\left(\frac{\rho_m}{\rho_o} - 1\right) + \nu_o\left[U - h\left(\frac{\partial u}{\partial y}\right)_{y=0}\right]$

Now $\int_0^h \frac{\partial u}{\partial x}\cdot\int u\,dy\,dy = \frac{\partial u}{\partial x}\iint_0^h u\,dy\,dy - \int_0^h \frac{\partial^2 u}{\partial x\,\partial y}\cdot\iint u\,dy\,dy\,dy$

The parallel plate case gives a value for the double integral $\iint_0^h u\,dy\,dy = \frac{Kh^4}{24}$. Here it may have a maximum value of the order of h^4 (where h, the oil film thickness, is very much less than unity) making the term $\int_0^h \frac{\partial u}{\partial x}\int u\,dy\,dy$ at least two orders of magnitude smaller than the other terms in the equation. Neglecting this term the expression becomes

$$W\int_0^h u\,dy = \frac{gh^2}{2}\left(\frac{\rho_m}{\rho_o} - 1\right) + \nu_o\left[U - h\left(\frac{\partial u}{\partial y}\right)_{y=0}\right] \quad \ldots\ldots\ldots\ldots 6.3.$$

Equations 6.2 and 6.3 give two expressions for W, i.e. $\frac{dh}{dt}$, in terms of the following unknowns:

h, the oil film thickness,

U, the upward speed at the oil-mercury interface,

$\left(\frac{\partial u}{\partial y}\right)_{y=h}$ the velocity gradient at the oil-mercury interface in the oil,

$\left(\frac{\partial u}{\partial y}\right)_{y=0}$ the velocity gradient at the oil-metal interface,

$\int_0^h u\,dy$ the area swept out in the film by the velocity profile,

and $\frac{\partial u}{\partial x}$ the vertical gradient of velocity.

Expressions for all these functions in terms of h or $\frac{dh}{dt}$, are needed.

6.2.1 Expressions for $\int_0^h u\,dy$:

Consideration of the total flow of fluid through the segment shown in fig. 6.1.b gives the relationship:

$$q_x + \frac{\partial q_x}{\partial x}.dx + W dx dz - q_x = 0$$

$$\text{i.e. } \frac{\partial q_x}{\partial x} = -W dz$$

where q_x is the total flow of fluid in the x direction at depth x.

Now $q_x = \int_0^h dq_x$ where $dq_x = \frac{dx\,dy\,dz}{dt}$

$$\therefore W = -\frac{\partial}{\partial x}\int_0^h \frac{dx\,dy}{dt}$$

$$\text{i.e. } W = -\frac{\partial}{\partial x}\int_0^h u\,dy \qquad \ldots\ldots\ldots\ldots\ldots\ldots 6.4.$$

6.2.2 Expression for $\left(\frac{\partial u}{\partial x}\right)_{y=h}$:

The value of $\frac{\partial u}{\partial x}$ required is that at the oil-mercury interface, i.e. at y = h. Considering the Navier-Stokes equation for the mercury at the interface gives

$$\frac{\partial u}{\partial t} + u\frac{\partial u}{\partial x} + \omega\frac{\partial u}{\partial y} = -g - \frac{1}{\rho_m}.\frac{\partial p}{\partial x} + \nu_m.\frac{\partial^2 u}{\partial y^2}$$

where ν_m is the kinematic viscosity of the mercury, which, due to its high density is very small. The vertical motion of the mercury at the interface is caused solely by the viscous drag of the rising oil and therefore the magnitude of u here will be much lower than in the mainstream of the fluid. The value of $\frac{\partial^2 u}{\partial y^2}$ will, therefore, be very small here and the term $\nu_m.\frac{\partial^2 u}{\partial y^2}$ may be neglected.

It was shown earlier that $\frac{\partial p}{\partial x} = -g\rho_m$ and the above equation becomes:

$$u\frac{\partial u}{\partial x} = -\omega\frac{\partial u}{\partial y} - \frac{\partial u}{\partial t}$$

or $$\frac{\partial u}{\partial x} = -\frac{1}{u}\left(\omega\frac{\partial u}{\partial y} + \frac{\partial u}{\partial t}\right)$$ in the mercury.

Assuming no slip at the oil mercury interface, then:-

$u = U$

$w = W$ } are continuous across the interface

and $\left(\frac{\partial u}{\partial x}\right)_{y=h}$

The tangential shear, τ, is also continuous at the interface,

i.e. $\tau = \eta_o\left(\frac{\partial u}{\partial y}\right)_o = \eta_m\left(\frac{\partial u}{\partial y}\right)_m$ at $y = h$

where η_o is the absolute viscosity of the oil,

η_m is the absolute viscosity of the mercury,

$\left(\frac{\partial u}{\partial y}\right)_o$ is the velocity gradient in the oil

and $\left(\frac{\partial u}{\partial y}\right)_m$ is the velocity gradient in the mercury.

The above expression may be rewritten:

$$\left(\frac{\partial u}{\partial x}\right)_{y=h} = -\frac{1}{U}\left(\frac{W\eta_o}{\eta_m}\cdot\left(\frac{\partial u}{\partial y}\right)_{y=h} + \frac{\partial u}{\partial t}\right) \quad \ldots\ldots\ldots\ldots 6.5.$$

6.2.3 Expression for $\left(\frac{\partial u}{\partial y}\right)_{y=h}$:

If expression 6.5 is substituted into equation 6.2 and relations for $\int_o^h u\,dy$ derived from both equations 6.2 and 6.3 are equated, then:

$$\int_o^h u\,dy = \frac{U\eta_m}{2\eta_o W\left(\frac{\partial u}{\partial y}\right)_{y=h}}\cdot\left(WU - \nu_o\left(\left(\frac{\partial u}{\partial y}\right)_{y=h} - \left(\frac{\partial u}{\partial y}\right)_{y=0}\right) - gh\left(\frac{\rho_m}{\rho_o} - 1\right)\right)$$

$$= \frac{\nu_o}{W}\left(U + \frac{gh^2}{2\eta_o}(\rho_m - \rho_o) - h\left(\frac{\partial u}{\partial y}\right)_{y=0}\right)$$

remembering that $\frac{\partial u}{\partial t}$ is neglected.

which simplifies to

$$\left(\frac{\partial u}{\partial y}\right)_{y=h} = \frac{U\eta_m\left(WU + \nu_o\left(\left(\frac{\partial u}{\partial y}\right)_{y=0} - \frac{gh}{\eta_o}(\rho_m - \rho_o)\right)\right)}{\left(2\eta_o U + gh^2(\rho_m - \rho_o) + 2\eta_o h\left(\frac{\partial u}{\partial y}\right)_{y=0} + U\eta_m\right)} \quad \ldots\ldots 6.6.$$

This gives just one expression for the three remaining factors, and in order that they may be isolated in terms of h & $\frac{dh}{dt}$ only, some approximations must be made to give the two extra expressions necessary.

6.2.4 First Approximation:

It can be seen from equation 6.3 that if a value for $\int_o^h u\,dy$ were substituted, an expression containing h, W, U and $\left(\frac{\partial u}{\partial y}\right)_{y=0}$ would be obtained. The similarity of the parallel plate case may be used to derive a reasonable value for this integral. In this case, once steady flow has evolved, equation 6.1 would become:

$$-g + g\frac{\rho_m}{\rho_o} + \nu_o \frac{\partial^2 u}{\partial y^2} = 0$$

i.e. $\frac{\partial^2 u}{\partial y^2} = -K$ where $K = \frac{g(\rho_m - \rho_o)}{\eta_o}$, a constant.

∴ Integrating across the oil film with respect to y gives:

$$\frac{\partial u}{\partial y} = -Ky + \text{constant}$$

at $y = 0$, $\frac{\partial u}{\partial y}$ is finite and positive, i.e. $\left(\frac{\partial u}{\partial y}\right)_{y=0}$

$$\therefore u = -\frac{Ky^2}{2} + y.\left(\frac{\partial u}{\partial y}\right)_{y=0}$$

and $$\int_o^h u\,dy = -\frac{Kh^3}{6} + \frac{h^2}{2}\left(\frac{\partial u}{\partial y}\right)_{y=0}$$

Substituting this in equation 6.3 gives

$$U = \frac{Wh^2}{2\nu_o}\left(\left(\frac{\partial u}{\partial y}\right)_{y=0} - \frac{hK}{3}\right) - \frac{Kh^2}{2} + h\left(\frac{\partial u}{\partial y}\right)_{y=0} \quad \ldots\ldots\ldots\ 6.7.$$

6.2.5 Second Approximation:

The value of u at y = h obtained from the expression derived for the parallel plate case in the previous section is:

$$U = -\frac{Kh^2}{2} + \left(\frac{\partial u}{\partial y}\right)_{y=0}.h.$$

Hence, if U is to be greater than zero, then $\left(\frac{\partial u}{\partial y}\right)_{y=0}$ must be greater than $\frac{Kh}{2}$,

i.e. let $\left(\frac{\partial u}{\partial y}\right)_{y=0} = \frac{K}{2}(h+d)$

where d is some small, unknown distance.

In fact, the velocity profile will not be perfectly parabolic as the equation for u predicts because of the ability of the mercury to move vertically at the oil interface. The parabolic profile and the proposed profile are compared in fig. 6.2. By postulating that the intercepts of the two profiles on the u = 0 line coincide, then a second expression for the unknown distance, d, may be obtained using the triangle, a, b, c.

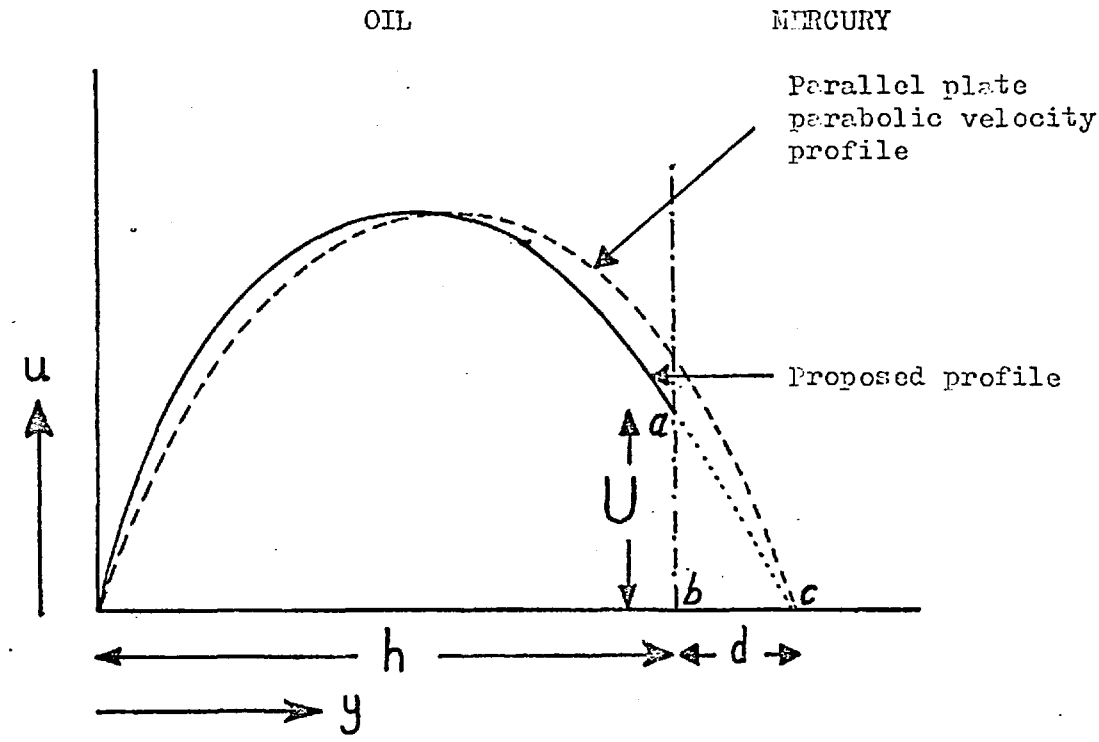


Fig. 6.2. Comparison of velocity profiles, for second approximation.

i.e. $$\frac{U}{d} \approx -\left(\frac{\partial u}{\partial y}\right)_{y=h}$$

This approximation is reasonable considering the extremely small magnitude of U in this problem.

Eliminating d from both expressions gives:

$$U = \left(\frac{\partial u}{\partial y}\right)_{y=h} \cdot \left(h - \frac{2}{K}\left(\frac{\partial u}{\partial y}\right)_{y=0}\right) \qquad \ldots\ldots\ldots\ldots\ldots\ldots \quad 6.8.$$

6.2.6 Final expressions for U, $\left(\frac{\partial u}{\partial y}\right)_{y=h}$ & $\left(\frac{\partial u}{\partial y}\right)_{y=0}$:

Expressions for these three variables may be obtained from the three simultaneous equations 6.6, 6.7 and 6.8.

Putting $$\left(\frac{\partial u}{\partial y}\right)_{y=0} = Y_1$$

and $$\left(\frac{\partial u}{\partial y}\right)_{y=h} = Y_2$$

and equating $\frac{U}{Y_2}$ in 6.6 and 6.8 gives:

$$\left(h - \frac{2Y_1}{K}\right) = \frac{\nu_o\left((2\eta_o + \eta_m)U + \eta_o h(Kh - 2Y_1)\right)}{\eta_m\left(WU + \nu_o(Y_1 - Kh)\right)}$$

Using the expression for U from equation 6.7 gives:

$$Y_1^2 + \frac{KhY_1}{2}\left(\frac{Wh}{2\nu_0}\left(\frac{2\eta_0+\eta_m}{\eta_m}\right)-2\right) - \frac{K^2h^2}{4}\left(\frac{Wh}{3\nu_0}\left(\frac{2\eta_0+\eta_m}{\eta_m}\right)-1\right) = 0$$

Neglecting the higher powers of Wh the solution of this quadratic is:

$$Y_1 = \frac{Kh}{2}\left(1 + \left(-\frac{Wh(2\eta_0+\eta_m)}{6\nu_0\eta_m}\right)^{\frac{1}{2}} - \frac{Wh(2\eta_0+\eta_m)}{4\nu_0\eta_m}\right) \quad \ldots\ldots 6.9.$$

Substituting Y_1 in equation 6.7 gives:

$$U = \frac{Kh^2}{2}\left(\left(-\frac{Wh(2\eta_0+\eta_m)}{6\nu_0\eta_m}\right)^{\frac{1}{2}} - \frac{Wh(6\eta_0+\eta_m)}{12\nu_0\eta_m}\right) \quad \ldots\ldots\ldots 6.10.$$

where terms in Wh^4 have been ignored.

Using this value of U in equation 6.8 gives:

$$Y_2 = \frac{Kh}{2}\left(G - \frac{Wh(6\eta_0+\eta_m)}{12\nu_0\eta_m}\right) \Big/ \left(\frac{Wh(2\eta_0+\eta_m)}{4\nu_0\eta_m} - G\right) \quad \ldots\ldots 6.11.$$

where $G = \left(\frac{-Wh(2\eta_0+\eta_m)}{6\nu_0\eta_m}\right)^{\frac{1}{2}}$

Before these expressions are substituted in equation 6.2 the $\frac{\partial u}{\partial t}$ terms are reintroduced to give a fuller description of the thinning process.

It was shown earlier that $\left(\frac{\partial u}{\partial x}\right)_{y=h} = -\frac{1}{U}\left(\frac{\eta_0 W Y_2}{\eta_m} + \frac{\partial U}{\partial t}\right)$

$\therefore$ equation 6.2 becomes

$$\nu_0 Kh + \nu_0(Y_2 - Y_1) = WU - 2\left(\frac{W\eta_0 Y_2}{U\eta_m} + \frac{1}{U}\frac{\partial U}{\partial t}\right)\int_0^h u\,dy + \int_0^h \frac{\partial u}{\partial t}.dy \quad .. 6.12.$$

Here, $\int_0^h \frac{\partial u}{\partial t}.dy$ & $\frac{1}{U}.\frac{\partial U}{\partial t}$ need expressing in terms of h.

$\therefore$ $\int_0^h \frac{\partial u}{\partial t}.dy$ may be written as $\int_0^h \frac{\partial u}{\partial t}.\frac{\partial y}{\partial t}.dt$

which gives $\int_0^h \frac{\partial u}{\partial t}.\frac{\partial y}{\partial t}.dt = [\omega u]_0^h - \int_0^h \frac{\partial \omega}{\partial t}.u\,dt.$

Generally, ω is extremely small so that the $\frac{\partial \omega}{\partial t}$ term may be ignored.

$\therefore$ $\int_0^h \frac{\partial u}{\partial t}.dy \approx WU$

&. $\frac{1}{U}.\frac{\partial U}{\partial t}$ may be obtained by using the expression for U from equation 6.10.

i.e. $\frac{1}{U}.\frac{\partial U}{\partial t} = \frac{5W}{2h}$

Equation 6.12 now may be rewritten as

$$\int_0^h u\,dy = \left(2WU - \nu_0(Kh + Y_2 - Y_1)\right) \Big/ 2\left(\frac{WY_2\eta_0}{U\eta_m} + \frac{5W}{2h}\right)$$

Substituting the expressions for U, Y_1 and Y_2 in the above equation, 6.4 becomes:

$$W = \frac{\partial}{\partial x}\left[\frac{\frac{Kh^2}{2}\left(hG + \frac{\nu_0}{2}\left(\frac{G}{W} - \frac{h(2\eta_0 + \eta_m)}{4\nu_0\eta_m}\right)\right)}{\left(\frac{\eta_0}{\eta_m}\right)\Big/\left(G - \frac{Wh(6\eta_0 + \eta_m)}{12\nu_0\eta_m}\right) - \frac{5}{2}}\right]$$

and carrying out the partial differentiation gives:

$$W = \frac{-Kh^2}{24\left(N - \frac{5}{2}G\right)}\left[3(2N+1)\frac{\partial h}{\partial x} - \frac{h}{R}(3N+1)\left(7W\frac{\partial h}{\partial x} + h\frac{\partial W}{\partial x}\right) - \frac{5h(2N+1+G(3N+1))}{2R\left(N - \frac{5}{2}G\right)}\left(W\frac{\partial h}{\partial x} + h\frac{\partial W}{\partial x}\right)\right]$$

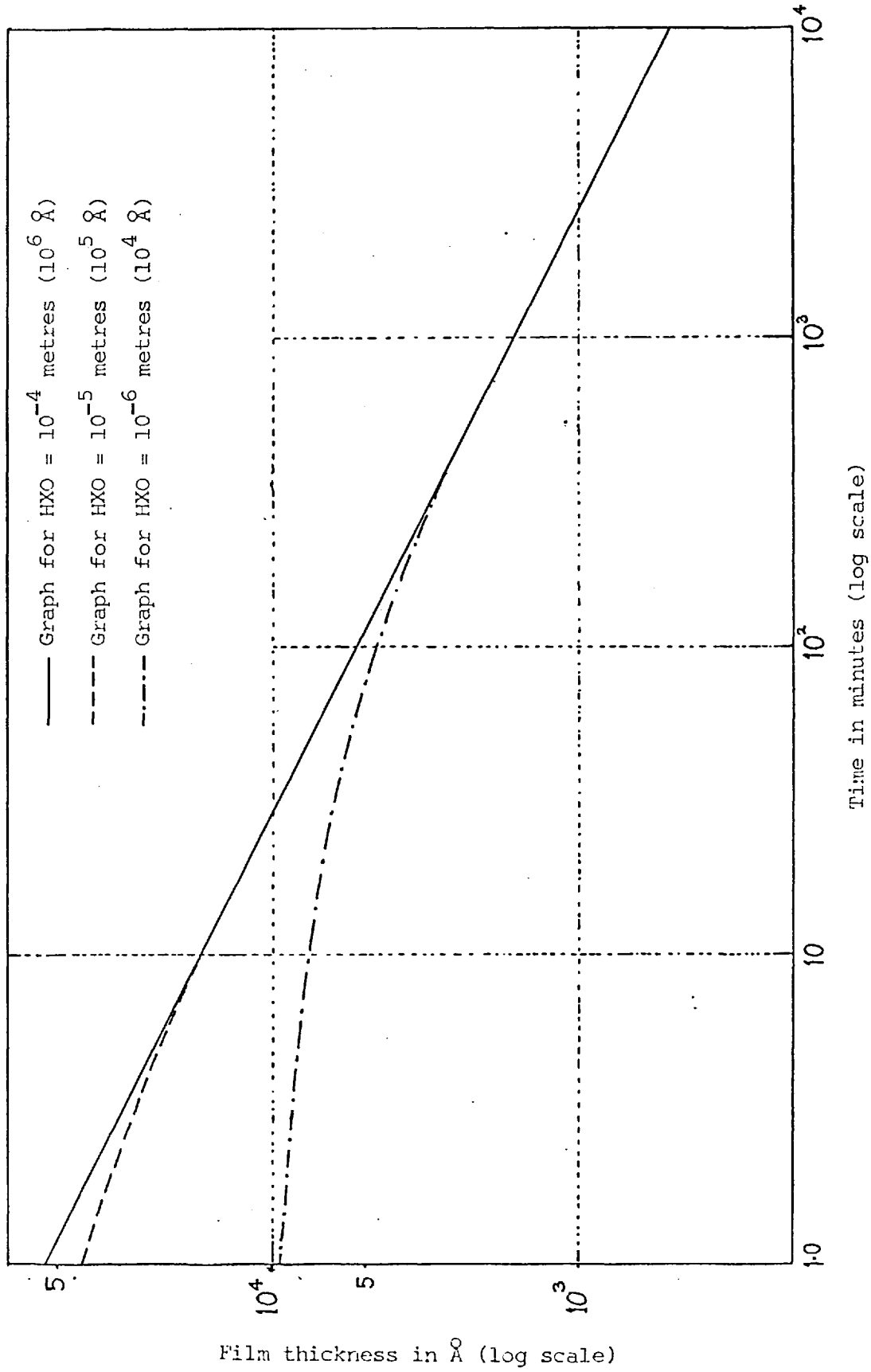
where $R = \left(\frac{-6\nu_0 Wh}{2N+1}\right)^{1/2}$

$N = \frac{\eta_0}{\eta_m}$ and $W = \frac{dh}{dt}$

This equation was solved by computer as shown in appendix C. Fig. 6.3 shows the calculated variation of film thickness with time for a newtonian fluid having the same viscosity as squalane at room temperature. The graph was computed for a depth corresponding to that of the chrome capacitor plate below the mercury surface. As explained in appendix C, this curve is characteristic of any fluid of the same viscosity for all reasonable starting conditions. Similar theoretical curves were computed for all the fluids tested as described in the next chapter, where they are compared with the experimental results.

In the foregoing derivation the only external force considered was gravity. In the apparatus used in this research where many polar fluid are tested electric double layers will inevitably form at the metal-fluid interfaces. The effect such double layers could have on the

Fig. 6.3 Theoretical variation of film thickness with time for newtonian fluid with same properties as squalane



results and the electro-kinetic forces they would introduce are discussed below.

6.3 The Eletric Double Layer

This electrical phenomenon has to do with the nature of the distribution of ions in solution, usually, but not necessarily, in the presence of an applied electric field. The most relevant consideration here is for a plane surface bearing a uniform charge density (the metal) in contact with an ionised solution. Double layers may also arise on micellar and colloidal formations, usually in aqueous solutions.

A simplified theory of double layer formation may be described by three similtaneous mechanisms. A positive potential is assumed to exist at the metal surface, which would fall off exponentially with distance into the solution but for the following factors:

(i) Positive charges are repelled from the surface, negative charges are attracted.

(ii) The system overall should be electrically neutral, i.e. no net charge should exist in the bulk of the solution. Close to the surface, however, an excess of negative over positive ions creates a net charge in the solution balanced by the equal and opposite net charge on the surface.

(iii) The local potential anywhere in the solution is affected by the local charge density, and the interrelation between the two must be considered.

Stern (2) considered the case of real ions and suggested that it could be handled by dividing the region near the surface into two parts. The first consisted of a layer of ions adsorbed at the surface and forming an inner, compact double layer. The second part consisted of a diffuse double layer, known as the Gouy layer. Stern's treatment

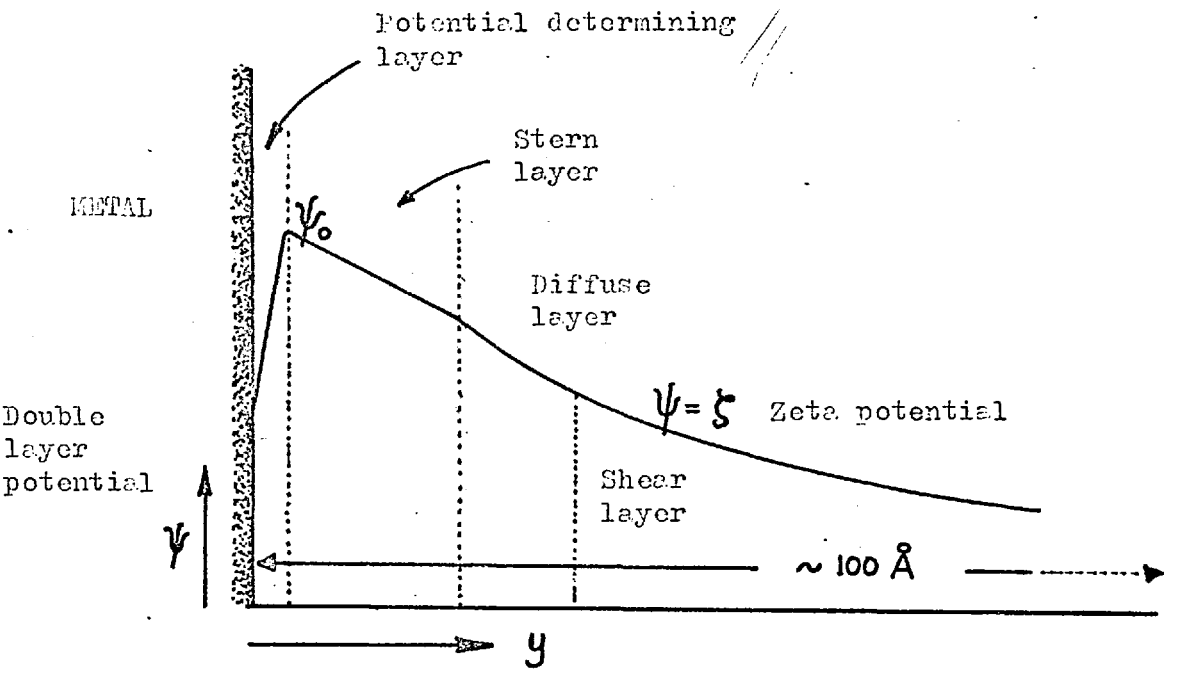


Fig. 6.4. Electric double layer showing variation of potential with distance from surface (from Adamson (3))

estimated the extent to which ions could enter the compact layer and the resulting reduction of the potential. An overall idea of the potential variation with distance is given in figure 6.4.

The absence of an applied potential at the metal surface does not mean that a double layer is not present. An inner layer of desolvated, chemically and/or physically adsorbed molecules will be ionised producing a potential whose size varies with the degree of adsorption. A Stern layer or diffuse Gouy layer will follow depending on the molecular dimensions of the ions initially adsorbed. The higher the ionic concentration in the bulk of the fluid the sharper does the potential of the diffuse layer fall off with distance.

The presence of water in the test fluids can be seen to be of importance in this respect. Its presence on the metal surface would affect the size of the potential produced by adsorption on the surface, usually increasing it. Its presence in the bulk of the solution would effect the fall off of this potential, making it sharper. The purification of the fluids prior to testing reduces the presence of water to

negligible quantities, but the wet cleaning process (chapter 2.6) would leave a layer of adsorbed water on the metal surface. As the tendency of most fluids tested to ionize is very low in the absence of water, then it follows that the ion-concentration in the bulk of the solutions would be very low. This would produce, therefore, in the case of wet cleaned surfaces, a quite large double layer potential falling off very slowly (and exponentially) in the non-ionised fluid. On the dry cleaned surfaces the initial potential would probably be lower, but the range would be similar. It is difficult to measure the electrical potentials in these double layers, but estimates for the zeta potential are reported in the range of 1 to 50 millivolts. The range of potentials applied by the modified bridge circuit, i.e. between 40 μvolts and 400 μvolts, was at least an order of magnitude below these zeta potentials and therefore considered negligible in their production. The zeta potential is positioned in the diffuse layer nearest to the stationary Stern layer, and is, therefore, somewhat less than the maximum potential. The effective range of this potential, taken as the point where it has fallen to $\frac{1}{e}$ of its maximum value at the surface, is usually of the order of 100Å.

Several properties of the electrical double layers are relevant to this research. Firstly, they have their own inherent capacity, due to the charge separation. As this separation is very small, i.e. of molecular dimensions or less, the capacitance is high. It has been measured by many workers for various solutions using electrocapillarity, and, for the low non-applied potentials due solely to adsorption is of the order of 50 → 100 $\mu F/cm^2$. As this capacitance is in series with that of the bulk fluid then the relation

$$\frac{1}{C_t} = \frac{1}{C_b} + \frac{1}{C_d}$$ will apply

where C_t = total capacitance

C_b = capacitance due to bulk of fluid

C_d = capacitance due to double layer

From this it can be seen that the much lower capacitances due to the bulk of the fluids (of the order of $10 \rightarrow 100$ nF/cm^2), will be measured virtually unaffected at the bridge.

Another property is that two plane, approximately parallel double layer systems will develop repulsion between them. This repulsion depends on the size of the potential at the surfaces and their separation. In this research these potentials are quite low and such repulsion would only come into effect at separations below 100Å. Adsorption on mercury is much less than on the chrome or steel substrates, however, so that the double layer potential will be even lower on the mercury surface. It seems reasonable, therefore, to ignore this repulsion in this work where anomolies in films of the order of 1,000Å thick are being investigated.

Finally, the electrokinetic phenomena, especially the streaming potential, should be considered. They occur where the motion of the charged diffuse layer in a moving film produces a current, and, therefore, a potential along the film. The motion of such charged particles past the zeta potential will also induce an electric field opposing such motion, simulating a higher viscosity, i.e. the electroviscous effect. Again, the size of the potentials involved in this research makes this effect very small. Furthermore, in the absence of any ionised molecules in the bulk of the fluid, i.e. especially if water is excluded, neither the streaming potential nor the retarding field will form.

CHAPTER 7

INVESTIGATION OF PHYSICAL ADSORPTION

7.1 Introduction

This chapter deals with the existence of physically adsorbed polymolecular layers on metal substrates. The trends shown in the results obtained with the ball apparatus (Chapter 5) coupled with the theory derived in Chapter 6 allow for a more thorough interpretation of the systematic results catalogued here. An improved apparatus is described which enhanced the reliability of the results obtained.

Before these results are discussed a short review of the forces relevant to physical adsorption and the most popular models of physical thick films is given.

7.1.1 Physical Interactions

Thorough treatment of these interactions may be found in several text books, e.g. Adamson (1), Akhmatov (2). The forces of attraction and repulsion are basically electrical in nature, falling into the following sections.

(i) Mutual interactions existing between ions, or between ions and their reflections in a conducting surface, or induced dipoles in a dielectric. These Coulombic interactions, especially between ions and metallic or charged surfaces, are known to influence the behaviour of particles or surfaces over several tens of Angstroms, and vary inversely with their separation. This is the general form of the effect of an electrical double layer of ions described in the previous Chapter (6.3).

(ii) Mutual interactions occuring between polar molecules, e.g. caroxylic acid dimers, or between such molecules and their reflections. Such dipole-dipole orientation interactions vary as $1/r^6$, where r is the dipole separation, and, under normal conditions, have an effective range of less than 10Å.

(iii) Interactions produced between polar molecules and the corresponding dipoles induced in non-polar species. These effects vary as $1/r^4$ again having a range below 10Å. It is worth mentioning that such systems may be considered in long chain polar molecules with asymmetric polar qualities, e.g. primary fatty acids, alcohols and amines. It is feasible that the polar "heads" of these molecules may induce dipoles in their attached non-polar hydrocarbon chains.

(iv) Dispersion, or London-Van der Waals interactions.

These are the resultant forces between two, or more, non-polar species. They are most satisfactorily explained by quantum mechanical considerations, being second order perturbations. London (3) was the first to treat them in this way, using two hydrogen atoms as an example, the appearance of the dispersion forces may be explained as follows:-

Each atom has no dipole moment as the probability of finding their electrons at any point on their respective orbits is the same, i.e. the average dipole moment is zero. Instantaneously, however, each atom has an electric moment equal to $e\underline{r}$, where e is the electronic charge and $\underline{r}$ is the orbital radius vector. Widely different relative spatial orientations are possible corresponding roughly to attractive and repulsive configurations. Quantum mechanical considerations show that long range London forces vary as $1/r^6$. Short range repulsive forces vary as $1/r^{12}$. Again the range is of 10Å or less although accumulations of London forces, e.g. in long chain molecules, increase their effective size and range.

Dispersion forces also occur between atoms and metal surfaces. They are usually weaker than the inter-atomic case because of the screening effect of the free electrons in the metal lattice.

Of these interactions two are known to have comparatively long range effects. The electrical double layer is one. The other is the long-range London-Van der Waals interaction between extended surfaces, the resultant attractive force overcoming the accumulated repulsion. It is very doubtful

that these forces alone, even when combined, could produce the long range interactions necessary to explain the results of Chapter 5. It is generally accepted that some further force is present which, either alone, or by its cumulative effects, can have a range of several thousand Angstroms. In most models for deep polymolecular films this force is assumed to exist, of necessity, yet its nature has yet to be defined. Some of these models are described below.

7.1.2 Models for Physically Adsorbed Thick Films

Most of these are based on a strongly adsorbed coherent monolayer, as visualised by Godfrey (4), see fig. 7.1. His idealised model is of a stearic acid monolayer on an iron-iron oxide substrate. Considering systems of identical molecules a layer-type or lamellar structure for further molecular adsorption onto the monolayer is the most popular model. Each of these layers usually is considered to consist of dimers of fatty acid aligned steeply to the substrate. A number of authors have advanced different but closely related variants of this model founded mainly on the evidence of the many X-ray and electron-diffraction studies carried out on these systems, e.g. by Bowden and Tabor (5), Woog (6) and Karplus (7).

An improvement on these theories was proposed by Akhmatov (2), who included the substrate conditions as being of vital importance. In his view the earlier models could only apply to substrates of extremely high class surface finishes. On the more usual polycrystalline, coarse grain substrates he proposed that a corresponding "polycrystalline zone" would develop within the boundary layer structure determined by the structure of the metal. To substantiate his theory, Akhmatov quotes the work of Beletskii (8), who found characteristic electron-diffraction patterns of single crystals in boundary layers on polycrystalline metal surfaces.

Akhmatov did not include the possibility of saponification in this model, even though he admitted the possibility of physical adsorption and chemisorption being "simultaneously present on the same metal surface, if its different

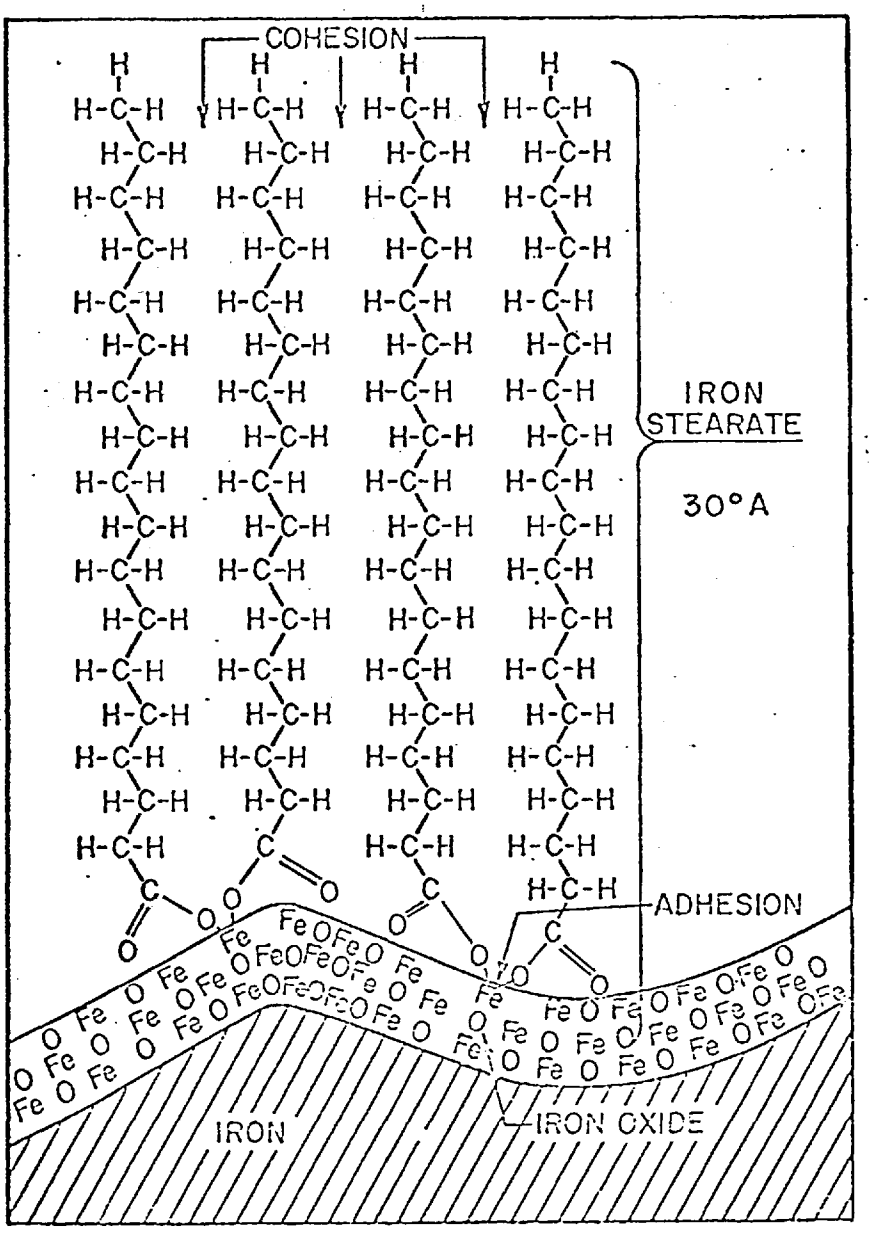


Fig. 7.1 Representation of a stearic acid monolayer on an iron-iron oxide substrate (from Godfrey (4))

regions have significantly different chemical activities." He makes little attempt to visualise the nature of the long range force, merely assuming its presence in the light of experimental results.

The model of Allen and Drauglis (9) is noteworthy as it attempts to isolate some of the facets of the unknown long range force. To do this they go through some of the probable processes involved in the formation of a multi-molecular layer, again of stearic acid. The final film model is almost identical to that of Akhmatov, but the two major assumptions used in its formation are:

(i) the rod-shaped, polar hydrocarbon molecules interact with one another to form ordered domains, i.e. random layers of laterally linked dimers, in the liquid state.

(ii) the bounding surfaces establish an orienting force which acts on the ordered domains of the liquid, aligning them with the surface layer(s). This orienting force is somehow promoted by the ordered layers further into the bulk of the fluid.

To justify the first assumption they mention the clustering tendency of molecules in liquid crystals. They also mention the difference between the electric field necessary to orient such liquid crystals (about 100 volts/cm) as opposed to that necessary to overcome the effect of intermolecular forces once internal ordering has been established (as high as 10^5 volts/cm). In defence of the second assumption they invoke the existence of such co-operative phenomena as ferro-magnetism, suggesting that a similar process may be devisive in producing long range order.

The research of Deryagin and co-workers(10) experimentally confirmed the electrical nature of adhesion forces in several boundary systems. Electric discharges were produced on tearing films from their substrates. Following this, Deryagin developed an electrical theory of adhesion (11). He asserted that in some systems the electric field predicted by electrophoresis (electric double layers - Chapter 6) becomes secondary to the "electrolyte concentration gradient" effect, which he designates as "diffusion phoresis". No experimental

verification of this theory as applied to the polymolecular boundary layers relevant to this research has been reported. His theory is important, however, as it indicates the possibility of long range electric field effects dependant on the constitution and molecular orientation of the boundary film.

Before such phenomena can be investigated the nature and energies of the bonds associated with each molecular interaction should be discussed.

7.1.3 Types of Molecular Bonding

In the multimolecular structure of the boundary layer of a predominantly physically adsorbed caroxylic acid there are other bonds in addition to that between the polar head groups and the metal. These involve the interaction of carboxyls in dimer rows, of non-polar methyl end groups and of the methylene (CH_2) radicals of the carbon chains. These forces are compared, in Table 7.1, with an intramolecular force.

Table 7.1

Interactions	Physical Nature of Forces	Interaction Energy k cal/mole
Interactions between carbon atoms and methylene chains:	Covalent Forces (intramolecular)	84
Interactions between carboxyl (or hydroxyl) radicals and metal surface:	Adsorption Forces	13
Interactions between carboxyls or hydroxyls in dimers:	Debye orientation forces and Hydrogen Bond	15
Interaction between methyl radicals:	London dispersion Forces	$\sim 10^{-1}$

A brief description of the physical nature of each of the three of these intermolecular interaction types follows:

(i) The bonding between the end groups (carboxyl or hydroxyl) in the dimers is strong, resulting from an orientation interaction of high energy coupled with hydrogen bonding. According to Akhmatov (2) each dimer is a quadrupole resulting in a very short range electric field.

(ii) Generally, the methyl radical (CH_3) has no electric moment so any bonding between adjacent methyl end groups must be due to the weak London-Van der Waals dispersion forces.

(iii) The methylene chains of normal hydrocarbons, polar and non-polar, are commonly assumed to be non-polar. This implies that interactions between carbon chains in molecular rows must be due to molecular Van der Waals forces. Assuming no orientation or polarisation effects the attraction will again be by London dispersion forces. As described earlier, these forces can accumulate, especially in close packed molecular structures, making the energy of this interaction relatively high. This may be a major contributory factor to the "chain matching" effects described in Chapter 4. The possibility of an overall electric moment being produced between the methylene chain links under conditions of stress, (i.e. bending) is discussed by Akhmatov (2).

Of these intermolecular forces the role played by hydrogen bonding is least understood. Some of the relevant properties of hydrogen bonding substances are reviewed below.

7.1.4 Hydrogen Bonding

The hydrogen bond is an attractive force between two molecules created by a hydrogen atom which, being chemically linked to one of the molecules (e.g. in a carboxyl or hydroxyl group) simultaneously interacts with an oxygen atom (for example) of the other molecule. These interactions are known between hydrogen and F,O and N atoms, and, to a lesser extent, C, Na, Cl and S atoms. The energy of this type of bond depends upon its position in the molecule and other steric conditions, and upon the nature of the other interacting atom,

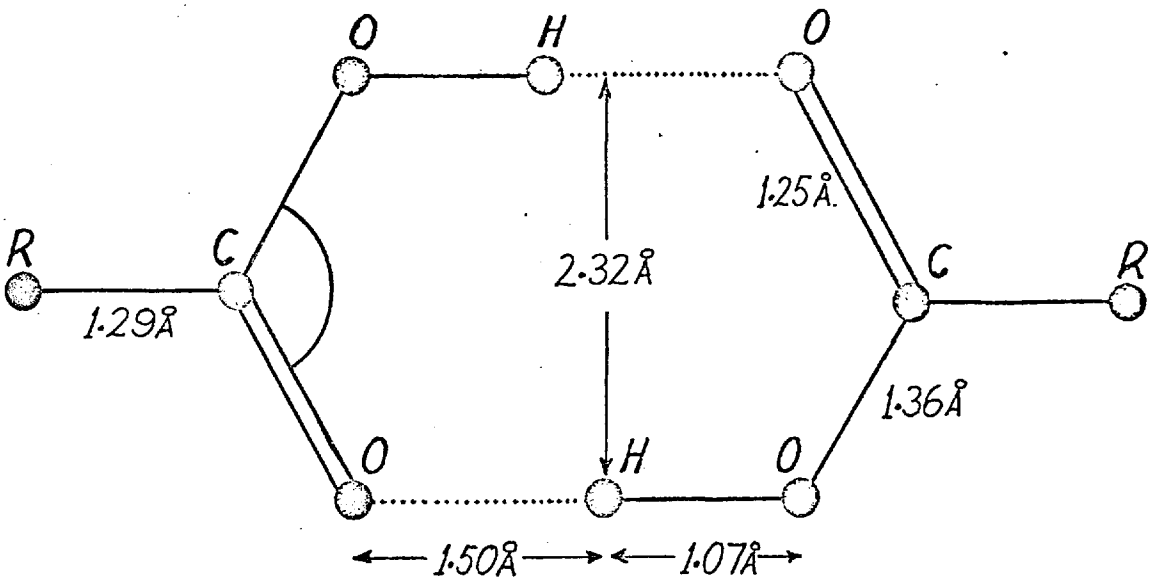


Fig. 7.2a Double hydrogen bond between carboxyl groups of two fatty acids molecules, forming a dimer

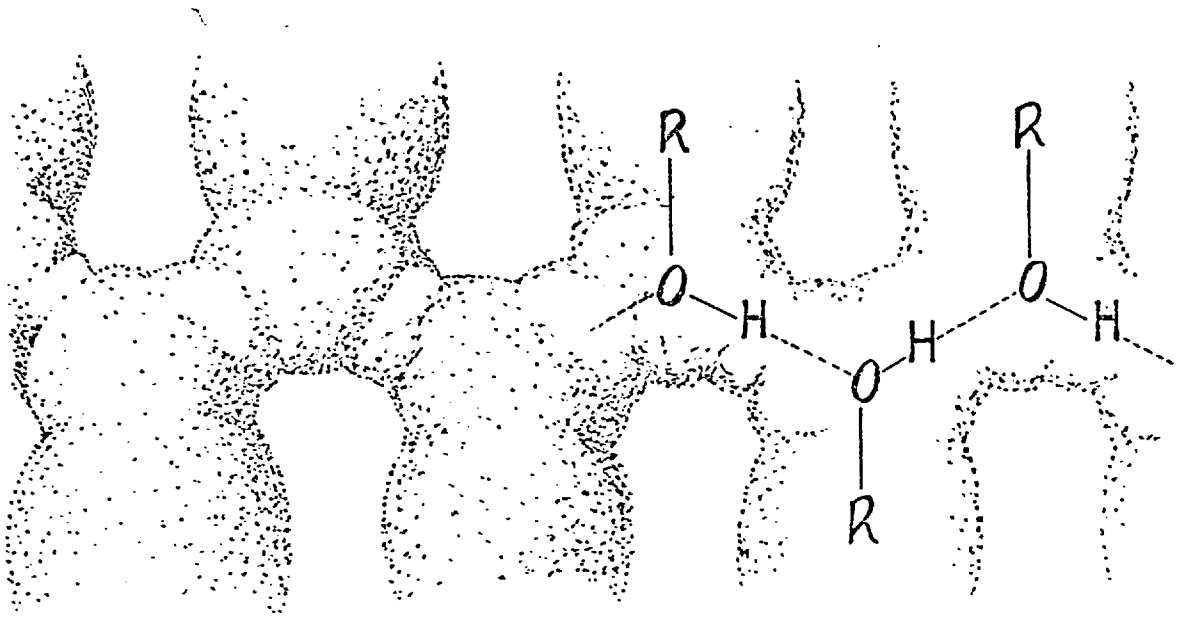


Fig. 7.2b A hydrogen bond chain in alcohols, showing electron clouds (from Pimentel and McClellan (12))

varying overall from 2 to 10 kcal/mole. The bonding energy of a dimer (i.e. a carboxyl-carboxyl interaction) is about 14 kcal/mole, each hydrogen bond being between 6 and 7 kcal/mole .

The mechanism of this bond is not yet fully understood, but it can be regarded as an especially powerful type of electrostatic attraction of the dispersion type. It can be thought of simply as arising between a non-bonding orbital and a protonated orbital because of the powerful attraction of the dense region of electron density within the former for a proton in the latter. More complex theories, such as "frequency modulation" and "Predissociation", all have some defficiences and a thorough quantum mechanical analysis has yet to be produced.

Hydrogen bonding for two molecular types is shown in figs. 7.2.a and 7.2.b. One is for a dimer of a saturated fatty acid, showing atomic separations in Angstroms. The second shows the combination of saturated fatty alcohol molecules giving a hydrogen bond chain. In both, as is generally the case, the hydrogen bond is indicated by a dotted line.

Hydrogen bonding molecules tend to have either proton donating groups or electron donating groups, i.e. are acidic or basic. Some molecules exhibit both qualities and generally have the strongest interactions. The classification of some compounds and compound types by their hydrogen bonding abilities is given in Table 7.2., taken from Pimentel and McClellan (12) produced in 1960. Hydrogen bonding has far reaching effects on many bulk properties of liquids (as well as solids and gases), but only the relevant topics are discussed here.

(a) Viscosity Variations:

Bulk viscosity measurements are not a particularly sensitive tool for detecting hydrogen bonds, but it is generally higher for those substances known to associate. The variation of bulk viscosity with

Table 7.2 Classification of Compounds by Hydrogen Bonding Type

Class of Compound	Molecule contains		Examples
	Proton Donor Groups (Acid)	Electron Donor Groups (Base)	
A	Yes	No	Mainly halogenated compounds with enough halogens to activate the hydrogens: $CHCl_3$, C_2HCl_5, etc.... and possibly C_2H_2 protons
B	No	Yes	Ketones, aldehydes, ethers, tertiary amines, esters, olefins.
AB	Yes	Yes	Water, alcohols, carboxylic acids, primary and secondary amines
N	No	No	Saturated hydrocarbons, CS_2, CCl_4

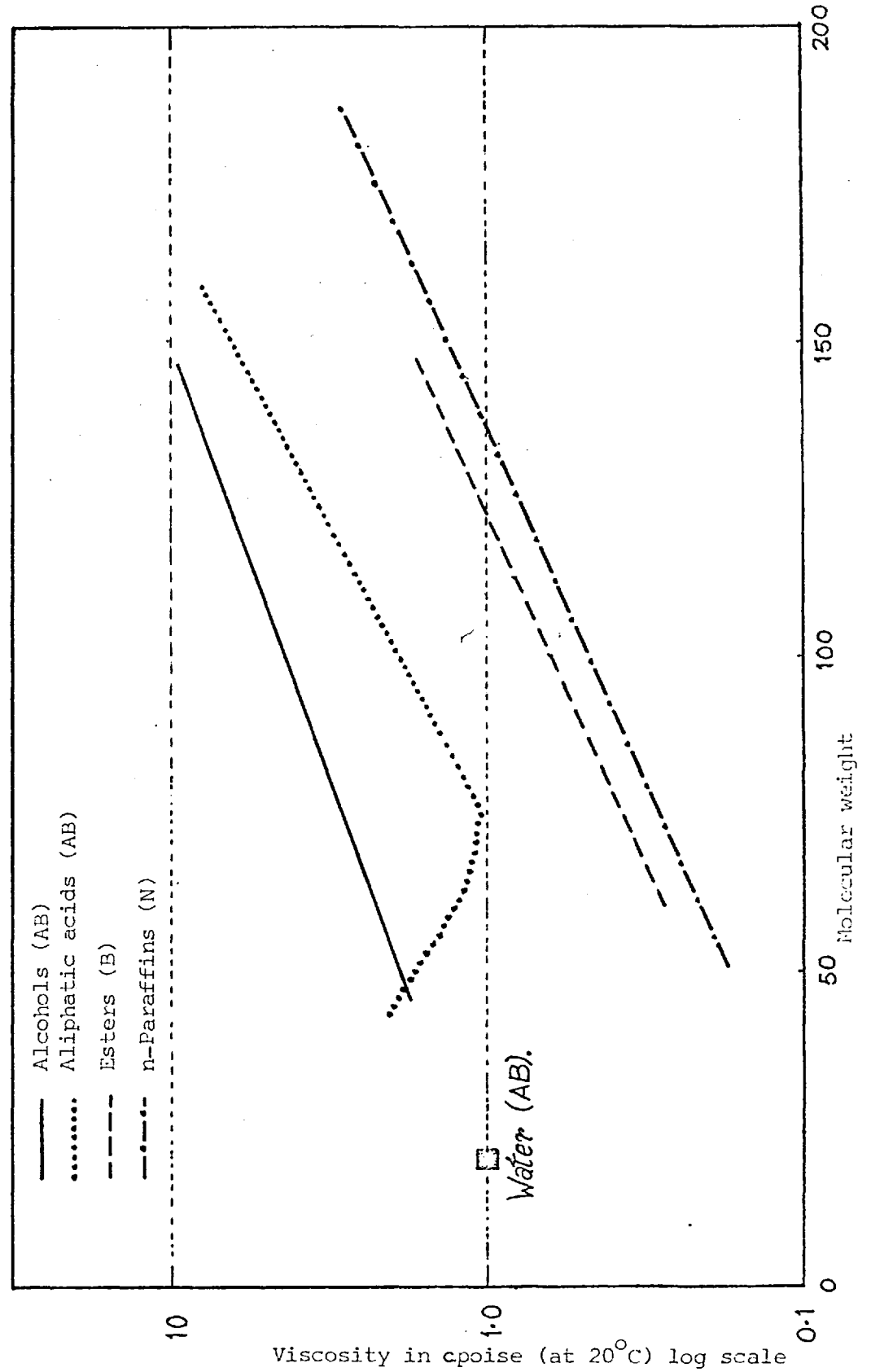


Fig. 7.3 Graph of viscosity v. molecular weight for some H-bonding and non-H-bonding compounds. The letters in brackets indicate the H-bonding class as in Table 7.2

molecular weight for different hydrocarbon types as presented by Kendall (13) is shown in fig. 7.3. The effect of hydrogen bonding is exhibited by the higher viscosities of the alcohols and acids compared with the non H-bonding esters, keton and n-paraffins. In the view of Pimentel and McClellan the enhanced viscosities may be attributed to the "increased size and reduced mobility of the hydrogen bonded complex".

As density is involved in the kinematic viscosity of fluids it is relevant to mention the effect on it of hydrogen bonding. Generally, the density is increased and the molar volume decreased. This reflects the unusually short interatomic distances of the hydrogen bond. The small increase in hydrogen bond formation with pressure seems reasonable in the light of these trends. The density increments are affected also by molecular structure, being less marked for the longer chain molecules.

(b) Dielectric Constant Variation:

It is not possible to make a simple statement about the effect of hydrogen bonding on values of dielectric constant or dipole moment, but the following generalisations are valid.

(i) Dielectric constant and dipole moment do not increase together.

(ii) High values of dielectric constant are usually found in intermolecularly hydrogen bonded substances in which non-cyclic association occurs.

(iii) If the dielectric constant is low for a substance in which association occurs, then intra molecular hydrogen bonding as opposed to inter molecular bonding is the most likely mechanism.

(iv) The arrangement of molecules within a polymeric unit can be roughly determined by comparing the measured dipole moment with values calculated by the vectorial addition of bond dipole moments for various arrangements.

The very high dielectric constant of water has caused it to be studied quite intensely. Several theories have been produced to explain this high value and again the idea of long range ordering (in liquid crystals) in such a

manner that the hydrogen bond dipoles do not cancel is often invoked. Organic hydroxyl compounds (e.g. aliphatic alcohols) can be thought of as being similar to water but with one hydrogen atom replaced by a large non-hydrogen bonding group. The size of this 'inert' long chain appreciably disrupts the order that can be achieved. The hydrogen bonded chain arrangement proposed for such molecules is shown in fig. 7.2.b. Harris (14) and co-workers deduced from dielectric constant values for pressures up to 200 atmospheres at 25-50°C that for alcohols with less steric hinderance (e.g. ethanol) an infinite chain length model fits the data.

(c) Conductance Variation:

Generally hydrogen bonds only markedly increase the conductance of systems when high degrees of order, ionization and orientation are present. A notable exception is water, whose H^+, H_3O^+ and OH^- ions have unusually high mobilities, which enhance the conductance. Pollock and Ubbelohde (15) demonstrated two points for solid organic acids. Conductance is high for crystals having a "cooperative assemblage of H-bonds", almost 100 times greater than it is in the solids with closed pairs of hydrogen bonds, i.e. crystalline dimers. Secondly, the interruption of the continuous chain (e.g. by water of crystallisation) decreases this conductance. These workers concluded that a hydrogen bond chain makes a good path for movement of protons (i.e. proton tunnelling).

(d) Pyroelectric Behaviour:

Pyroelectric systems are those containing elements of stable permanent polarization. Pimentel and McClellan state that "hydrogen bonding is one of the important ordering mechanisms responsible for permanent polarization". A special kind of pyroelectricity where the polarity is reversible in an applied field, namely ferroelectricity, occurs in a few known crystals, e.g. Rochelle salt. A large amount of research has been done on these substances recently (e.g. R. Blinc and S. Svetina (16, 17)), hydrogen bonding proving to be the all important mechanism.

The participation of hydrogen bonding in adsorption systems has been suspected for some time by several researchers, notably Akhmatov (2), but no definitive results along these lines have been produced. The apparatus used in this research can detect several hydrogen bonding effects, i.e. viscosity, conducitivity and dielectric constant variations. Some results of Chapter 5 imply that the trends in these properties shown by the bulk fluids where association occurs may be accentuated under boundary layer conditions. Further investigations of these effects with improved apparatus comparing the results of fluids known to associate with those that do not were carried out in the hope that some relationship between hydrogen bonding and the unknown long range force may become apparent.

7.2 Experimental Apparatus and Procedure

Several deficiencies in the ball apparatus needed overcoming before sufficiently accurate readings could be taken for comparison of the film thicknesses with theory. The faults were:

(i) The spherical shape, complicating the analysis of fluid flow under the hydrostatic pressure of mercury, and preventing satisfactory polishing of the surface.

(ii) Surface asperities of up to 400 Å, reducing the accuracy of film thickness measurements, and creating marked field concentrations which promoted dielectric breakdown.

(iii) The unknown factor where the insulated wire joined the ball, creating possible field concentrations and film weaknesses.

(iv) The difficulty in determining the overall cleanliness of the ball.

The plate apparatus was designed to overcome these problems, see fig. 7.4. It consisted of a layer of chromium vacuum deposited onto an optically flat glass slide. Any asperities were thus reduced to the order of 100Å. A connecting wire was attached to one end of the chromium strip with conducting

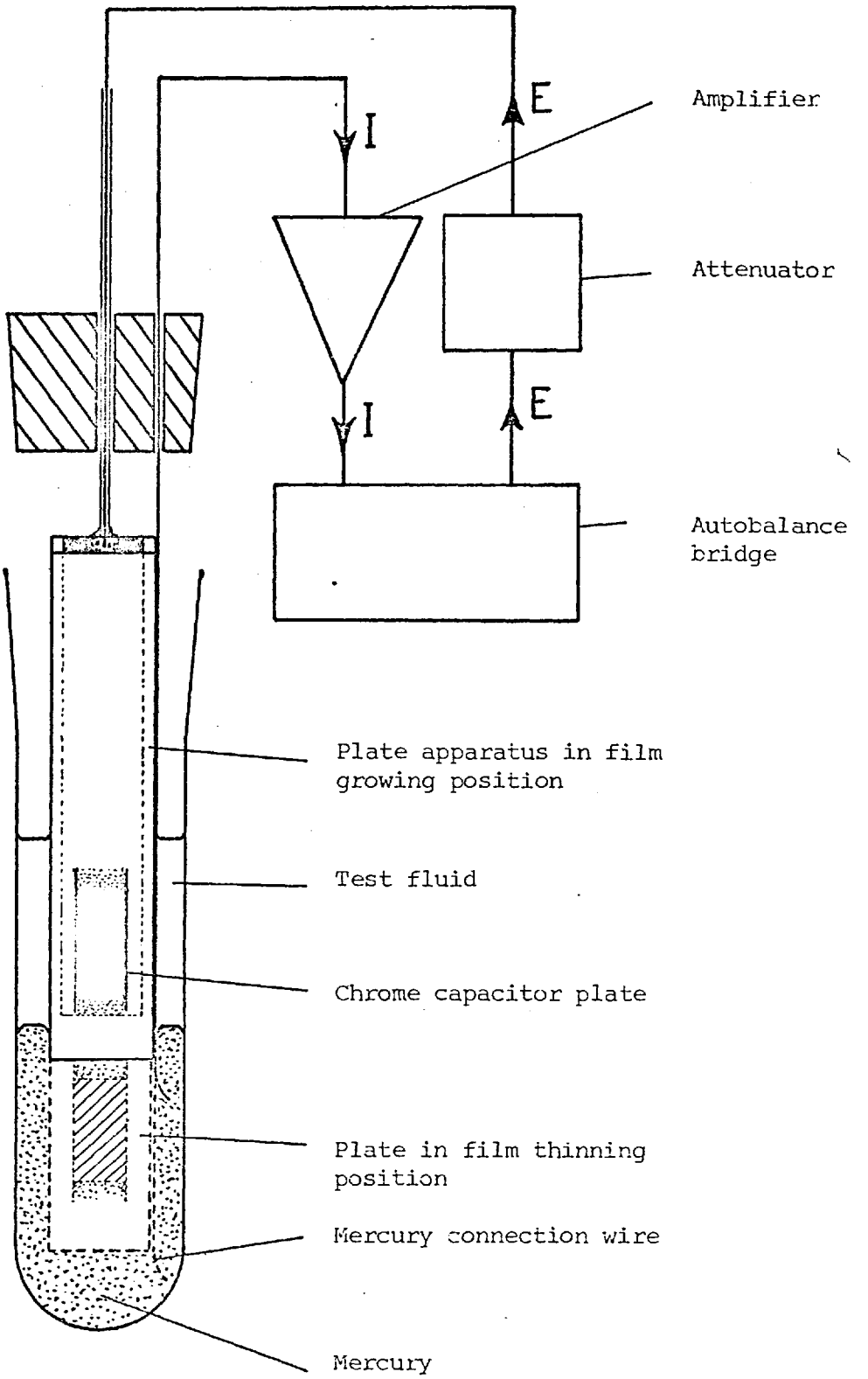


Fig. 7.4 Plate Apparatus

epoxy resin. A second glass slide containing a square hole of area much less than the chromium capacitor plate, i.e. 0.5 cm^2 ($5 \times 10^{-5} m^2$) was sealed over the metalised surface. The two edges of this hole which were perpendicular to the vertical flow of the test fluid were tapered to prevent any restrictions. The apparatus was fixed around the edges with an epoxy resin, within the mercury connection wire was embedded down one side.

In this apparatus only glass and the extremely smooth chrome plate came into contact with the test fluids. The electric field concentrations which would occur at the edges of the chrome plating were masked by the glass, and so could not interfere with the capacitance measurements. The planar geometry of the apparatus simplified the theory and made the cleaning much more certain.

The procedure in these experiments was identical to that used with the ball apparatus. The wet and dry cleaning processes were used as described earlier. The thinning curves of each fluid were plotted on log-log paper together with the corresponding curves obtained from the computed theory. The relevant bulk properties for all the pure fluids tested are shown in Table 7.3.

The pure hydrocarbons and the esters were purified as described in Chapter 2.6.3. In the cases where small concentrations of polar molecules were dissolved in hexadecane the solutions were found in bulk to retain the properties of the saturated hydrocarbon .

The tests on each fluid were repeated at least three times, all at room temperature (21 - 23°C) and with 30 minute growing periods, unless otherwise stated. The errors were calculated from distribution of these results, as

Table 7.3 Properties at 21°C

Test Fluid	Absolute Viscosity in c.poise	Density in g/cm^3	Dielectric Constant	Hydrogen bonding properties (Table 7.2)
Hexadecane	3.48	0.77	2.15	None
Squalane	26.4	0.81	2.15	None
Oleic Acid	28.8	0.88	2.4	AB
N-decanol	8.6	0.83	6.8	AB
Pentaerythritol-tetravalerate	27.0	1.01	3.57	B
Di(2 ethylhexyl)-adipate	11.4	0.92	4.05	B

before. On the few occasions when the conductivity rose enough to effect the capacitance readings (before complete dielectric breakdown), the errors incurred were calculated using the calibration curves of Chapter 2.4.2.

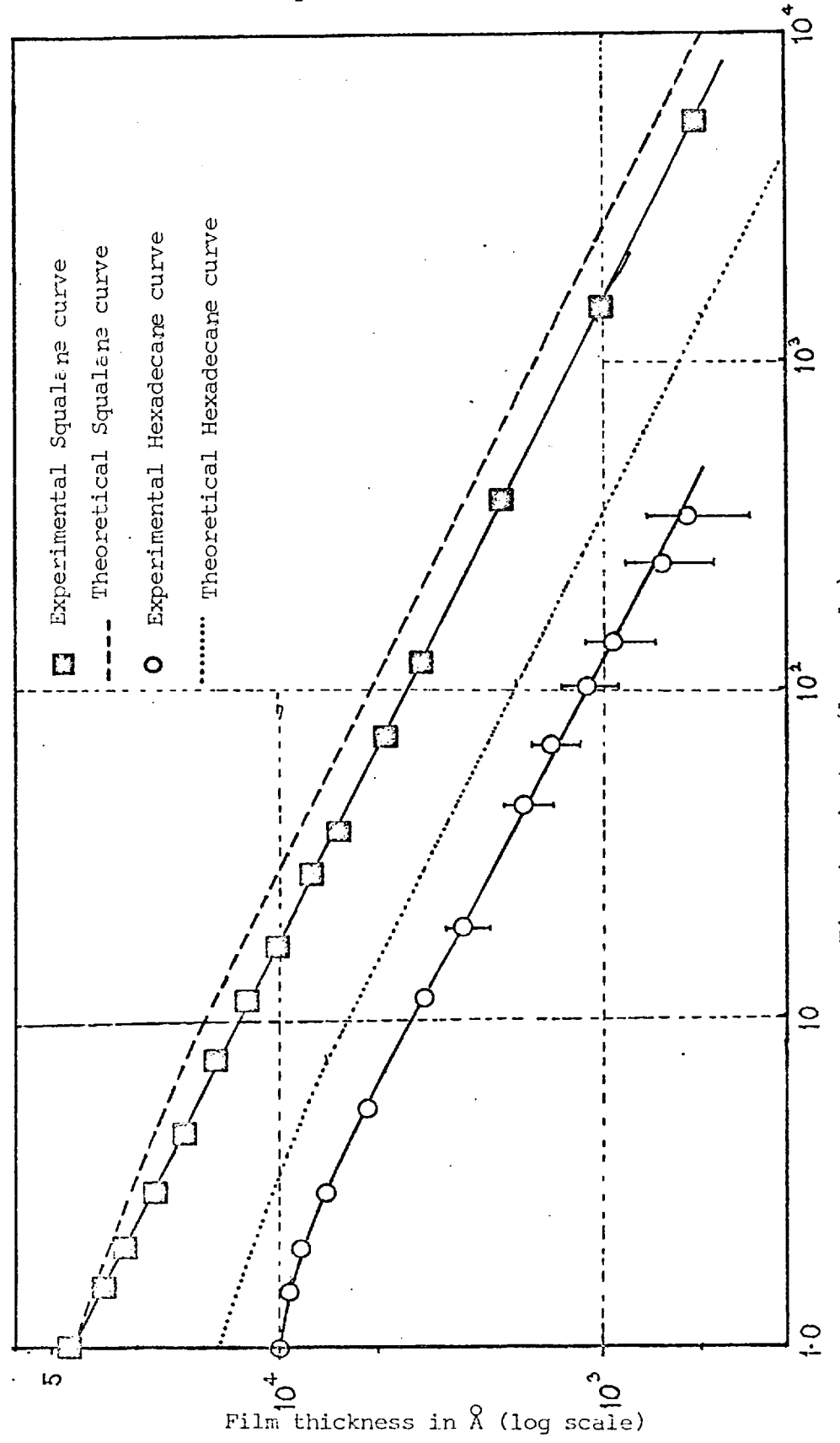
7.3 Results and Discussion

7.3.1 The Pure Hydrocarbons

These tests were carried out mainly to compare the theoretical predictions with the experimental thinning curves, as the hydrocarbons, especially squalane, appeared to behave as newtonian fluids in earlier experiments with the ball apparatus (Chapter 5.3.2). The theoretical and experimental thinning curves of squalane and hexadecane are shown in fig. 7.5. The two curves for each fluid show good agreement. It can be seen that for squalane the two graphs are parallel although the fluid appeared to thin slightly faster than theoretically predicted. This small discrepancy may be explained as follows:-
First there is the increase in the actual surface area due to roughness and asperities over the area used. For the highly polished surfaces used in this work the difference would result in calculated film thicknesses too low by 4% to 7%. The film thicknesses are calculated assuming uniform depth of the fluid across the capacitor plate. In practice the film will most likely be thinner over the asperity peaks and thicker over the valleys. Smith (18) discusses this point concluding that it would also result in the values obtained for the film thickness being too low. This effect is closely related to the surface roughness so that the discrepancy would probably be of the same order, i.e. 4% to 7%.

The tests carried out with hexadecane produced variable results, early dielectric breakdown occuring on several occasions. The results obtained here, however, were far more consistant than those obtained with the ball apparatus and show good agreement with the theory. The graphs show that the fluid thinned too quickly by comparison with theory, even if the uncertainties in the surface area and film thickness discussed for squalane are taken into account. This

Fig. 7.5 Experimental and theoretical thinning curves of hydrocarbons



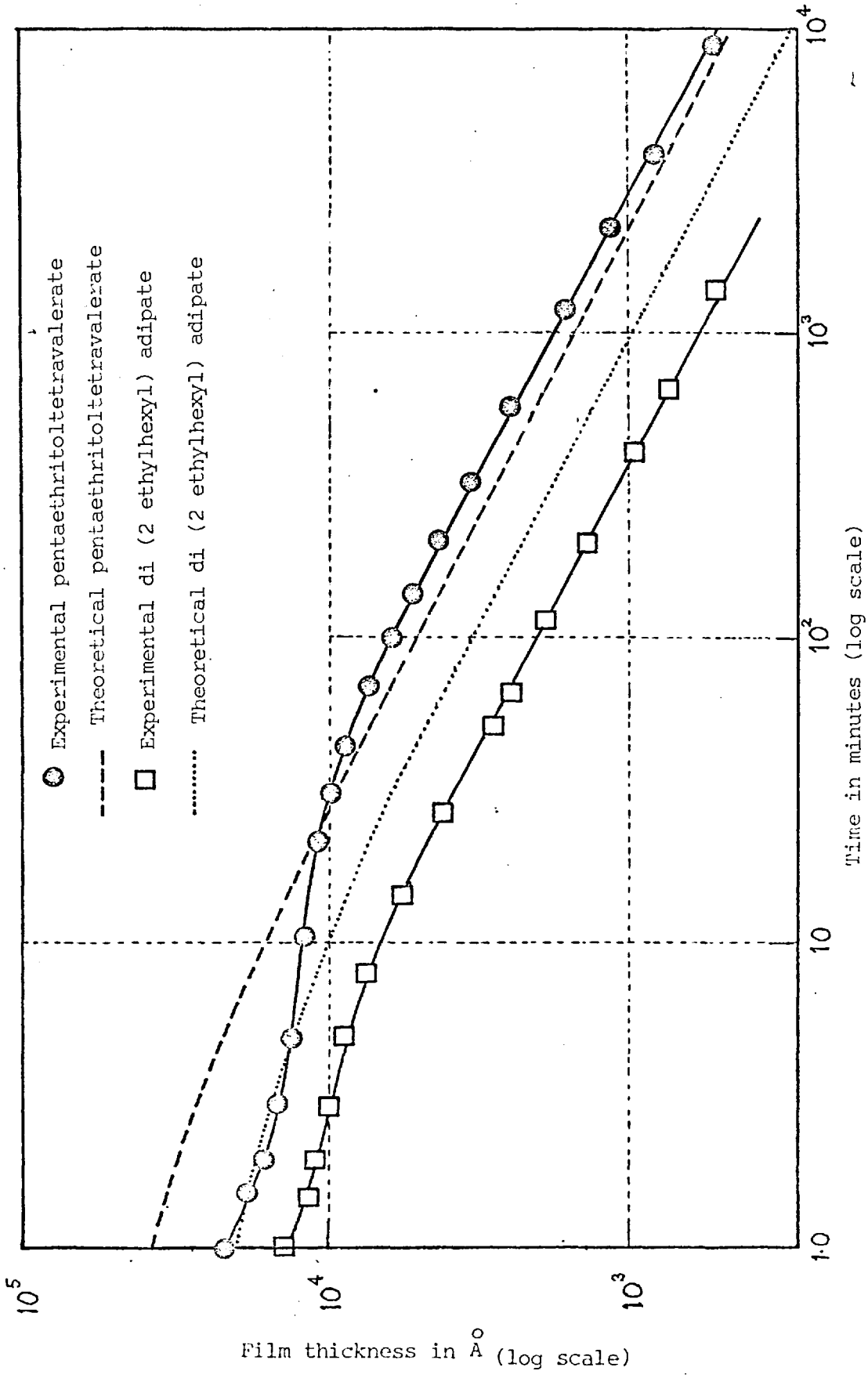
indicates that the viscosity of hexadecane in these thin films is slightly lower than its bulk value. The decrease may be explained by the fact that hexadecane consists of long chain non-polar molecules. It is generally accepted that such non-polar long chain molecules tend to lie flat along a non-polar metal substrate, although with virtually no bonding. As the ambient temperature was only 3°C above the melting point of hexadecane there would be little thermal motion to disrupt this orientation near the surface. Houwink (19) reports that long chain molecules tend to align themselves in the direction of any flow when thermal agitation remains a minor factor, and that such ordering, once initiated, tends to increase. These factors could well combine in this apparatus to give a thin film of hexadecane with molecules predominantly oriented in the direction of flow. An apparent decrease in the cross-sectional area of the molecules, perpendicular to the flow, and, therefore, a corresponding decrease in the viscosity would result.

7.3.2 The Esters

The thinning curves of the two esters tested are shown in fig. 7.6. Both fluids thinned to below 500Å with a gradient of $-\frac{1}{2}$, i.e. parallel to their theoretical counterparts. No electrical instabilities were observed in the films until final dielectric breakdown occurred. The Di (2 ethyl hexyl)-adipate appears to have retained its bulk viscosity throughout the thinning, its slight displacement from its theoretical curve being similar to the case for squalane.

Pentaerythritoltetravalerate shows a viscosity increase, the thinning curve being higher than predicted by theory. At any time the film thickness is too large by a factor of up to 40%, which corresponds to a viscosity increase of up to 100%, i.e. from 27 centipoise to about 50 centipoise. This increase occurs between 20,000Å and 10,000Å, after which it remains constant until electrical breakdown at about 500Å. This is explained if near to the metal surface (at about 10,000Å and below) the molecules accumulate in such a way as

Fig. 7.6 Experimental and theoretical thinning curves of the esters



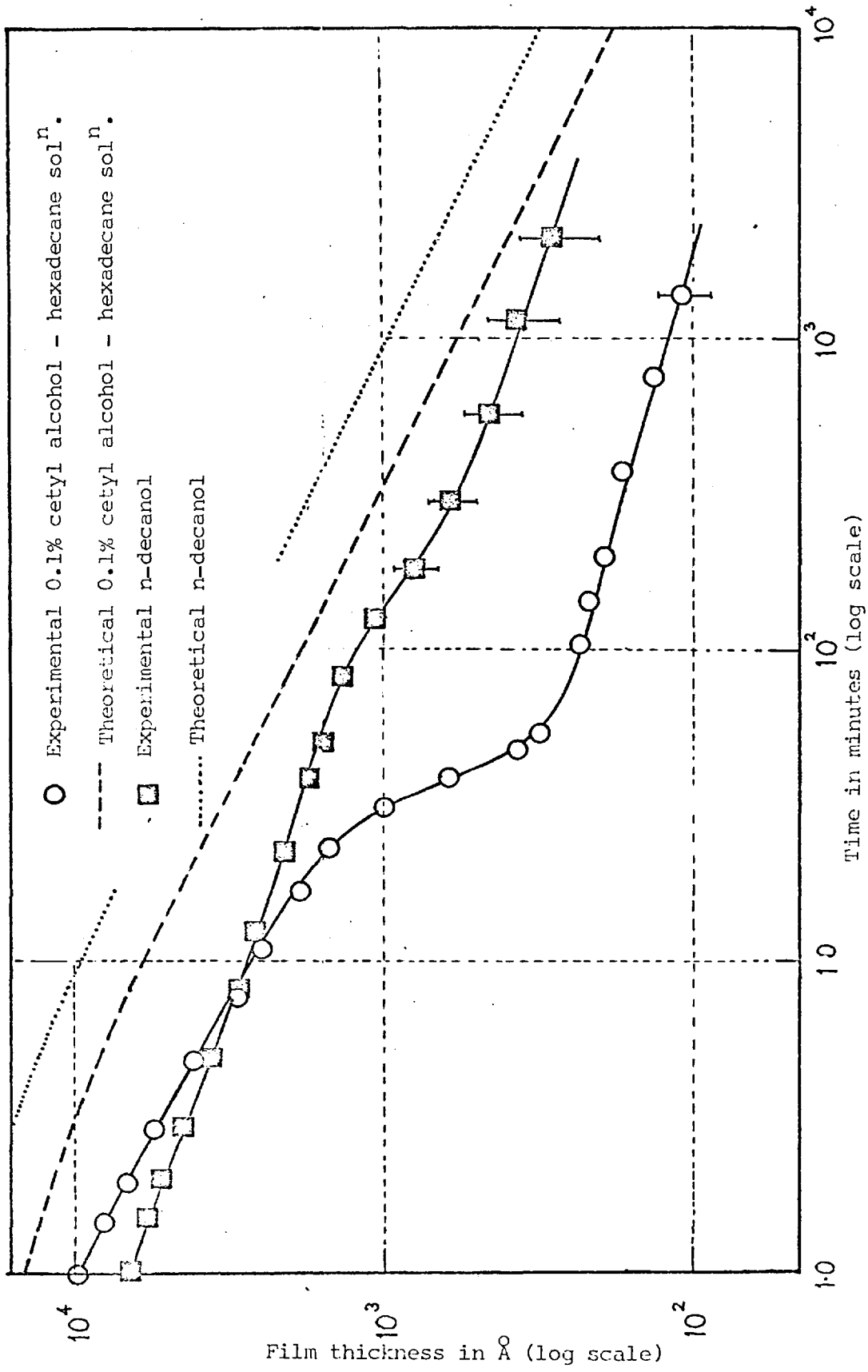
to markedly increase the viscosity of the film, but that no enhanced bonding to the substrate occurs. Such a molecular accumulation could form in micellar type structures around water molecules. A relatively small number of water molecules would diffuse from the damp metal oxide substrate into the bulk of the film. Here they could form hydrogen-bonded complexes with the electron-donor group of the ester, in this case exposed oxygen atoms. Such an accumulation would show the non-polar ends of the ester molecules to the bulk of the film, i.e. non-polar macromolecules would be produced. The ester molecules alone cannot hydrogen-bond together as they have no proton donating groups, so that no long range macro-molecular chains and/or long range ordering can be produced by this mechanism. The increased viscosity therefore can be explained by the formation of micelles around water molecules from the substrate, and their non-polar nature is consistent with the fluid continuing to thin in a newtonian fashion down to 500Å, there being no enhanced bonding to the substrate.

The retention of its bulk properties indicates that Di(2 ethyl hexyl)-adipate cannot form these micellar structures. This may be accounted for by the two double bonded oxygens of each molecule being quite stably bonded in six-component rings within the molecule, i.e. intra-molecular bonding. This could statistically reduce any macromolecular formations around water molecules to a marked extent. Little or no viscosity increments would be expected.

7.3.3 The Alcohols

The curves of fig. 7.7 show large differences between the theoretical and experimental results. The0.1% cetylalcohol solution in hexadecane thinned at a similar rate (i.e. viscosity) to the pure hexadecane (fig. 75) until it reached 2,000Å after about 20 minutes. Here there was apparently a sudden increase in the thinning rate which corresponds to either a large viscosity decrease or an increase in the dielectric constant of the fluid (see Chapter 5). A viscosity decrease of such proportions (down to about $\frac{1}{4}$ of the bulk value)

Fig. 7.7 Experimental and theoretical thinning curves of the alcohols



cannot be explained by an physical means, including that used for pure hexadecane in section 7.3.1. It appears, therefore, that the dielectric constant of the solution increased by at least 100% (i.e. to about 4) for a film thickness of 2,000Å and below. After this the film thinned with a gradient of less than $-\frac{1}{2}$, i.e. its viscosity was continuously increasing, until electrical breakdown occurred. Assuming the dielectric constant did increase, then the viscosity increments started when the fluid was still 2,000Å thick, reaching a value of about 8 centipoise before electrical breakdown.

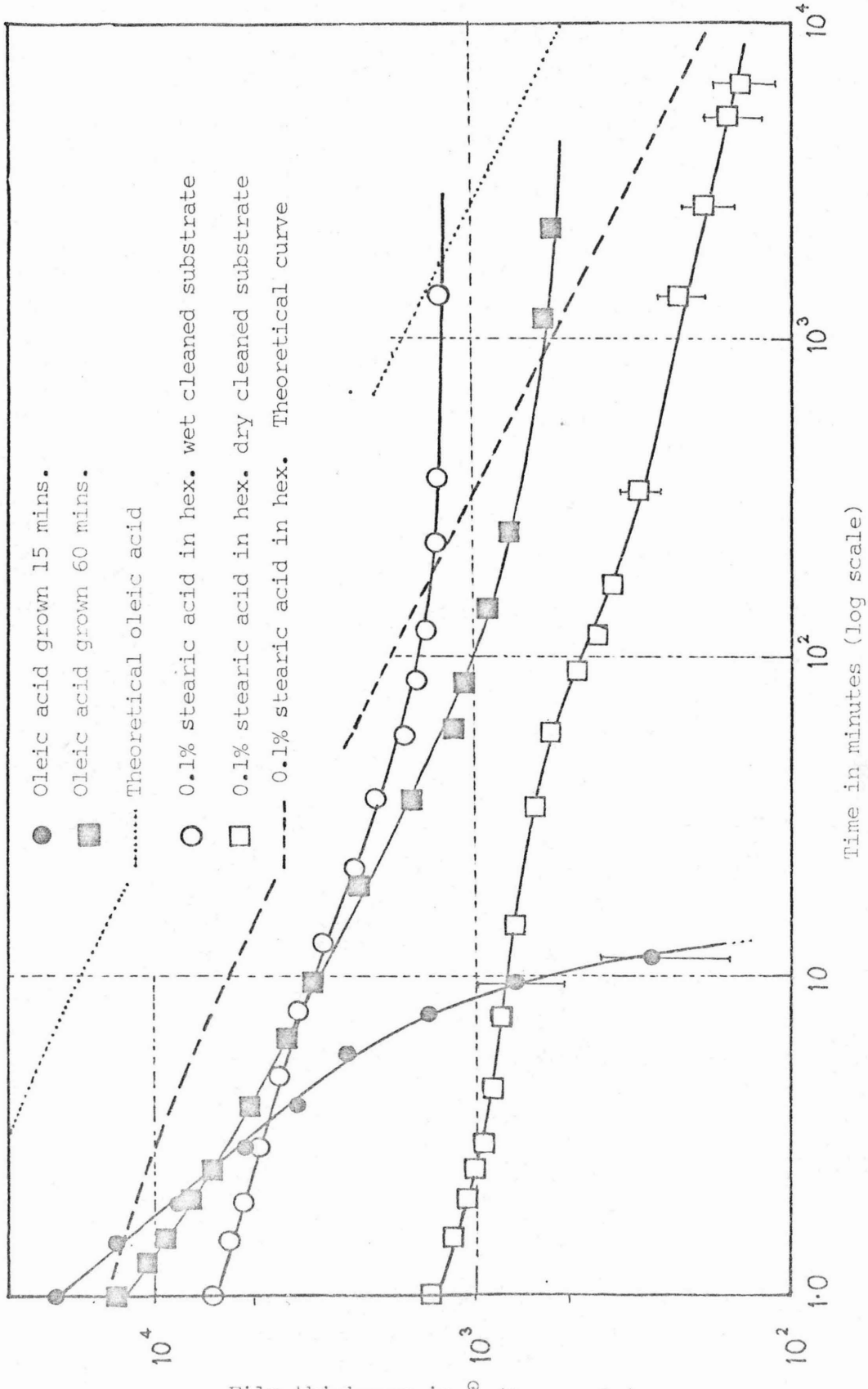
These results can be explained if the cetyl alcohol has been adsorbed onto the metal substrate to form a film over 1,000Å deep consisting largely of the alcohol. The increase in the dielectric constant corresponds to the attainment of a high degree of order in the film and the increasing viscosity suggests a continued strengthening of the bonding in the structure.

The thinning curve for n-decanol is far below the theoretical plot for a fluid of the same viscosity. This again is explained by a corresponding increase in the dielectric constant due to long range ordering of the molecules of approximately 100% (i.e. up to about 12). In this case, however, the increment took place within the first minute of thinning, and at a film depth of at least 10,000Å. The fluid then thinned with a gradient of less than $-\frac{1}{2}$, corresponding to a continous increase in the viscosity, until electrical breakdown occurred. After 100 minutes of thinning a step in the graph indicates a further dielectric constant increase, after which the conductance of the film rose quite markedly. By correcting for the dielectric constant increments the film was calculated as being over 2,000Å thick after thinning for one day, at which time the viscosity had increased to the order of 40 centipoise.

7.3.4 The Fatty Acids

The two fluids tested were a 0.1% solution of stearic acid in hexadecane and pure oleic acid, their graphs are shown in fig. 7.8.

Fig. 7.8 Experimental and theoretical thinning curves for fatty acids on wet and dry cleaned surfaces



The stearic acid solutions thinned on the wet cleaned chromium surfaces to give classical chemisorbed thick films around 1,300Å thick. It is noticeable, however, that at first even this solution thinned below the theoretically predicted curve for pure hexadecane. On the dry cleaned substrates produced in the ionic bombardment apparatus the stearic acid solution thinned similarly to the fatty alcohols. Again the dielectric constant appears to have increased within the first minute, by the order of over 300%. There was a further dielectric increase when the film was around 5,000Å thick, followed by large increments in the conducitivity. After 5 days of thinning the film was at least 1,000Å thick, and the viscosity had risen to the order of 70 centipoise. These results again are explained by a liquid crystalline structure reaching over 10,000Å into the film, the order in this structure increasing as the film thins to a viscous film about 1,000Å thick. It is important to remember that the stearic acid in the solution could not react chemically with the oxide and hydroxide free metal substrate.

The two thinning curves of oleic acid were produced for growing periods of 15 minutes and 60 minutes. The results for the short growing period are similar to those reported in Chapter 5, as the film became highly conducting after 10 minutes of thinning. By comparison with the theoretical plot a very large and continuous increase in the dielectric constant is indicated. These results were obtained on a wet cleaned metal substrate, i.e. the oxide and hydroxide layers were not removed, and therefore a chemisorbed thick film, similar to that produced by the stearic acid solution, was expected to form. When the growing period was increased to 60 minutes the thinning curve shows the presence of a chemisorbed film. The displacement of the graph from the theoretical curve suggests a dielectric increase of over 300%, and, allowing for this, the residual film would have been over 2,000Å thick after 2 days of thinning (i.e. a film of similar thickness to that produced by stearic acid under equivalent conditions).

The increments in the dielectric constant and conductivity correspond to long range correlation in the liquid fatty acid over 20,000Å from the metal oxide surface. The difference between the two experimental curves suggests that the larger amount of chemical reaction product (formed during the longer growing period) retards both the dielectric constant and conductivity increments in the oleic acid films. It was shown in Chapter 4 that 15 minutes was an insufficient time to allow a coherent film of reaction product to form over the metal surface, so that, in some regions, not enough metal soap was present to interfere with the physical long range order in the pure acid, and hence dielectric breakdown occur ed. How and why this reaction product can interfere with any long range physical orientation are discussed later in this chapter.

7.4 Summary and Conclusions

The results described in this chapter can be summarised as follows:

(i) The pure long chain hydrocarbons thinned very similarly to the theoretical predictions, and retained their bulk properties at least down to film thicknesses of 500Å.

(ii) The thinning of the esters also bore a close relationship to the theory, the only change from bulk fluid properties being the small viscosity increase of Pentaerythritoltetravalerate for films below 10,000Å.

(iii) The fatty alcohols showed large increases in their dielectric constants and their viscosities. With the pure liquid alcohol, n-decanol, these effects occured within the first minute of thinning at a thickness of over 10,000Å. The 0.1% solution of cetylalcohol in hexadecane did not show these increments until the film had thinned below 2,000Å. This was probably because at this thickness the alcohol concentration had increased enough (by preferential adsorption) for long range orientation of the molecules to begin.

(iv) The fatty acids also showed large increases in their viscosities. For the 0.1% solution of stearic acid in hexadecane the dielectric constant increased only when the formation of the metal soap was prevented. This incre ase

was, however, even larger than that shown by the alcohols. The pure liquid acid (oleic acid) exhibited dielectric constant increments in all cases, although the greater the amount of chemical reaction product formed the smaller was this increase in the relative permittivity. The films of both acids showed large increments in their conductivity for thicknesses below 5,000Å when the production of the metal soaps was very low.

By referring to table 7.3 it can be seen that those fluids whose thin films exhibit large variations from their bulk properties (i.e. the fatty alcohols and acids) are the fluids capable of extensive hydrogen bonding. The way in which intermolecular hydrogen bonding affects the bulk viscosity, dielectric constant and conductivity of fluids has been described earlier in this chapter (7.1.4). These effects have been magnified within the thin films investigated in these experiments. This can be explained if the degree of hydrogen bonding was increased under these conditions, and such an increase can only occur in fluids when long range ordering of the constituent molecules is present. The molecular orientations and the structure of the long range order regime which could produce the large changes detected in the viscosities and dielectric constants of the associating fluids are discussed below.

7.4.1 Proposed Structure of Physically Adsorbed Films

The theory of molecular orientation put forward by Allen and Dauglis (9), described in section 7.1.2, cannot explain the above results. The repeated layers of fatty acid dimers aligned perpendicularly to the substrate surface would be of very low polarity. Such a structure could exhibit no increase in its overall polarisation and therefore its bulk dielectric constant should not change. Also, the slip planes produced by the neighbouring methyl-methyl end groups are incompatible with the viscosity increments detected. Finally such a self-cancelling structure should have a lower conductivity than the disordered

liquid state due to the decrease in ion mobility - again in opposition to the experimental results.

It is proposed here that the perpendicular orientation of dimeric layers in their theory is incorrect. The polarity of dimers of fatty acids or alcohols is much lower than that of the individual molecules due to the cancelling nature of the interacting dipoles and hydrogen bonds. The resulting quadrupole moment in the centre of the complex has a very small range, much less than the total length of the dimer, according to Akhmatov (2). Larger complexes of a basically similar nature to dimers, such as the associated alcohol chain of fig. 7.2.b will also have a very low overall polarity. These 'quasi-non-polar polymers would tend to align anti-parallel to any force field. In this system the field is perpendicular to the substrate due to the electric double layer produced by the metal and the primary mono-layer so that the polymers would tend to lie flat against the exposed methyl end groups, as in fig. 7.9.a.

Those dimers and polymers lying closest to the monolayer would experience an electric field due to the double layer of a similar size to the intermolecular bonding field. Each individual molecular dipole would tend to reorientate, to some extent, in the direction of the electric double layer field, i.e. perpendicular to the substrate surface. The resulting bending of the dimer and polymer structures would decrease the strength of the hydrogen bonding, but simultaneously increase the local strength of the electric double layer field whilst promoting it further into the fluid film. Possible realignments of the molecules in dimers of a fatty alcohol and a fatty acid under these conditions are shown in fig. 7.9.b.

These bent polymers could close pack onto the methyl end groups of the primary monolayer forming a further polar layer strongly bonded laterally by multi-intermolecular hydrogen bonding. Once established, a further polar layer would form above this one, again enhancing the electric field perpendicular to the substrate, and establishing it further into the fluid. In this way a highly ordered, semi-crystalline structure could form deep into the fluid, as shown in

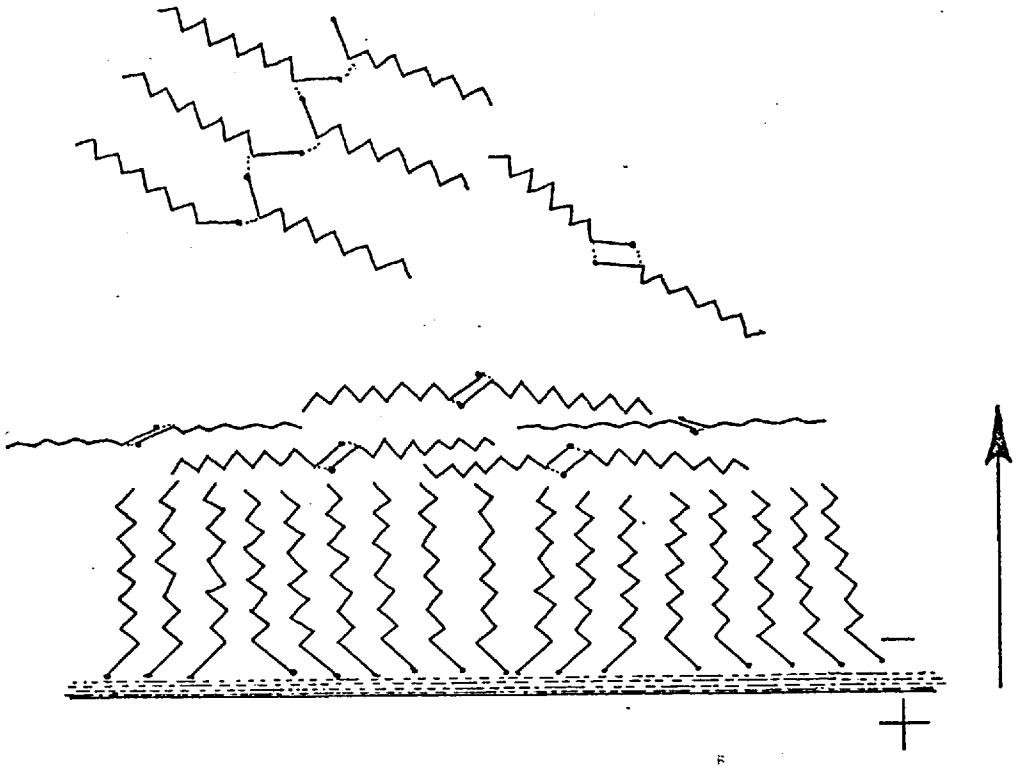


Fig. 7.9a Orientation in double layer field of dimers and polymer chains above primary monolayers

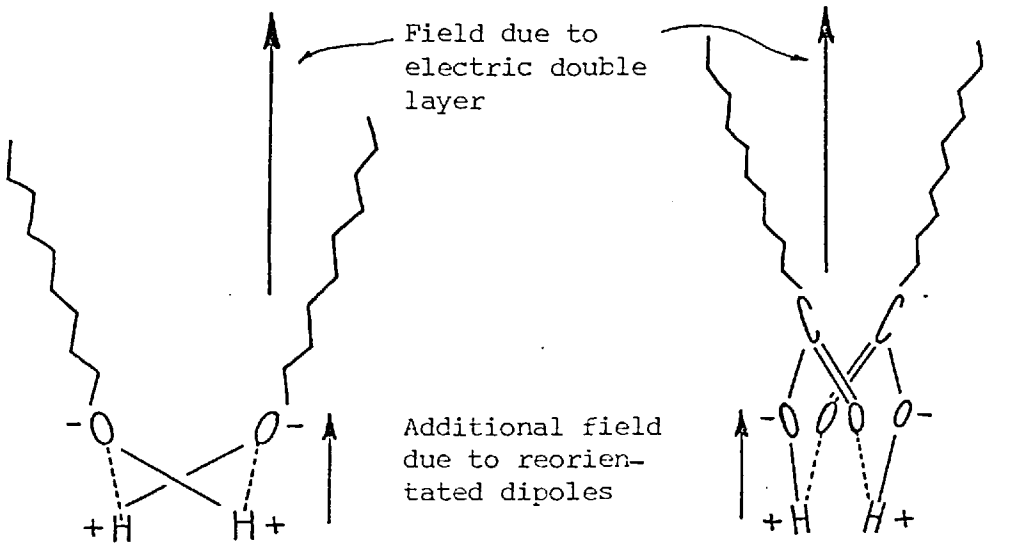


Fig. 7.9b Proposed realignment of fatty acid and alcohol dimers in double layer field

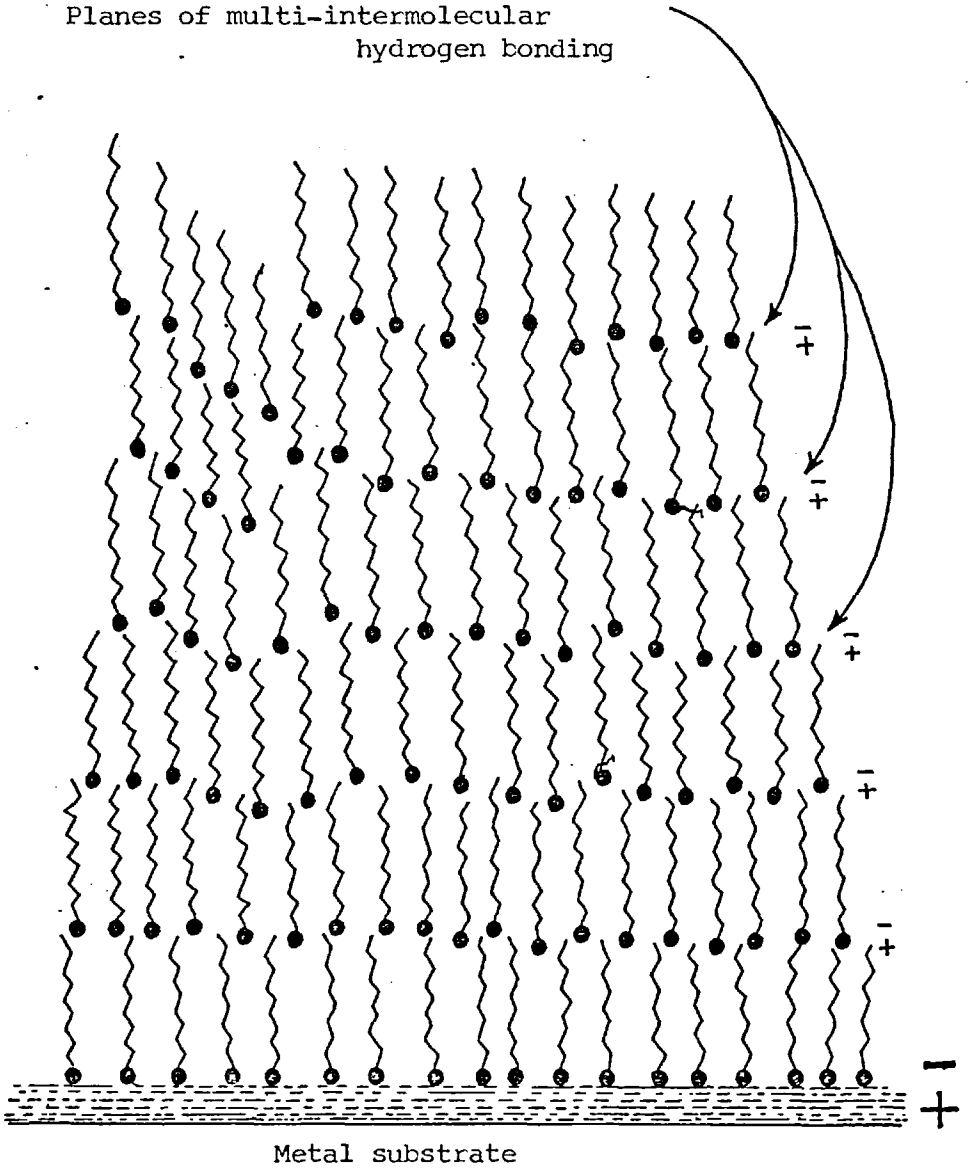


Fig. 7.10 Proposed structure of hydrogen bonding polar fluid films on metal substrate. The permanent spontaneous polarization produces the long range field.

fig. 7.10. Such a structure would have a unique polar axis and would exhibit pyroelectric properties, i.e. it would have a spontaneous polarization. According to Hill (20), the extent of the spontaneous polarization which can arise in these structures is of the order which would only be induced in normal crystals by fields of 10^5 to 10^8 volts/cm. By comparison, the alternating field applied by the capacitance measurement circuit of between 1.0 and 10 volts/cm would be negligible.

The long range ordered structure described above would satisfy the experimental results of this chapter in every respect. It is evident that the fluid molecules must be both polar and capable of intermolecular hydrogen bonding. The resulting spontaneous polarization accounts for the large increments observed in the dielectric constants of the films. The replacement of the methyl-methyl slip planes with ones containing extensive lateral hydrogen bonding would result in the continued viscosity increments reported. The promotion of the electric field deep into the fluid tallies with the observed anomolous effects 10,000Å from the metal surface. The enhanced conductivities measured are almost certainly due to proton 'hopping' or tunnelling. This conduction process would take place in the hydrogen bonding planes, the conducting links between one plane and the next formed by defects in the multi-planar structure. Such lattice defects would be situated where non-polar or non-hydrogen bonding molecules were trapped in the structure. If these interfering molecules became predominant they would greatly reduce the order and the range of the semi-crystalline structure. This would explain the decrease of dielectric constant variations observed with the fatty acids when large amounts of metal soap were present, and also the lower range of the effects observed for cetyl alcohol dissolved in hexadecane.

CHAPTER 8

CONCLUSION AND FUTURE WORK

The mercury squeeze-film apparatus has been developed in two ways to investigate more fully several properties of fluid films between 50,000Å and 200Å. The existence of at least two quite different types of strongly adherent polymolecular fluid layers on metal substrates has been clearly established.

8.1 Shear Strength of Chemisorbed Thick Films

The thick films produced by long chain carboxylic acids on damp metal oxide surfaces were sheared tangentially by pumping the mercury past them. The films formed by the myristic, stearic and palmitic acids proved especially resistant to shearing, thinning to about 1,500Å under a force of 150 newtons/metre^2 (or much more if turbulence occurred, see Appendix B). Electrical instabilities in these films whilst undergoing shear made it necessary to observe them interferometrically. This latter technique confirmed that the films consisted of interwoven soap fibrils between 1,000Å and 5,000Å in length. The bulk of the results obtained were found to be in general agreement with those of Fuks (Chapter 4, refs. 2, 3).

An important observation was the marked increase in shear strength exhibited by the thick films formed from solutions of chain matching fatty acids and solvents. These films also showed much greater electrical resistance, corresponding to well developed coherent films of reaction product (i.e. metal soap). The chain matching phenomenon strongly supports the theory that the chemisorbed films have a quasi-crystalline structure. Such a structure would grow much more extensively and be inherently stronger when the metal soap molecules and solvent molecules are of similar dimensions.

8.2 Investigation of Physical Adsorption

The plate apparatus was developed to measure the thinning of the test fluids down to~200Å under the hydrostatic pressure of mercury. By comparing these results with theoretical curves the apparatus could be used as a thin film

viscometer. The saturated paraffins were shown to retain their bulk properties throughout. The esters exhibited little change in their properties, although where micellar formations were possible small viscosity increments were found.

The most interesting results were obtained for those fluids capable of cooperative hydrogen bonding, i.e. the fatty acids and alcohols. These fluids all showed increments in their dielectric constants, viscosities and conductivities for film thicknesses below 10,000Å. These results made it evident that a high degree of molecular ordering of a physical nature extended deep into the film from the metal substrate. The current theories of such long range alignment incorporate large accumulations of single dimers or dimeric chains which can satisfactorily explain neither the above results nor many obtained by previous workers. A revised theory was proposed in which the dimeric accumulations have bent and realigned within the range of the electrical double layer field near the surface to form a permanently polarized highly ordered pyroelectric structure.

This theory may also account for the electrical breakdowns of the chemisorbed thick films whilst undergoing shear, as described in Chapter 3. The fluid above the film weak spots reasonably could be expected to consist mainly of unreacted fatty acid as little or no chemical adsorption could have occurred at these points. If basically physical adsorption then took place at these points forming the proposed pyroelectric structure then the enhanced conductivity (due to proton tunnelling) and the large potential caused by the spontaneous permanent polarization would accelerate electrical breakdown.

8.3 Possible Future Research

Much more research needs to be carried out into the shear strength of the chemisorbed thick films so that their role in practical lubricating systems may be established. Some pointers to this work follow:

(i) The films should be exposed to much higher tangential shear, until physical breakdown occurs for every case. Here the large increase in shear with the advent of turbulence could be utilized, although accurate measurement of the shearing force would be a problem.

(ii) A much larger range of solvents and acidic additives should be tested with special emphasis on the occurrence of chain matching.

(iii) The investigation of the effect of large temperature variations on the thick film properties could also prove interesting.

(iv) Stainless steel has not yet been used as the substrate in the shear experiments. With this metal the effect on the shear strength of the thick films of increased surface roughness might be observed, an important point from the lubrication aspect.

(v) The interferometric system could be improved so that more accurate optical measurements of film thicknesses might be made simultaneously with the capacitance measurements.

Possibilities for the continued reasearch into the mechanisms of physical adsorption of fluids on various substrates are manyfold:

(i) So far only tests on stainless steel and chrome substrates have been made. Using interferometric measurements of film thicknesses as an alternative to capacitance measurements the adsorption of fluids on many interesting but non-conducting substrates may be studied. Such surfaces would also be useful for tests on fluids with relatively high conductivities and dielectric constants, e.g. distilled water.

(ii) The state of these substrates prior to testing might also be varied. Apart from the "wet" and "dry" cleaning techniques, the surface energies could be greatly affected using high voltage discharges both before and during the experiments.

(iii) Temperature variations should give very clear insight into the mechanisms of the dielectric properties and conductivities of these films.

Dielectric dispersion measurements using a large range of applied frequencies would be very useful in this repsect, but the technique would be very difficult to perfect in this system. More direct measurements could be made on the electrical properties of the films, e.g. detection of rectification, and the disrupting effect of slight amounts of additional water in the fluids.

(iv) Many different and more complex solutions ought to be tested from a practical viewpoint. Included in these would be industrially proved oil mixtures and some of their constituent parts, to help establish the role of each fraction and study possible interference between some additivies. Other worthy tests would be those on important physiological fluids, e.g. sinovial fluid.

APPENDIX A

The Effect of Turbulence in the Cell Apparatus

In chapter 2.3.3 it was mentioned that at high flow rates, equivalent to a pressure drop across the cell of 34 cm. of mercury, the Reynolds number, R_e, approached the critical value of 2,000, above which it is generally accepted that turbulent flow replaces laminar flow. The shear produced by laminar flow for low Reynolds number was calculated earlier (chapter 2.3.3), but here the approximate shear resulting from turbulent flow must be estimated.

In fact in this system, R_e will not rise greatly above 2,000. Assuming therefore, that it is in the range $2{,}000 < R_e < 10^5$, then the Blasius law will apply, i.e.

$$C_f = 0.079\ R_e^{-\frac{1}{4}} \qquad \ldots\ldots\ldots\ldots \quad (A.1)$$

where C_f is the skin-friction coefficient.

An expression for the shear stress at the wall, τ, under these conditions is:-

$$\tau = C_f \times \frac{1}{2} \rho_m u_m^2 \qquad \ldots\ldots\ldots\ldots \quad (A.2)$$

where ρ_m is the density of mercury

and u_m is the average velocity of the mercury in the channel.

u_m may be calculated from the relationship:

$$u_m = 0.817 \times 8.6 \left(\frac{\tau}{\rho_m}\right)^{\frac{4}{7}} \times \nu_m^{-\frac{1}{7}} \times \left(\frac{h_c}{2}\right)^{\frac{1}{7}} \qquad \ldots\ldots\ldots\ldots \quad (A.3)$$

where ν_m is the kinematic viscosity of mercury

and h_c is the channel separation.

These three equations may be combined to give an expression for τ in terms of R_e, ν_m, ρ_m, η_m and h_c, all of which have known values. This

expression simplifies to

$$\tau \approx \left[\frac{R_e^{\frac{1}{4}}}{2}\right]^7 \times \frac{4\eta_m^2}{h_c^2 \rho_m} \qquad \ldots\ldots\ldots\ldots\ldots\ldots (A.4)$$

Substituting the values of the various constants gives:

$$\tau \approx 10 \times \left[\frac{R_e^{\frac{1}{4}}}{2}\right]^7 \qquad \ldots\ldots\ldots\ldots\ldots\ldots (A.5)$$

The Reynolds number, R_e, calculated from the maximum flow rate in the cell is in the range:

$2{,}000 < R_e < 2{,}500$. Using these two values in equation (A.5) gives values of shear in the range 5×10^3 newtons/metre^2 $< \tau <$ 9×10^3 newtons/metre^2. Comparing this range with the maximum shear of 1.5×10^2 newtons/metre^2 calculated assuming laminar flow indicates a very large increase in shear experienced at the channel walls resulting from the transition to turbulent flow.

This increase can be explained by considering the effect on the mercury velocity profile with the advent of turbulence. As the value of R_e increases over the critical value (~2,000) turbulence will replace laminar flow within the boundary layer at a point close to the entry of the channel. This turbulent boundary layer will then spread inwards as the flow continues downstream, until it has fully developed. It will produce, therefore, a velocity profile which is far from the parabolic model for laminar flow, (see fig. A.1). The velocity is almost constant across the centre of the flow channel, but the velocity gradient near the channel walls will be much larger than for the parabolic case. As the velocity gradient at any point in a fluid defines the shear stress in the fluid at that point it follows that, for the same rate of flow, turbulent flow will produce a much larger shear at the channel walls than laminar flow.

With respect to the results of chapter 4 it is an interesting

point that if turbulence did arise then the thick films withstood a much larger shear than 150 newtons/metre^2. The approximate calculations above indicate that the shear which thinned them down to between 1,500 Å and 2,000 Å could have been of the order of 5 x 10^3 newtons/metre^2, i.e. ~50 gm/cm^2. By comparing these values with the graph of fig. 4.1b, they can be seen to fit the results produced by Fuks much more closely than reported in chapter 4. The apparently greater shear strength of the thick films produced in this research could be explained by the added resiliance produced by chain matching, as discussed earlier.

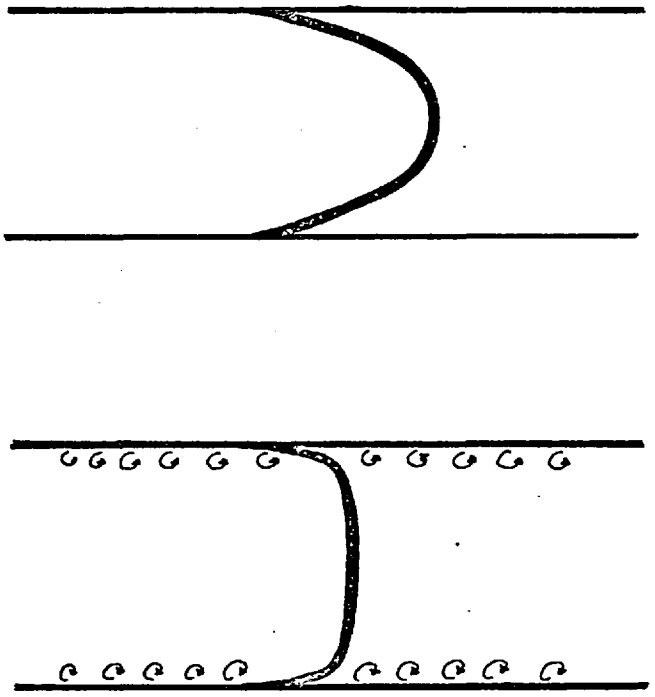


Fig. A.1 Comparison of velocity profiles for laminar and turbulent flow

APPENDIX B

Table of results obtained by Fuks (Chap. 4, ref. 3)

Table B.1 Influence of Shear and Fatty Acid on Residual Film Thickness of a Turbine Oil (Viscosity = 35 c.poise)

Fatty Acid Additive	None	0.1% Palmitic	0.1% Palmitic	0.1% Behenic
Chain	..... C_{25} *	$CH_3(CH_2)_{14}COOH$	$CH_3(CH_2)_{14}COOH$	$CH_3(CH_2)_{20}COOH$
Molecular weight	350 *	256	256	340
Normal stress (psi)	8.5	8.5	25	12
Static Film Thickness (Å)	1,200	1,900	1,200	1,900
Shear Stress (psi)	1.15	0.54	1.28	0.45
Sheared Film Thickness (Å)	800	1,200	900	1,300

Table B.2 Stress Relationship for Stearic Acid in Various Solvents

Solvent	Chain	Molecular Weight	Shear Stress, psi	Normal Stress, psi
Benzene	C_6H_6	78	0.03	42.5
Hexane	$CH_3(CH_2)_4CH_3$	86	....	54
Isooctane	$(CH_3)_2CH(CH_2)_4CH_3$	114	0.045	57
Dodecane	$CH_3(CH_2)_{10}CH_3$	170	0.073	74
MS.-20	$C_{35\ to\ 40}$ *	300-400 *	3.1	310

* Estimated

APPENDIX C

Computed Solution of Differential Thinning Equation

The partial differential equation derived in chapter 6 is:

$$W = \frac{-KH^2}{24(N-\frac{5}{2}G)}\left[3(2N+1)\frac{\partial h}{\partial x} - \frac{h}{R}\left((3N+1)(7W\frac{\partial h}{\partial x} + h\frac{\partial W}{\partial x}) + \frac{5(2N+1+G(3N+1))}{(2N-5G)}\cdot(W\frac{\partial h}{\partial x} + h\frac{\partial W}{\partial x})\right)\right]$$

This can be solved for h using the Gauss-Siedel iterative technique on a two dimensional mesh where x and t are the two dimensions. For this method a clearer expression for h is necessary. Non-dimensionalisation also simplifies the computation.

C.1 Non-Dimensionalisation

The equation is clarified by letting

$$F = (N - \frac{5}{2}G)$$

$$Q = 2N+1$$

and $$S = 3N+1$$

which reduces it to:

$$\frac{dh}{dt} = \frac{-Kh^2}{24F}\left[3Q\frac{\partial h}{\partial x} - \frac{h}{R}\left(6SW\frac{\partial h}{\partial x} + \left(\frac{5(Q+GS)}{2F} + S\right)\left(W\frac{\partial h}{\partial x} + h\frac{\partial W}{\partial x}\right)\right)\right] \quad \ldots C.1.$$

The non-dimensionalised values of h, x and t may be used where:

$$\left.\begin{aligned} X &= \frac{x}{L} \\ H &= \frac{h}{L} \\ \& \; T &= \nu_o t/L^2 \end{aligned}\right\} \quad \ldots\ldots\ldots\ldots\ldots\ldots\ldots C.2.$$

L can be any value of length, and is set here as the length of the plate apparatus; ν_o is the kinematic viscosity of the test fluid, and has dimensions $[L^2T^{-1}]$.

By substituting the expressions of C.2 in the functions G and R the non-dimensionalised equations become:

$$\left.\begin{aligned} G &= \left(-\frac{Q}{6} H.W\right)^{\frac{1}{2}} \\ \text{and } R &= \nu_o \left(-\frac{6}{Q} HW\right)^{\frac{1}{2}} \end{aligned}\right\} \qquad \ldots\ldots\ldots\ldots\ldots\ldots C.3.1.$$

where W is now $\frac{dH}{dT}$.

Using the expressions of C.2 to non-dimensionalise the equation C.1 gives:

$$\frac{dH}{dT} = -\frac{KL^3.H^2}{24\nu_o F}\left[3Q\frac{\partial H}{\partial X} - \frac{H}{P}\left(6SW\frac{\partial H}{\partial X} + \left(\frac{5}{2F}(Q+GS)+S\right)\left(W\frac{\partial H}{\partial X} + H\frac{\partial W}{\partial X}\right)\right)\right]$$

where $P = \left(-\frac{6}{Q} HW\right)^{\frac{1}{2}}$ C.3.2.

Defining A as

$$A = 6SW\frac{\partial H}{\partial X} + \left(\frac{5}{2F}(Q+GS)+S\right)\left(W\frac{\partial H}{\partial X} + H\frac{\partial W}{\partial X}\right)$$

reduces the equation to:

$$\frac{dH}{dT} = W = -\frac{KL^3.H^2}{24\nu_o F}\left(3Q\frac{\partial H}{\partial X} - \frac{AH}{P}\right)$$

which is, in terms of H:

$$H. = \left(-24\nu_o F.W \Big/ KL^3\left(3Q\frac{\partial H}{\partial X} - \frac{AH}{P}\right)\right)^{\frac{1}{2}} \quad \ldots\ldots \quad C.4.$$

The iteration process carried out by the computer uses the old value of H at a particular mesh point (i.e. H(I,J)) on the right hand side of equation C.4 to calculate the new value on the left hand side. This new value is used in the next iteration and so on.

When computed, equation C.4 could not be made to converge, mainly because the function within the square root repeatedly went negative during the iteration process. Another expression for H(I,J) could be obtained from its differential with respect to X, which may be written:

$$\frac{\partial H}{\partial X} = \frac{H(I+1,J) - H(I,J)}{\Delta X}$$

where the I suffix refers to the x dimension

and the J suffix refers to the t dimension

(from Crandall (C.1)).

Thus equation C.4 becomes:

$$H(I,J) = H(I+1,J) + \left(\frac{8\nu_0 F}{KQL^3.H^2}.\frac{dH}{dT} + \frac{A.H}{3QP}\right).\Delta X \ldots\ldots \text{C.5.}$$

C.2 Boundary Conditions

As this is a propagation problem only one boundary condition need be specified, i.e. the variation of H with x at a particular time. This relationship was obtained from an approximated form of the basic equation where terms in H^3 and higher powers were neglected. Equation C.3.2. reduces to:

$$\frac{dH}{dT} = \frac{-KL^3}{24\nu_0 F}.3QH^2\frac{\partial H}{\partial X}$$

where F now $\approx$ N.

i.e. $$\frac{dH}{dT} = -CH^2\frac{\partial H}{\partial X} \qquad \ldots\ldots\ldots\ldots \text{C.6.}$$

where $$C = \frac{KL^3}{8\nu_0}.\left(2+\frac{1}{N}\right)$$

Assuming H is a separable function in terms of X and T, i.e.

$$H(X,T) = H(X).H(T)$$

equation C.6 becomes

$$H(X)\frac{dH(T)}{dT} = -C.H(X)^2.H(T)^3.\frac{\partial H(X)}{\partial X}$$

i.e. $$\frac{1}{H(T)^3}.\frac{dH(T)}{dT} = -C.H(X).\frac{\partial H(X)}{\partial X}$$

This is a justification of the above assumption, as each side of the equation is a function of a different variable. Both expressions, therefore, must equal a constant, B.

Taking the variables inside the differentials the expression is:

$$\frac{d(H(T))^{-2}}{dT} = C.\frac{\partial H(X)^2}{\partial X} = B.$$

Integrating these give:

$$\frac{1}{H(T)^2} = BT + C_1$$

$$H(X)^2 = \frac{B}{C}.X + C_2$$

where C_1 and C_2 are constants.

$$\therefore H(X,T) = H(X).H(T) \qquad \text{i.e.} = \left(\frac{BX/C + C_2}{BT + C_1}\right)^{1/2} \ldots . C.7.$$

This simplified solution is encouraging as it predicts that the film thickness is inversely proportional to the square root of the period of thinning. This concurs with the experimental evidence and the Stefan-Reynolds expression.

To evaluate the constants C_1, C_2 and B certain starting values for H must be assumed. These were varied to illustrate the dependence of the thinning curve on the experimental starting conditions. A typical example is demonstrated below.

at X = 0, T = 0 put H = 0

i.e. H(0,0) = 0

This boundary condition results from the fact that the glass slide rests on the mercury surface prior to the addition of the test fluid, and therefore, at the very bottom, there will be no oil film.

$$\therefore \text{from C.7} \qquad \frac{C_2}{C_1} = 0 \qquad \text{i.e.} \quad C_2 = 0$$

At x = 1, T = 0, H = HXO

$$\therefore HXO = \left(\frac{B}{CC_1}\right)^{1/2}$$

equation C.7 becomes:

$$H = HXO\left(\frac{X}{HXO^2.CT + 1}\right)^{1/2} \ldots \ldots . C.7.1.$$

Differing experimental starting conditions can be simulated by varying HXO between 10^{-3} metres and 10,000Å (10^{-6} metres) in equation C.7.1 which defines H over the two dimensional grid.

C.3 The Programme

Expression C.5, which defines H in terms of $\frac{dH}{dT}$, $\frac{dH}{dX}$, $\frac{dH}{dX}$ and lesser terms containing H, is solved by the programme shown below. The fact that some lesser functions of H involved the square roots of a negative expression proved troublesome. If these expressions became positive at any point then the iteration cycle became complex and therefore meaningless. In physical terms it is impossible for these expressions to rise above zero, yet, as the iteration cycle involves oscillation around the solution until it converges to that solution, such an eventuality could, and did, arise. To safeguard against this, therefore, several "test procedures" were included in the programme which by-passed the problem.

By varying the values of the constants relating the properties of the fluids tested, the theoretical thinning curve for each fluid was calculated.

```
      PROGRAM ANS(INPUT,OUTPUT,TAPE5=INPUT,TAPE6=OUTPUT)
C
C*****     DATA
C*************************************************
      DIMENSION H(51,51),RS(51,51),X(91,2),T(91,2),RSDU(3),DHT(51,51),
     1DHX(51,51),DHX(51,51)
C*****   DEFINE VISCOSITIES AND DENSITIES.
      VISHG=1.51*10.**(-3)
      DENHG=13.6*10.**3
C*****    OIL IS SQUALANE.
      VISOIL=2.64*10.**(-2)
      DENOIL=8.1*10.**2
C*****  DEFINE ITERATION CONSTANTS.
      GRAV=9.81
      ELLE=3.*10.**(-2)
      CAY=GRAV*(DENHG-DENOIL)/VISOIL
      ENNE=VISOIL/VISHG
      COO=2.*ENNE+1.
      ESSE=3.*ENNE+1.
      CEE=CAY*ELLE**3*DENOIL*(2.+1./ENNE)/8./VISOIL
      RP=.1
      IN=51
      JN=51
      INM=IN-1
      JNM=JN-1
```

```
C*****      VARY STARTING CONDITIONS
C*************************************************
      IJK=0
    3 IJK=IJK+1
      H00=0.000
      IF(IJK.EQ.1) HX0=10.**(-2)
      IF(IJK.EQ.2) HX0=10.**(-3)
      NMAX=100
C
C
C*****          SET X-CO-ORDINATES
C*************************************************
      X(1,1)=0.2
      DO 10 I=2,IN
      X(I,1)=X(I-1,1)+0.8/FLOAT(INM)
   10 X(I,2)=X(I,1)-X(I-1,1)
      X(1,2)=X(2,2)
C*****          SET T-CO-ORDINATES
C
C
C*****   ITERATION REPEATS FOR 1, 10, 100, 1000 ,10000 MIN CYCLES
C*************************************************
      T(JN,1)=0.
      TIME=VISOIL/DENOIL/ELLE**2*60.
      K=0
    2 K=K+1
      T(1,1)=T(JN,1)
      DO 11 J=2,JN
      T(J,1)=T(J-1,1)+TIME/FLOAT(JNM)
   11 T(J,2)=T(J,1)-T(J-1,1)
      T(1,2)=T(2,2)
C
C
C*****      SET INITIAL H-VALUES
C*************************************************
      DO 12 I=1,IN
      RS(I,1)=0.
      START=((HX0**2-H00**2)*X(I,1))**.5+H00
      IF(K.EQ.1) H(I,1)=START/(CEE*(HX0**2-H00**2)*T(1,1)+1.)**.5
      IF(K.NE.1) H(I,1)=H(I,JN)
      DO 13 J=2,JN
      RS(I,J)=0.
   13 H(I,J) =START/(CEE*(HX0**2-H00**2)*T(J,1)+1.)**.5
   12 CONTINUE
C
C
C*****    ITERATION CYCLE BEGINS
C*************************************************
      NITER=0
    1 NITER=NITER+1
      RSDU(1)=0.
C
C*****   CALCULATE DIFFERENTIALS AND CONSTITUENT FUNCTIONS.
C*************************************************
      DO 14 J=2,JN
      DO 14 I=1,IN
      IF(I.EQ.1) GO TO 44
      IF(I.EQ.IN) GO TO 55
      DHX(I,J)=(H(I+1,J)-H(I-1,J))/2./X(I,2)
      GO TO 57
```

```
   44 DHX(1,J)=(-3.*H(1,J)+4.*H(2,J)-H(3,J))/2./X(1,2)
   55 DHX(IN,J)=(3.*H(IN,J)-4.*H(INM,J)+H(IN-2,J))/2./X(INM,2)
   57 IF(J.EQ.JN) GO TO 66
      DHT(I,J)=(H(I,J+1)-H(I,J-1))/2./T(J,2)
   66 DHT(I,JN)=(3.*H(I,JN)-4.*H(I,JNM)+H(I,JN-2))/2./T(JNM,2)
      Z=H(I,J)
      IF(Z.LE.0.) GO TO 22
      IF(DHT(I,J).GE.0.) GO TO 9
      GEE=(-COO*Z*DHT(I,J)/6.)**.5
    9 IF(DHT(I,J).GE.0.) GEE=0.
   22 IF(Z.LE.0.) GEE=0.
      EFFE=ENNE-2.5*GEE
      IF(EFFE.LE.0.) EFFE=ENNE
      CON=8.*VISOIL/(CAY*DENOIL*ELLE**3*COO)
C
C
C*****     CALCULATE H(I,J).
C*************************************************
      IF(I.EQ.IN) GO TO 16
      H(I,J)=H(I+1,J)+CON*EFFE*DHT(I,J)*X(I,2)/Z**2
   16 H(IN,J)=2.*H(INM,J)-H(IN-2,J)
   17 H(I,J)=RP*(H(I,J)-Z)+Z
      IF(ABS(H(I,J)).LT.10.**(-20)) RS(I,J)=0.
      IF(ABS(H(I,J)).LT.10.**(-20)) GO TO 14
      RS(I,J)=1.-Z/H(I,J)
C
C*****    CHECK FOR CONVERGENCE.
C*************************************************
   14 IF( ABS(RS(I,J)).GT. ABS(RSDU(1))) RSDU(1)=RS(I,J)
      IF((NITER+NMAX-1)/NMAX-NITER/NMAX) 999,998,999
  998 WRITE(6,502)
      WRITE(6,500) ((H(I,J),I=1,IN,5),J=1,JN,5)
      WRITE(6,503)
      WRITE(6,500) ((RS(I,J),I=1,IN,5),J=1,JN,5)
      WRITE(6,504) NITER
  999 CONTINUE
      IF(NITER.GE.NMAX) GO TO 78
      IF(ABS(RSDU(1)).GT..001) GO TO 1
      WRITE(6,502)
      WRITE(6,500) ((H(I,J),I=1,IN,5),J=1,JN,5)
      WRITE(6,503)
      WRITE(6,500) ((RS(I,J),I=1,IN,5),J=1,JN,5)
      WRITE(6,504) NITER
      TIME=TIME*10.
      IF(K.LT.5) GO TO 2
      GO TO 77
   78 WRITE(6,505) NITER
  505 FORMAT(32H THE PROCESS DID NOT CONVERGE IN,I5,11H ITERATIONS)
   77 IF(IJK.LT.2) GO TO 3
  500 FORMAT(1H ,(11E11.4))
  501 FORMAT(1H ,3I5)
  502 FORMAT(1H ,10X,30HDISTRIBUTION OF FILM THICKNESS/
     111X,30H------------------------------//)
  503 FORMAT(1H ,//1H ,23X,14HRESIDUAL TABLE/21X,14H--------------)
  504 FORMAT(1H ,//7H NITER=,I5)
      STOP
      END
```

X	DISTRIBUTION OF FILM THICKNESS (Non Dimensional) 0·2	0·3	0·4	0·5	TIME (mins)
	0.4472E-03	0.5292E-03	0.6903E-03	0.6633E-03	0·0
	0.4049E-03	0.4791E-03	0.5432E-03	0.6005E-03	
	0.3727E-03	0.4409E-03	0.5000E-03	0.5528E-03	
	0.3471E-03	0.4107E-03	0.4657E-03	0.5148E-03	
	0.3261E-03	0.3859E-03	0.4376E-03	0.4838E-03	
	0.3086E-03	0.3651E-03	0.4141E-03	0.4577E-03	0·5
	0.2936E-03	0.3474E-03	0.3939E-03	0.4355E-03	
	0.2806E-03	0.3320E-03	0.3765E-03	0.4162E-03	
	0.2692E-03	0.3185E-03	0.3612E-03	0.3993E-03	
	0.2591E-03	0.3065E-03	0.3476E-03	0.3843E-03	
	0.2500E-03	0.2958E-03	0.3354E-03	0.3708E-03	1·0
	0.2500E-03	0.2958E-03	0.3354E-03	0.3708E-03	"
	0.1924E-03	0.2277E-03	0.2582E-03	0.2855E-03	
	0.1622E-03	0.1919E-03	0.2176E-03	0.2406E-03	
	0.1429E-03	0.1691E-03	0.1917E-03	0.2119E-03	
	0.1291E-03	0.1528E-03	0.1732E-03	0.1915E-03	
	0.1187E-03	0.1404E-03	0.1592E-03	0.1760E-03	
	0.1104E-03	0.1307E-03	0.1482E-03	0.1638E-03	
	0.1037E-03	0.1227E-03	0.1391E-03	0.1538E-03	
	0.9805E-04	0.1161E-03	0.1316E-03	0.1454E-03	
	0.9325E-04	0.1103E-03	0.1251E-03	0.1383E-03	
	0.8909E-04	0.1054E-03	0.1195E-03	0.1321E-03	10
	0.8909E-04	0.1054E-03	0.1195E-03	0.1321E-03	"
	0.6539E-04	0.7732E-04	0.8733E-04	0.9655E-04	
	0.5376E-04	0.6361E-04	0.7213E-04	0.7974E-04	
	0.4683E-04	0.5541E-04	0.6283E-04	0.6946E-04	
	0.4203E-04	0.4973E-04	0.5639E-04	0.6235E-04	
	0.3846E-04	0.4551E-04	0.5161E-04	0.5705E-04	
	0.3567E-04	0.4220E-04	0.4786E-04	0.5291E-04	
	0.3341E-04	0.3953E-04	0.4482E-04	0.4955E-04	
	0.3153E-04	0.3730E-04	0.4230E-04	0.4676E-04	
	0.2993E-04	0.3542E-04	0.4016E-04	0.4440E-04	
	0.2856E-04	0.3379E-04	0.3832E-04	0.4236E-04	10^2
	0.2856E-04	0.3379E-04	0.3832E-04	0.4236E-04	"
	0.2073E-04	0.2453E-04	0.2782E-04	0.3075E-04	
	0.1798E-04	0.2021E-04	0.2292E-04	0.2534E-04	
	0.1486E-04	0.1759E-04	0.1994E-04	0.2205E-04	
	0.1333E-04	0.1577E-04	0.1789E-04	0.1978E-04	
	0.1219E-04	0.1443E-04	0.1636E-04	0.1809E-04	
	0.1130E-04	0.1337E-04	0.1517E-04	0.1677E-04	
	0.1058E-04	0.1252E-04	0.1420E-04	0.1570E-04	
	0.9987E-05	0.1182E-04	0.1341E-04	0.1481E-04	
	0.9480E-05	0.1122E-04	0.1272E-04	0.1406E-04	
	0.9044E-05	0.1070E-04	0.1213E-04	0.1341E-04	10^3
	0.9044E-05	0.1070E-04	0.1213E-04	0.1341E-04	"
	0.6561E-05	0.7764E-05	0.8803E-05	0.9733E-05	
	0.5405E-05	0.6396E-05	0.7252E-05	0.8017E-05	
	0.4702E-05	0.5564E-05	0.6309E-05	0.6975E-05	
	0.4217E-05	0.4991E-05	0.5659E-05	0.6255E-05	
	0.3857E-05	0.4563E-05	0.5175E-05	0.5721E-05	
	0.3575E-05	0.4230E-05	0.4797E-05	0.5303E-05	
	0.3348E-05	0.3961E-05	0.4492E-05	0.4966E-05	
	0.3159E-05	0.3737E-05	0.4238E-05	0.4685E-05	
	0.2998E-05	0.3548E-05	0.4023E-05	0.4447E-05	
	0.2860E-05	0.3384E-05	0.3838E-05	0.4243E-05	10^4

REFERENCES

Chapter 1

(1) Reynolds, O., Phil. Trans. Roy. Soc., 177, 157, (1886).

(2) Grubin, A.N. (in Russian), Cent. Sci. Res. Inst. for Tech. and Mech. Eng. (Moscow 1949), Book No. 30, D.S.I.R. Trans. No. 337.

(3) Lord Rayleigh, Phil. Mag., 48 331, (1899).

(4) Langmuir, A., Trans. Faraday Soc., 15, 62, (1920).

(5) Levine, O., and Zisman, W.A., J. Phys. Chem., 61, 1068, (1957).

(6) Bigelow, W.C., Pickett, D.L., and Zisman, W.A., J. Colloid Sci., 1, 513, (1946).

(7) Bigelow, W.C., Glass, E., and Zisman, W.A., J. Colloid Sci., 2, 563, (1947).

(8) Levine, O., and Zisman, W.A., J. Phy. Chem., 61, 1188, (1957).

(9) Cottington, R.L., Shafrin, E.G., and Zisman, W.A., J. Phys. Chem. 62, 513, (1958).

(10) Bewig, K.W., and Zisman, W.A., J. Phys. Chem., 67, 130, (1963).

(11) Hardy, Sir W., and Nottage, M., Proc. Roy. Soc., A118, 209, (1927).

(12) Hardy, Sir W., Collected Works, Cambridge University Press, (1936).

(13) Trillat, J.J., Ann. Phys., 6, 5, (1926).

(14) Smith, A.J., Ph.D. thesis, University of London, (1971).

(15) Duff, A.W., Phil. Mag., 9, 6, (1905).

(16) Barnard, D.P., Wilson, R.E., J. Ind. Eng. Chem., 14, 682, (1922).

(17) Dover, M.V., J. Ind. Eng. Chem., 18, 499, (1926).

(18) Needs, S., Trans. A.S.M.E., 62, 331, (1940).

Chapter 1 continued.

(19) Tausz, J., Szekely, P., Erdol und Teer, 9, 331, (1933).

(20) Deryagin, B.V., Samygin, M.M., Acad. Nauk S.S.S.R., 1, 59, (1941).

(21) Deryagin, B.V., Zeits. Phys., 84, 657, (1933).

(22) Deryagin, B.V., Zeits. Sovjetunion, 4, 431, (1933).

(23) Deryagin, B.V., Nature, 138, 330, (1936).

(24) Deryagin, B.V., Kusakov, M.M., Acta Physiochem., U.S.S.R., 10, 25, and 153, (1939).

(25) Deryagin, B.V., Kusakov, M.M., Lebedeva, L., Comptes Rendues U.S.S.R., 23, 671, (1939).

(26) Deryagin, B.V., Karasev, V.V., Zakhavaeva, N.N., Lazanev, V.P., Sov. Phys. J.E.T.P., 27, 980, (1957).

(27) Henniker, J.C., Rev. Mod. Phys., 21, No. 2, 322, (1949).

(28) Deryagin, B.V., Wear, 1, 277, (1957).

(29) Zakhavaeva, N.N., Deryagin, B.V., Khomutov, A.M., Andreev, S.V., Research in Surface Forces, II, p. 156, Consultant's Bureau, N.Y., (1966).

(30) Deryagin, B.V., Zakhavaeva, N.N., Andreev, S.V., Milovidov, A.A., Research in Surface Forces, I, Consultant's Bureau, N.Y., (1963).

(31) Fuks, G.I., Bratova, G.S., Dok. Acad. Nauk, 153, No. 5, 1106, (1963).

(32) Fuks, G.I., Research in Surface Forces, 1, p. 79, Consultant's Bureau, N.Y., (1963).

(33) Fuks, G.I., Research in Surface Forces, 2, p. 159, Consultant's Bureau, N.Y., (1966).

(34) Askwith, T.C., Cameron, A., Crouch, R.F., Proc. Roy. Soc., A 291, 500, (1966).

Chapter 1 continued.

(35) Smith, A.J., Cameron, A., Special Discussion, Faraday Soc., (1971).

(36) Bulkley, R., U.S. Bureau of Standards J. Research, 6, 89, (1930).

(37) Bastow, S.H., Bowden, F.P., Proc. Roy. Soc., A 134, 404, (1931).

(38) Bastow, S.H., Bowden, F.P., Proc. Roy. Soc., A 151, 220, (1935).

(39) Hayward, A.T.J., Isdale, J.D., Brit. J. Appl. Phys., Ser. 2, 2, 251-9, (1969).

(40) Griffiths, A.A., Phil. Trans. Roy. Soc., A 221, 163, (1920).

(41) Frewing, J.J., Proc. Roy. Soc., A 182, 270, (1944).

(42) Bowden, F.P., Gregory, J.N., Tabor, D., Nature, 156, 97, (1945).

(43) Gregory, J.N., Spink, J.A., Nature, 159, 403, (1947).

(44) Greenhill, E.B., Trans. Faraday Soc., 45, 631, (1949).

(45) Prutton, C.F., Frey, D.R., Turnbull, D., Ind. Eng. Chem., 37, 90, (1945).

(46) Dennison, G.H., Ind. Eng. Chem., 36, 477, (1944).

(47) Tingle, E.D., Trans. Faraday Soc., 46, 93, (1950).

(48) Tingle, E.D., Nature, 160, 710, (1947).

(49) Shooter, K.V., Brit. J. App. Phys., Supplement No. 1, 49, (1951).

(50) Rowe, G.W., I.M.E. Conf. on Lubrication and Wear, Paper 5, (1957).

(51) Russel, J.A., Campbell, W.E., Barton, R.A., Ku, P.M., A.S.L.E. Trans., 8, 48, (1965).

(52) Lancaster, J.K., Rouse, R.L., Research, 4, 44, (1951).

(53) Hirst, W., Lancaster, J.K., Trans. Faraday Soc., 47, 315, (1951).

Chapter 1 continued.

(54) Akhmatov., A.S., Molecular Physics of Boundary Lubrication, Israel Programme for Scientific Translations, Jerusalem, (1966).

(55) Allen, C.M., Drauglis, E., Wear, 14, 363, (1969).

(56) Bowden, F.P., Tabor D., The Friction and Lubrication of Solids, Oxford University Press, (1950).

(57) Frewing, J.J., Proc. Roy. Soc., A 181, 23, (1942).

(58) Bowden, F.P., Throssel, W.R., Proc. Roy. Soc., A 209, 297, (1951).

(59) Bickerman, J.J., Proc. Roy. Soc., A 170, 130, (1939).

Chapter 2

(1) Smith, A.J., Cameron, A., Special Discussion, Faraday Soc., Cambridge, (1971).

(2) Wayne-Kerr Monograph No. 1, The Transformer Ratio-Arm Bridge, Wayne Kerr Ltd., New Malden, Surrey.

(3) Smith, A.J., Ph.D. Thesis, University of London, (1971).

(4) Cameron, A., Gohar, R., Theoretical and Experimental Studies of the Oil Film in Lubricated Point Contact, Proc. Roy. Soc., A 291, 520, (1966).

(5) Tolansky, S., An Introduction to Interferometry, Longmans, London, (1966).

(6) Steel, W.H., Interferometry, Cambridge University Press, London, (1967).

(7) Gentle, C.R., Ph.D. Thesis, University of London, (1971).

Chapter 3

(1) Smith, A.J., Ph.D. Thesis, University of London, (1971).

(2) Smith, A.J., Cameron, A., Proc. Roy. Soc., A 328, 541-560, (1972).

(3) Lancaster, J.K., Rouse, R.L., Research, 4, 44, (1951).

(4) Fuks, G.I., Bratova, G.S., Dok. Acad. Nauk, 153, No. 5, 1106, (1963).

(5) Fuks, G.I., Research in Surface Forces, I, p. 79, Consultant's Bureau, N.Y., (1963).

(6) Fuks, G.I., Research in Surface Forces, II, p. 159, Consultant's Bureau, N.Y., (1966).

(7) Talmud, D.L., Bresler, S.E., Surface Phenomena, GTTI, Moskva, (1934).

(8) Zoltoev, K.D., Mechanical and Electrical Properties of Liquid Films, Candidate's Thesis, Moskva, (1952).

(9) Twisleton-Wykeham-Fiennes, W.G., Ph.D. Thesis, University of London, (1971).

(10) Kok, J.A., Poll, J.W., and Vroonhoven, C., Dielectrics, 91, (May 1963).

(11) Pearson, G.L., Phy. Rev. 56, 471, (1939).

(12) Holm, R., 'Electric Contacts Handbook', Third Ed., Springer-Verlag, Berlin, (1958).

(13) Jachym, B., Act. Phys. Polon., 26 (6), 1061, (1964).

(14) Deryagin, B.V., and Krotova, N.A., Adhesion.Studies on Adhesion and Gluing Action, Izd. AN. S.S.S.R., (1949).

(15) Karasev, V.V., Krotova, N.A., and Deryagin, B.V., DAN, 88, 777, (1953).

Chapter 4

(1) Needs, S.J., 'Boundary Film Investigations', A.S.M.E., Trans., 62, 331, (1940).

(2) Fuks, G.I., Research in Surface Forces, 1, p. 79, Consultant's Bureau, N.Y., (1964).

(3) Fuks, G.I., Research in Surface Forces, 2, p. 159, Consultant's Bureau, N.Y., (1966).

(4) Terzaghi, K., Discussion of Ref. (1), p. 343.

(5) Smith, A.J., Ph.D. Thesis, University of London, (1971).

(6) Gentle, C.R., and Day, R.S., Effect of some Antiwear Additives on the Elastohydrodynamic Lubrication of a Point Contact, Tribology Convention, I.Mech.E., (1972).

(7) Akhmatov, A.S., Molecular Physics of Boundary Lubrication, Israel Programme for Scientific Translations, Jerusalem, (1966).

(8) Bowden, F.P., Tabor, D., The Friction and Lubrication of Solids, Oxford University Press, p. 200, (1950).

(9) Thiessen, P.A., and Spychalski, R., Z. phys. Chem., A156, 435, (1931).

(10) Askwith, T.C., Cameron, A., Crouch, R.F., Proc. Roy. Soc., A 291, 500, (1966).

Chapter 5

(1) Smith, A.J., Ph.D. Thesis, University of London (1971).

(2) Bowden, F.P., Tabor, D., The friction and Lubrication of Solids, Oxford University Press, p. 218, (1950).

(3) Moore, W.J., Physical Chemistry, Longmans, p. 303, (1965).

(4) Needs, S., Trans. A.S.M.E., 62, 331, (1940).

(5) Fuks, G.I., Research in Surface Forces, I, p. 79, Consultant's Bureau, N.Y., (1963).

(6) Askwith, T.C., Cameron, A., Crouch, R.F., Proc. Roy. Soc., A 291, 500, (1966).

(7) Parker, R.J., Kannel, J.W., Elastohydrodynamic Film Thickness between Rolling Discs with a Synthetic Paraffinic Oil to 589°K., NASA Technical Note TN D-6411, Washington, D.C., (1971).

(8) Gentle, C.R., Day, R.S., Effect of some Antiwear Additives on the Elastohydrodynamic Lubrication of a Point Contact, Tribology Convention, I.Mech.E., (1972).

Chapter 6

(1) Smith, A.J., Ph.D. Thesis, University of London, (1971).

(2) Stern, O.Z., Electrochem., 30, 508, (1924).

(3) Adamson, A.W., Physical Chemistry of Surfaces, p. 221, Interscience, London, (1967).

Chapter 7

(1) Adamson, A.W., Physical Chemistry of Surfaces, Interscience Publishers, London, (1967).

(2) Akhmatov, A.S., Molecular Physics of Boundary Lubrication, Israel Programme for Scientific Translations, Jerusalem, (1966).

(3) London, F., Trans. Farad. Soc., 33, 8, (1937).

(4) Godfrey, D., Symposium on Properties of Surfaces, A.S.T.M. Special Publication No. 340, p. 109, (1962).

(5) Bowden, F.P., Tabor, D., Friction and Lubrication of Solids, Clarendon Press, Oxford, (1950).

(6) Woog, P., Contribution a l'étude du graissage, Delgrave, Paris, (1926).

(7) Karplus, H., Petroleum Z., 25, 375, (1929).

(8) Beletskii, M.S., X-ray and Electron-Diffraction Studies of the Structure of the Films of Surface Active Substances Absorbed by the Surface of Deformed Aluminium, Doctorate's Thesis, Vsesoyuznyi Alyuminievomagnievyi Institut, Leningrad, (1954).

(9) Allen, C.M., Drauglis, E., Wear, 14, 363, (1969).

(10) Karasev, V.V., Krotova, N.A., Deryagin, B.V., Dan, 88, 777, (1953).

(11) Deryagin, B.V., Research in Surface Forces, 2, Consultant's Bureau, N.Y., (1966).

(12) Pimentel, G.C., McClellan, A.L., The Hydrogen Bond., Freeman, London, (1960).

(13) Kendall, C.E., H-bond effect on Viscosity, Chem. and Ind., 1944, 211.

(14) Harris, F.E., Haycock, E.W., Alder, B.J., J. Chem. Phys., 21, 1943-8, (1953).

(15) Pollack, J. McC., Ubbelohde, A.R., Electrical conductivity: theory for hydrogen bonded crystals, Trans. Farad. Soc., 52, 1112, (1956).

(16) Blinc, R., and Svetina, S., Cluster Approximations for Order-Disorder-Type Hydrogen Bonded Ferroelectrics, I, Small Clusters; Phys. Rev., 147, 423, (1966).

(17) Blinc, R., and Svetina, S., As above, Part II; Application to KH_2PO_4, Phys. Rev. 147, 430, (1966).

(18) Smith, A.J., Ph.D. Thesis, University of London, (1971).

(19) Houwink, R., Elasticity, Plasticity and Structure of Matter, Cambridge University Press, (1940).

(20) Hill, N.E., et al., Dielectric Properties and Molecular Behaviour, Van Nostrand Reinhold Co., Ltd., London, p. 433, (1969).

Appendix C

C.1 Crandall, S.H., Engineering Analysis, McGraw Hill, (1956).